**ADDIS ABABA UNIVERSITY**

**ADDIS ABABA INSTITUTE OF TECHNOLOGY**

**SCHOOL OF CIVIL AND ENVIRONMENTAL ENGINEERING**

# Prediction of Compressive Strength of Concrete using Artificial Neural Network, Fuzzy System Model and Thermodynamic Methods (A Comparative Study)

**A Thesis Submitted to the School of Graduate Studies of Addis Ababa University in Partial Fulfillment of the Requirements for the Degree of Masters of Science in Structural Engineering**

**By Nebiyu Siraj**

**Advisor: Dr. Esayas Gebreyouhannes**

**October 19, 2015**

**ADDIS ABABA UNIVERSITY**

**ADDIS ABABA INSTITUTE OF THECHNOLOGY**

**SCHOOL OF CIVIL AND ENVIRONMENTAL ENGINEERING**

# **P**rediction of **C**ompressive **S**trength of **C**oncrete using **A**rtificial **N**eural **N**etwork, **F**uzzy **S**ystem **M**odel and **T**hermodynamic **M**ethods (A Comparative Study)

**Nebiyu Siraj**

**Approved by the Board of Examiners:**

| | |
|---|---|
| ______________________________ | __________________ |
| **Advisor** | **Signature** |
| ______________________________ | __________________ |
| **Internal Examiner** | **Signature** |
| ______________________________ | __________________ |
| **Exterior Examiner** | **Signature** |
| ______________________________ | __________________ |
| **Chair Person** | **Signature** |

**Addis Ababa, Ethiopia**

## Declaration

I, the undersigned, declare that this thesis work, to the best of my knowledge and belief, is my original work, has not been presented for a degree in this or any other universities, and all sources of materials used for the thesis work have been fully acknowledged.

Nebiyu Siraj_ ____________________

**Candidate** **Signature**

Date of Submission: October 19, 2015

This is to certify that the above declaration made by the candidate is correct to the best of my knowledge.

**Dr. Esayas Gebreyouhannes** ____________________

**Thesis Advisor** **Signature**

## ACKNOWLEDGEMENTS

It is with immense pleasure that I express my gratitude to my advisor, Dr. Esayas Gebreyouhannes for being an inspiring figure throughout my academic life. His support has always transcended beyond the valuable comments, directions and suggestions in my thesis work; of which I am eternally grateful.

I would also like to thank Mr. Nasir Bedewi for his initial suggestion and motivation for the title of the thesis paper. His guidance, even in some demanding circumstances compounded with his unrelenting remarks have been invaluable during the continuous process of refining my paper.

My heartfelt thanks extends to Mr. Abraham Assefa for his pedagogy in contemporary methodologies and his time; and Dr. Abrham G., Melaeke S., Samson W. and Mekdes T for their insightful comments. My special thanks goes to Mina Ahmed for her unyielding support, love and advice.

Last but not least, I would like to thank, with all my heart, my family for their patience, encouragement and love.

## TABLE OF CONTENTS

## ABSTRACT

Utilization of concrete, as a material for building structures has been one of the major triumphs of mankind. Driven by increased standard of living and ever-rising population, the need for ‘better’ concrete is now the current trend. This in turn necessitates a representative measure of concrete quality that can be used as a benchmark. Amongst the possible alternatives, compressive strength of concrete is the main parameter used in design and assessment of quality in massive structures built with the likes of reinforced concrete, composite materials etc. Such endeavor is the challenge of the structural engineer while coming up with appropriate material and structural designs and controlling the quality of the concrete throughout the construction stage.

This thesis aims at adressing these challenges. The need to bypass the 28-day or accelerated compressive strength testing at the laboratory, especially in speedy constructions is duly recognized. Hence, compressive strength predicting models using the principles of artificial intelligence are proposed. These models apply fuzzy logic and artificial neural networks as a tool to predict the compressive strength of concrete at a given day. The Matlab software was also used to create a program that employs a user-friendly Graphical User Interface tool. To help in the comparative study, regression analysis was done to represent a statistical approach.

There have been many reported incidents where a structure encounters material failure before it reaches its capacity. Knowing the behavior of the concrete is therefore very important. Hence, one needs to strike the balance between structural and material design. This is apparent in massive structures like dams or concrete structures built in extreme weather conditions.

In an attempt to study of the behavior of the concrete, thermodynamic method is adopted. This was done with the help of a software called DuCOM-COM 3D. Here, hydration of the concrete is closely studied and a compressive strength predicting model has been proposed.

The models were found to give good predictions of compressive strength. Sugeno type fuzzy inference system performed better under the fuzzy logic approach and the artificial neural network approach mapped the compressive strength outputs with a much better accuracy. The thermodynamic approach also gave very good results for specific cement types and provided a much elaborate analysis for a mechanistic study of concrete properties such as degree of hydration, temperature rise, free water content, porosity and most importantly, stepwise development of compressive strength.

**Keywords:** compressive strength, fuzzy logic, artificial neural network, thermodynamics

## LIST OF TABLES

## LIST OF FIGURES

# LIST OF ABBREVIATIONS

| | |
|---|---|
| EBCS | Ethiopian Building Code of Standards |
| NIST | The National Institute of Standardization |
| ANN | Artificial Neural Network |
| FL | Fuzzy Logic |
| ANFIS | Adaptive Network based Fuzzy Inference Systems |
| FLC | Fuzzy Logic Control |
| FIS | Fuzzy Inference System |
| CA | Coarse Aggregate |
| FA | Fine Aggregate |
| W/C | Water to cement ratio |
| GUI | Graphical User Interface |

# 1. INTRODUCTION

## 1.1 BACKGROUND

Concrete is one of the most common building materials on earth. Its use in virtually all construction sites has made it a loyal companion for mankind. From the ages dating past the Roman Empire, concrete has helped in spearheading the development and expansion of many civilizations.

Concrete is dubbed the 'magical material' not only because what was once a fluid, flowing material turns into a strong, rigid building block; its wide spread availability and affordability, its nature to be molded into any desired shape, its versatility and adaptability, its high compressive strength, stiffness and durability [1] are also its inherent characteristics short of pure magic.

The area in concrete development continues to fascinate many researchers today. The prospects stretch to Reactive Powder Concrete which is still in development. Such concrete has ultra-high strength with a compressive strength range from 200 to 800 MPa [1].

Ethiopia also aspires to make use of the benefits of concrete; carrying out mega-projects using this material as a major building block. This is evident in the country's current commitment in the Grand Renaissance Dam, as well as Gilgel Gibe III, Gilgel Gibe IV. Several previously built bridges, dams etc. also underline such reality.

Hence, it is only logical to lay out a common understanding framework in which people involved in the making and utilizing of concrete could make use of while describing concrete. In this regard, a measure of concrete quality can be used as a benchmark, both while concrete production and construction stages.

Among many of its other characteristics, compressive strength of a concrete is one of the major features to determine its quality. The need to study compressive strength stems from its importance as it directly relates to a certain technical standard requirements. The implication exhibited by compression strength on properties like durability can also be used to the advantage of the structural designer, material engineer as well as other stakeholders in the concrete manufacturing and construction industry. This signifies the need to have a standard measure for the prediction of concrete compression strength.

The usual practice is to take representative samples from the mix and carryout testing in the laboratory. Third and seventh day testing is carried out to know the early-age strength gaining properties of the concrete. Concrete attains the majority of its final strength after 28 days so the samples will have to take that long to be tested. The 28$^{th}$ day testing is also used as a benchmark to compute the compressive strength of concrete at any other given age. Such procedures are the likes of standards specified in design codes.

However, these design codes fail to grasp the real scenario when the concrete constituents are more than the conventional cement, aggregate and water. The compressive strength of concrete is thus complex, becoming more and more intricate as the constituent materials differ.

Furthermore, inter-relationship of concrete constituents at a molecular level cannot be explicitly stated when the type of concrete differs (e.g. high strength concrete, high performance concrete) because unaccounted factors like pozollanic material and super plasticizers come into play. In such cases, the empirical relationship given in codes fails to grasp the real scenario as factors like 'effect of plasticizers', 'casting temperature' etc. get a chance to affect the outcome of the compressive strength.

In fast track projects where 28-day test results are not to be waited for, a sound and reliable model capable of determining the compressive strength of a concrete sample at any age is important. This can avoid the time spent on waiting for laboratory results, which can be interpreted in auspicious monetary values due to speedy construction.

Therefore, alternative approaches need to be sought for. The applications of these alternative approaches must be discussed and their areas of applications explored.

## 1.2 RESEARCH SIGNIFICANCE

This research has benefits both to the construction industry and the research community. It introduces new methods as a way to solve problems in civil engineering. These new methods, if properly utilized, have the potential to save time and cost which would otherwise be squandered using the conventional approaches.

This research can shed light on the contemporary approaches being used today, to solve problems in civil engineering. Introduction of these methods will thus empower the engineer with new and better tools while modelling and computation.

As this research affirms giving due attention to reaction mechanisms in concrete at a molecular level, pursuing it can facilitate a favorable environment for the study of modification of concrete properties.

Structural models making use of the strength development patterns of concrete, computed through this research can also make use of prediction models forwarded by this research. A thermodynamic study is important for durability analysis of massive concrete structures as it can give a good picture of the temperature rise in concrete. Hence, thermal cracking of (especially) massive concrete structures can somehow be mitigated.

## 1.3 OBJECTIVE

### 1.3.1 General Objectives

The general objectives of this thesis include:

- Introduce the concepts of the major compressive strength predicting methods; namely, Empirical, Artificial Intelligence and Mechanistic approaches.
- Introduce Artificial Intelligence methods as an alternative to solving other problems in Civil Engineering.

### 1.3.2 Specific Objectives

The specific objectives of this thesis include:

- To come up with compressive strength predicting models using regression analysis, fuzzy logic, artificial neural network and thermodynamic methods.
- To critically analyze each model with regards to applicability and performance.

## 1.4 SCOPE OF THE RESEARCH

This thesis focuses on the compressive strength computation of "normal strength concrete" with OPC type cement, water and aggregate as the main ingredients. The effects of admixtures as well as pozzolanic materials such as fly ash and blast furnace slag have not been considered. However, these effects will be separately studied in brief, in the thermodynamic method. Furthermore; particle shape and surface texture, fineness of cement, type of sand, specific gravity and related matters are not considered.

Testing for compression strengths is assumed to take place with the same laboratory conditions for all the samples. Laboratory tests carried out for differing sample sizes have also not been considered. All test samples are cubes with a dimension of 150mm.

## 1.5 METHODOLOGY

The compressive strength prediction of concrete will be studied after a thorough revision of current trends.

The compressive strength of concrete will be modelled according to multilinear regression, fuzzy logic, artificial neural network and thermodynamic methods. The modelling process will make use of concrete compression test results obtained from laboratory experiments.

After the modelling process, results from these methods will be compared with the use of error portraying parameters. Comparison of the models will be made and areas of application for both the construction industry and the research community will be suggested.

## 1.6 STRUCTURE OF THE PAPER

The structure adopted in this thesis is portrayed in its contents. There are four major chapters included in this thesis. Chapter one deals with introduction of concrete, its significance as a major building material and discusses some of the major approaches to predict its compressive strength.

From the discussed approaches, three, namely statistical methods, artificial intelligence methods and thermodynamic methods are further investigated in the literature review (Chapter two). Works done by several researchers are used to lay the foundation for assessing the theoretical principles behind these approaches.

Concrete compressive strength predicting models are produced in chapter three. Several models using each of the three prime approaches are presented here using two separate data sets.

Chapter four will discuss the findings and compares the outputs of the predicting models with respect to their performance (error measurements). The applicability of each model, along with advantage and disadvantage of each model will also be discussed before conclusions can be drawn and recommendations for future work are made.

# 2. LITERATURE REVIEW ON COMPRESSION STRENGTH, AND COMPRESSION STRENGTH PREDICTION METHODS OF CONCRETE

## 2.1 CONCRETE

Concrete is a stone like material obtained by permitting a carefully proportioned mixture of cement, sand and gravel or other aggregate, and water to harden in forms of the shape and dimensions of the desired structure [2]. The term concrete has a Latin ancestry. It is derived from the word "*concretus*" (meaning compact or condensed), from "*con-*" (together) and "*cretus*" (to grow) [3].

Concrete's recent progress, coupled with its dexterity while usage with steel has granted it preference over other construction materials. Many buildings today make use of this dexterity offered by concrete.

One most important element in the make-up of concrete is cement. From its omnipresence as early as 300 BC in the Roman Empire [3] while building the Coliseum and Pantheon, cement still continues to dominate today. This is because of the role it plays in concrete. A simple manipulation in the clinker composition allows the cement, thereby the concrete, to assume any desired property. This capacity of concrete to morph into different types; owes greatly to the type of cement, in addition to the composition of constituent materials.

As cement production is not the main focus of this thesis, the whole process in the cement kiln and what happens at those high temperatures is not discussed. However, among the different constituents of concrete, this ingredient is given more weight as it is believed to contribute the lion's share in concrete properties. This contribution is also dealt with in thermodynamic approaches.

### 2.1.1 Classification of Concrete

**Normal Concrete:** This concrete is 'normal' as it is comprised of the conventional ingredients (aggregate, water and cement). It is also called normal weight concrete or normal strength concrete. It has a setting time of 30-90 minutes depending on moisture in the atmosphere, fineness of cement etc. The common strength value is 10MPa to

40MPa. At about 28 days 75-80% of the total strength is attained. Ninety five percent of the strength is achieved at almost 90 days [1].

**High Performance Concrete:** This mix has the following main properties: high strength, high workability, high durability, ease of placement, compaction without segregation, early age strength, long life in severe environments. The water to cement ration in this type of concrete can go as low as 0.25.

**High Strength Concrete:** Such concrete type is defined by ACI as a concrete with compressive strength greater than 6000 psi (41 MPa). This type of concrete requires a very low water to cement ratio during mix. It is usually made by having water to cement ratio of 0.35or lower. Creating this mix necessitates the use of plasticizers to maintain workability. Such concrete mix is also liable to quality compromise which highlights the need of a high level of control during production, transportation and placement.

**Air Entrained Concrete:** One of the triumphs in the field of concrete technology. It is used where the concrete is vulnerable to freezing and thawing action. Air entrained admixture is introduced into the concrete mix. Despite its lower strength as compared to the normal concrete, the air entrainment helps mitigate the uncertainty caused by the water inside the concrete mix as it freezes and expands.

**Light weight concrete:** This concrete type has a substantially lower mass per unit volume than the concrete made of ordinary ingredients. Its major advantage is reducing dead loads; it can be used in places where loads need to be minimized.

**Self-compacting concrete:** The concrete where no vibration is required. The concrete is compacted due to its own weight. It is also called self-consolidated concrete or flowing concrete. It can also be categorized as high performance concrete as the ingredients are the same, but in this type of concrete workability is increased. This concrete is characterized by extreme fluidity which means no vibrators are required, its placement is easier, aggregate segregation is also not present. It is used in locations unreachable for vibratos such as underground structure, deep wells etc. This saves a significant amount of labor cost, reduces wear and tear on formwork and also has faster pouring time [1].

### 2.1.2 Compressive Strength of Concrete

Generally, the term *concrete strength* is taken to refer to the uniaxial compressive strength as measured by a compression test [4], obtained from cylinders with a height to diameter ratio of 2 to 1 or from cubes of usually 150mm. Cubes are used in Great Britain, Germany and many other countries in Europe. Cylinders are the standard specimen in the United States, France, Canada, Australia, and New Zealand. In our country, tests are made on both cubes and cylinders but testing using cubes is usually practiced.

Such tests are measures of the response of the concrete to a uniaxial compressive strength, and are the most common of tests on hardened concrete because of the following [5]:

- It is commonly assumed that most of the important properties of concrete are directly related (at least qualitatively) to the compressive strength.
- Since concrete has very little tensile strength, it is used primarily in a compressive mode, and therefore it is the compressive strength that is important in engineering practice.
- The structural design codes are based mainly on the compressive strength of concrete.
- The test is easy and relatively inexpensive to carry out.
- Most of the quality control and compliance criteria in standards and specification adopt compressive strength as primary criteria.

### 2.1.3 Prediction of Compressive Strength

There are several methods of compressive strength prediction methods. Some of the major methods, employed by many researchers around the world are discussed below.

#### *2.1.3.1 Empirical Methods*

Empirical methods try to directly depict the experiment process into a certain relationship. The relationship is a measure of the constituents' role in producing the final outcome. They usually rely on rigorous experimental analysis so that the produced relationship is able to fit the outcomes in the laboratory. While predicting compressive strength, most empirical relationship try to relate the strength to the water cement ratio, as the two almost always have an inverse relationship. In other cases, the models make use of an already known compressive strength and apply empirically computed coefficients to relate the known compressive strength with the required compressive strength.

For example, for a mean temperature of 20°C and curing in accordance with EN 12390, the compressive strength of concrete at various ages $f_{cm}(t)$ may be estimated from expressions below [6].

$$f_{cm}(t) = \beta_{cc}(t)\, f_{cm} \qquad (2\text{-}1)$$

$$\beta_{cc}(t) = exp\left\{ s\left[ 1 - \left( \frac{28}{t} \right)^{1/2} \right] \right\} \qquad (2\text{-}2)$$

Where:

| | |
|---|---|
| $f_{cm}(t)$ | is the mean concrete compressive strength at an age of *t* days |
| $f_{cm}$ | is the mean compressive strength at 28 days according to Table 3.1 [6]. |
| $\beta_{cc}(t)$ | is a coefficient which depends on the age of the concrete t |
| *t* | is the age of the concrete in days |
| *s* | is a coefficient which depends on the type of cement: |

= 0.20 for cement of strength Classes CEM 42.5 R, CEM 52.5 N and CEM 52.5R (Class R[1])
= 0.25 for cement of strength Classes CEM 32.5 R, CEM 42.5 N (Class N[2])
= 0.38 for cement of strength Classes CEM 32.5 N (Class S[3])

Where the concrete does not conform with the specification for compressive strength at 28 days the use of expressions (2-1) and (2-2) is not appropriate. The compressive strength at a time (t) is then computed as a function of 'age dependent coefficient' multiplied by the mean compressive strength at 28days. This age dependent coefficient takes into account the age of concrete (in days) and the type of cement class (Class R, N or S) [6]. Such empirical relationship can only work if the mean compressive strength used is at 28days.

Empirical methods give a better feeling of the final outcome as interactions between constituent materials can be studied. However, they may take a considerable amount of time compared with other available methods especially if the model sought for is

---

[1] Rapid Hardening High Strength Cements
[2] Normal and Rapid Hardening Cements
[3] Slow Hardening Cements

subject to intricacy due to a larger number of input parameters. Their application may also be limited to certain specific cases in which coefficients were set or experiments were carried out.

#### *2.1.3.2 Computational Modelling*

Finite element analysis is based on complex thermodynamic equations. Such modelling is usually computer-aided endeavor. They rely on a correct representation of the concrete microstructure. Such endeavor entails randomly casting the cement in a unit cell space, to effectively represent the hydrations (and other mechanisms) of the varying particle sizes in the cement using a computer simulation (pixel based). The mechanisms may also be encoded empirically, after calibration against experimental information.

#### *2.1.3.3 Mechanical Modelling*

Mechanical modelling entails a representation of the parameters as a combination of two features, namely the spring and the dashpot. While employing such principle to predict the compression strength of concrete, the usual approach is to consider the cement matrix as the spring and the time element (age of testing) as the dashpot [7]. The accuracy with the model decreases when the model is checked against testing dataset. Furthermore, the dashpot component negatively affects the outcome of the compressive strength especially at earlier ages.

#### *2.1.3.4 Statistical Methods*

Statistical methods make use of experimental data and employ mathematical equations to best describe the relationships between inputs and outputs. The most known statistical method is the multilinear regression technique. Statistical methods may be easy to understand and even easier to use, but their reliance on data can sometimes handicap a user. They also perform inferior compared to the other available methods and depend on the type of mathematical function chosen to fit the data.

#### *2.1.3.5 Artificial Intelligence*

The Webster's New World College Dictionary, defines artificial intelligence as the capability of computers or programs to operate in ways to mimic human thought process, such as reasoning and learning. This may bring one to inquire about the type of problems requiring computers to mimic the human brain. These include inference based on knowledge reasoning with uncertain or incomplete information, various forms of perception and learning, and applications to problems such as control, prediction, classification, and optimization [8]. In civil engineering problems, they can be used to model a phenomenon when the mechanism is not fully understood.

Examples of AI methods include neural networks and genetic algorithms, which bear resemblance to microscopic biological models in structure (artificial neural networks analogous to the one in the brain) and in performance (genetic algorithms analogous to genes: the computer's program components 'mutate', produce better and better solutions as they adapt). Other relatively contemporary forms of AI include fuzzy systems and Adaptive Network based Fuzzy Inference Systems (ANFIS). ANFIS features combination of artificial neural networks and fuzzy systems. A network obtained in such manner has an excellent ability of training by means of neural networks and linguistic interpretation of variables via fuzzy logic [9].

Artificial Intelligence methods are powerful in terms of their capacity to learn and produce appropriate models even for a vastly ranging information. However, this information must be enough so that a 'close to reality' inference can be made.

### 2.1.4 Factors affecting compressive strength values

The compressive strength of concrete at an age t depends on the type of cement, temperature and curing conditions; among some. (EBCS EN 1992-1-1:2013). Furthermore, testing and measuring procedures may affect the outcome of the final compressive strength. Such disparity arising in the compression strength is summarized in Table 1 [5].

Table 1 Variations in Compressive Strengths of Concrete [5]

| No. | Variation due to the properties of concrete | No. | Variation due to the testing methods |
|---|---|---|---|
| 1 | **Changes in w/c ratio caused by:** | 1 | **Improper sampling procedures** |
| | Poor control of water | | |
| | Excessive variation of moisture in aggregate or variable aggregate measurement. | | |
| 2 | **Variation in water requirement caused by:** | 2 | **Variation due to fabrication technique** |
| | Changes in aggregate grading, absorption, particle shape | | Handling, storing, and curing of newly made cylinders |
| | Changes in cementitious and Admixture properties | | Poor quality, damaged or distorted molds |
| | Change in air content | | |
| | Delivery time and temp. changes | | |
| 3 | **Variation in characteristic and Proportions of ingredients:** | 3 | **Changes in curing** |
| | Aggregates | | Temperature variation |
| | Cementitious materials | | Variable moisture control |
| | Admixtures | | Delays in bringing cylinders to the lab. |
| 4 | **Variation in mixing, transporting** | 4 | **Poor testing procedures** |
| | Placing and consolidations | | Specimen preparation |
| | Variation in concrete temperature and curing | | Test procedures |

## 2.2 REGRESSION ANALYSIS

Regression analysis is deemed a major aspect of statistical approach of modelling technique. Zain et al. [10] highlighted the use of statistical approach over other techniques in their relative ease of computing coefficients which can also be interpreted with regard to time saving. However, such approach is often complex and circuitous, particularly for non-linear relationships [11]. This element of their feature is temporarily shunned in this section. Statistical models are mathematically rigorous and can be used to define confidence interval for the predictions. Furthermore influence of the major ingredients on the output can be observed by carrying out correlation analysis.

The performance of each regression equation can be assessed using a parameter called $R^2$, also known as correlation coefficient. $R^2$ is the predicting power of a model. It is a measure of the capacity of the model to explain the variability in the output due to the variability in the input values. It ranges from 0 (when the estimated regression model explains none of the variation in Y) to 1 (when all points lie on the regression line).

Zain et al. [10] introduced slump test results and density of concrete, in addition to the mix proportions of the constituent materials for predicting the compressive strength of high performance concrete. This was done to get a better representation of the strength gaining process for the different ages of testing. Introducing those independent variables gave proved to improve the final multi-variable power equation, with a correlation coefficient reaching 99.99%. Mahmoud [7] also forwarded his statistical compressive strength predicting model and found good correlations with experimental results. His model focused on forwarding an aid for designing concrete mixes so the inputs were generalized according to a predetermined matrix mixture.

The ease in modelling, compounded by the relatively smaller amount of time needed, has long made regression methods appealing. However, as the non-linearity between reactants and products increases (which is usually the case in concrete), the predicting power of each regression model highly subsides. This is visible in Subasi's research [12], when he tried to compare this technique with artificial neural network method and found the latter to give much better predictions.

## 2.3 FUZZY LOGIC

The concept of fuzzy logic was first introduced by Lotfi Zadeh [13]. As a pioneer of the fuzzy logic concept, which has revolutionized the way humans think about modelling the world around them, he has laid the groundwork for the development of many fuzzy inference system methodologies including Mamdani, Takagi and Sugeno.

### 2.3.1 Theoretical Background

Fuzzy logic is determined as a set of mathematical principles for knowledge representation based on degrees of membership rather than on crisp membership of classical binary logic [14]. This differs a great deal with the classical Boolean logic which has logical values of either 'completely false' (=0) or 'completely true' (= 1). The Boolean logic represents knowledge with clear demarcations (such as black or white).

More often than not, one finds reality to be completely different. The parameters within a set are seldom defined in pure black and white as there may exist an element with some degree of belongingness to both sets; usually labeled as the gray area. For example, one may have the data of ten people in a set categorized as 'tall' ranging from 1.75m to 2.20m and 'short' ranging from 1.50m to 1.74m. The category 'tall'; if crisp sets were to be used to describe these people, would give equal recognition for the person with a height 1.75m or 2.1m. The same is true for the members in the 'short' set. In other words, a person with a height of 1.74m or 1.75m is not rightly represented in the set. At such instances, consideration of a crisp set could be deemed weak. Such concept of dichotomy was also summarized by Witold Pedrycz and Fernando Gomide as 'painfully simplified' and 'in many circumstances, lacking rapport with reality' [13].

The above crisp set can be modeled with a stronger, better representation using fuzzy sets. A fuzzy set is a class of objects with a continuum of grades of membership, as defined by Zadeh [13]. Such as set is characterized by a membership (characteristic) function which assigns to each object a grade of membership ranging between zero and one.

A membership function is the relationship between the values of an element and its degree of membership in a set. A vehicle that quantifies different degrees of membership, it should be reflective of the problem at hand for which we construct fuzzy sets [13]. Triangular and trapezoidal membership functions are most commonly used but selection depends on the level of detail we intend to capture.

**Triangular membership functions**: Are the simplest possible models of membership as they are fully defined by only three parameters [13]. They can be described by their piecewise linear segments shown in equation (2-3) [15].

$$A(x, a, m, b) = \begin{cases} 0, & if\ x \le a \\ \dfrac{x-a}{m-a}, & if\ x \in [a,\ m) \\ \dfrac{b-x}{b-m} & if\ x \in [m, b] \\ 0, & if\ x \ge b \end{cases} \qquad (2\text{-}3)$$

Where:

X is defined within the set of real numbers R

a and b are the lower and upper bounds respectively[4]

m = typical value of the fuzzy set

Figure 1 shows a typical triangular membership function bound between 2 and 6. As the values of the fuzzy set digress from 4, one can see the degree of belongingness to the set decrease linearly both to the left and right, ultimately to zero.

[4] The extreme elements of the universe of discourse that delineate the elements belonging to A with non-zero membership degrees.

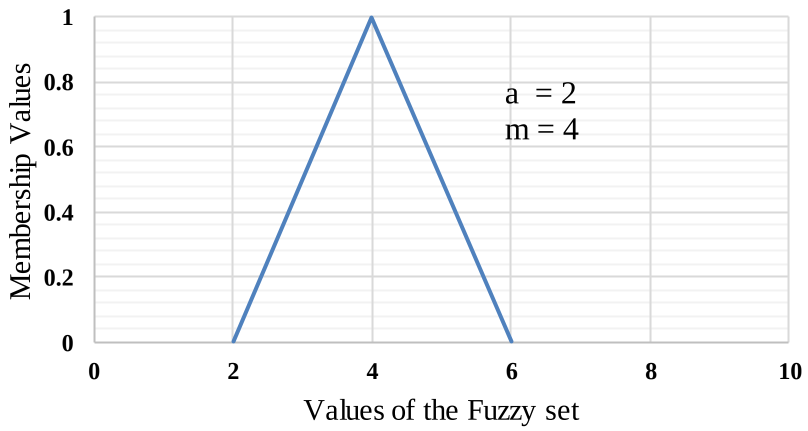


Figure 1- Typical triangular membership function [15]

**Trapezoidal membership functions:** They bear almost similar form as triangular membership functions with an additional parameter describing the change in shape. Their piecewise linear function is described in equation (2-4) as [15]:

$$A(x, a, m, n, b) = \begin{cases} 0, & if\ x \le a \\ \dfrac{x-a}{m-a}, & if\ x \in [a,\ m) \\ 1, & if\ x \in [a,\ n) \\ \dfrac{b-x}{b-m} & if\ x \in [n, b] \\ 0, & if\ x \ge b \end{cases} \qquad (2\text{-}4)$$

Figure 2 shows a typical trapezoidal membership function. Unlike the previous membership function, one can see the full belongingness of fuzzy set values around four.

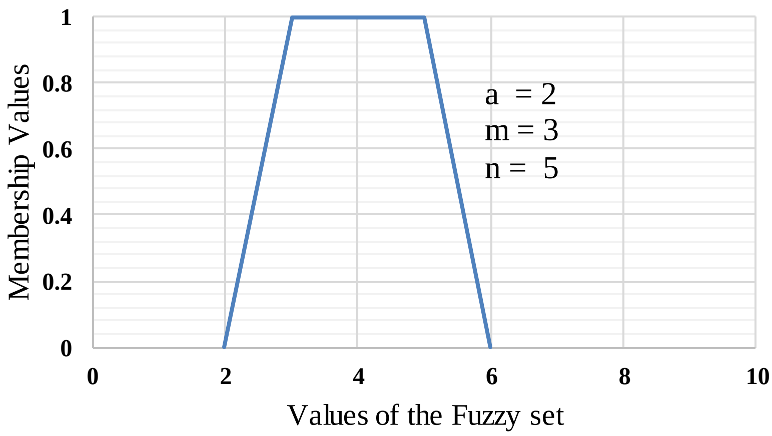


Figure 2- Typical trapezoidal membership function [15]

**Gaussian membership functions:** These membership functions are described by the equation (2-5) [13].

$$A(x,m,\sigma) = \exp\left(-\frac{(x-m)^2}{\sigma^2}\right) \qquad (2\text{-}5)$$

Where:

m = typical value of the fuzzy set

σ = denotation of the spread of A[5]

Figure 3 shows a typical membership function with m=4 and varying spread values. One can see that as the value of the spread increases, the nature of the Gaussian membership function changes. It is therefore up to the user to choose a fitting representation of their system.

[5] Higher values of σ correspond to larger spreads of the fuzzy sets

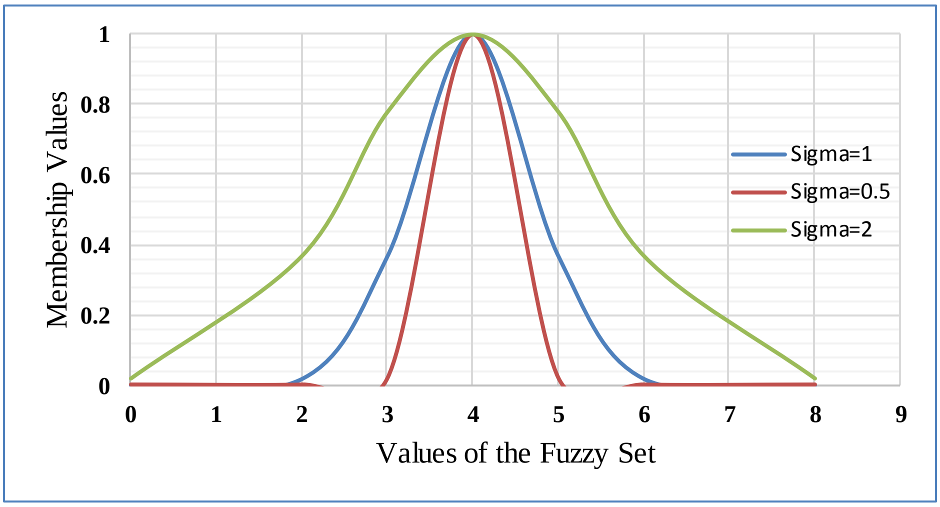


Figure 3- Gausiian membership functions with varying sigma values [15]

The degree of membership introduced in fuzzy sets allows one to give recognition to the members of the set. Varying the membership values within the set, a fuzzy set could be used to express the ten people in the previous example as short, very short, tall and very tall. Each members in the set would be given different weights, according to 'how tall' or 'how short' the individual is. The higher a membership value signifies a higher degree of belongingness of an element within a set. A person with a height of 1.75m will therefore not be given equal consideration as a 2.1m tall person.

Fuzzy sets offer an important and unique feature of describing information granules whose contributing elements may belong to varying degrees of membership (belongingness). This helps us to describe the concepts that are commonly encountered in real world. The notions, such as low income, high inflation, small approximation error, and many others, are examples of concepts to which yes-no quantification does not apply or becomes quite artificial and restrictive.

This classification of sets is very powerful because different data encompass significantly large amount of vagueness. Reasoning: the special feature of human beings can therefore be applied to some degree if a fuzzy set theory was to be used. The theory differs from probability theory which was deemed as the only measure of uncertainty until recently.

These two theories describe different kinds of uncertainty. Probability theory deals with expectation of future event, based on something known now while fuzzy set theory deals with uncertainty resulting from imprecision related to linguistic terms (e.g., wet, very wet, rapidly increasing etc.) or from measurement uncertainty.

Furthermore, probability is theory of random events; based on an event that can be repeated numerous times to generate a probability distribution function while fuzzy set theory is not concerned with events, but rather concepts; as it does not require an event to be repeatable- it just describes extent to which event matches the meaning of concept [15]. Probability theory involves crisp set theory and therefore, partial membership in a class is not entertained, only the frequency or the likelihood of an element belonging in a certain class. Fuzzy set theory deals with the similarity of an element to a class.

Fuzzy logic control is a powerful mathematical tool used to model non-linear systems and to develop complex controllers. Each ingredient in the make-up of concrete plays its role individually, as well as reacting with the other ingredients. This will create non-linearity with ingredient composition versus final compressive strength. This non linearity can be mitigated with the use of FLC as such control is used when the complexity of a system preludes the application of other modelling techniques. Due to their use of imprecise information, FLC applications tend to generate so-called expert and intelligent systems [13].

The basic concepts which underlie fuzzy systems are those of linguistic variable and fuzzy IF-THEN rule. A linguistic variable, as its name suggests, is a variable whose values are words rather than numbers, e.g., small, young, very hot and quite slow [15]. Fuzzy IF-THEN rules are of the general form: if antecedent(s) then consequent(s), where antecedent and consequent are fuzzy propositions that contain linguistic variables.

A fuzzy IF-THEN rule is exemplified by "if the temperature is high then the fan-speed should be high". With the objective of modeling complex and dynamic systems, FRBSs handle fuzzy rules by mimicking human reasoning (much of which is approximate rather than exact), reaching a high level of robustness with respect to variations in the system's parameters, disturbances, etc [13]

A fuzzy inference system (FIS) is a system that uses fuzzy set theory to map inputs (features in the case of fuzzy classification) to outputs (classes in the case of fuzzy classification). While using computers, the use of fuzzy expert systems (FES) to simplify fuzzification and the subsequent processes is opted for. Emulating human reasoning attribute, FES can be designed for knowledge based (where expert rules are used to produce fuzzy expert rules) or data based (where data obtained will be stored for each specific task of expert system) [13].

Knowledge based rule system makes use of expert knowledge to create rules and membership functions. This system requires that rules be accurately defined but once rules are set, modelling can be carried out even with a few amount of data. Data based rule system is a data-driven technique to create membership functions. This method depends on the amount of data to create a good inference; so that problems like overfitting can be avoided [13].

The fuzzy inference systems applied in this thesis are of Mamdani and Sugeno types. Both will be discussed briefly here, as their approach to predicting the compressive strength (output value) varies.

### 2.3.2 Steps in developing FL models

Using Mamdani inference system, one must go through these steps to compute the output.

Step 1: Determining a set of fuzzy rules: This is where input and output variables are defined. The user may input a crisp value (a number) or a linguistic term. These rules are usually in the form: 'if (antecedents) then (consequents)'. The antecedents and consequents would have to be membership functions so that fuzzy rules can be created. In the case of a data driven system, the antecedents and consequents may take the form input and output values respectively. The fuzzy rules obtained for the prediction of compressive strength are of the form:

If ***(cement = a)*** and ***(water = b)*** and ***(coarse aggregate = c)*** and ***(fine aggregate = d)***, then ***(compressive strength = Y).***

Fuzzy rules with a total number equaling the amount of instances were created accordingly, for development of the prediction model.

Step 2: Fuzzifying the inputs using the input membership functions: Fuzzification enables inputs to be mapped to values from 0 to 1 using the set of input membership functions. These membership functions are capable of representing vague concepts where fuzzy rule based system of modelling is applied.

The following steps (implication, aggregation and defuzzification) take different routes in Sugeno type as they are fixed and cannot be edited in the fuzzy logic toolbox. The implication method is simply multiplication, and the aggregation operator includes all of the singletons [16].

Step 3: After giving respective weights to the fuzzy rules, the fuzzified inputs are combined according to the fuzzy rules to establish a rule strength. The concepts "and", "or", and "not" are utilized here. These are differentiated in terms of the users desire to minimize or maximize the output.

A simple computation of "and" is achieved by taking the minimum of the membership values involved [13].

Step 4: Combining the consequences to get an output distribution (Aggregation)

Step 5: Defuzzifying the output distribution. Where Mamdani fuzzy type is used, outputs are in the form of fuzzy sets. However, the output is a crisp value when Sugeno-type fuzzy inference is used. This output may have a form: 'if x is A and y is B, then z = k' for a typical fuzzy rule in zero-order model or 'if x is A and y is B then z = p*x + q*y + r' for the more general first-order Sugeno fuzzy model. There are also higher models; but they add too much to the intricacy of the model, less to the accuracy of the output and are not supported by the fuzzy rule toolbox.

Matlab software has been utilized to carry out the computer analysis for Mamdani and Sugeno type fuzzy inference systems. The whole process can be carried out using the fuzzy inference engine provided on Matlab, shown in Figure 4 [16].

.

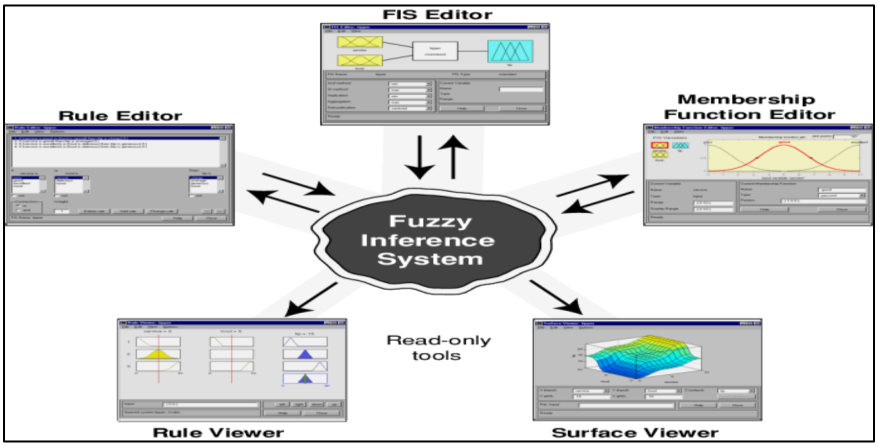


Figure 4- Matlab FIS Engine

As it is shown in the figure, the fuzzy inference system supported on Matlab has Editing tools and Read-Only tools. The editing tools are used during the modelling process. In general, the FIS Editor allows the user to edit the model parameters. The membership functions of the input and output (only for the case of Mamdani FIS) are edited by the Membership Function Editor. The Rule Editor allows the user to omit, add, or give the rule weights for the model.

The Rule and Surface viewer are aids for interpreting the model outputs. The surface gives general information about the parameters affecting the model's behavior while the rule viewer shows the process while arriving to a final crisp output.

### 2.3.3 Application of Fuzzy Logic in Civil Engineering

Fuzzy logic has played a key part in solving civil engineering problems. Its use in predicting the compressive strength of different types of concrete was given a special attention here in relation to the objective of this thesis. In this regard, several researchers have found this tool to be effective for the prediction of compressive strength of concrete [17], [18], [19], [20], [21].

Apart from its use in modelling of predictions, its application as a controller in drip irrigation was a recent one; on its way to realization is under study in School of Electrical Engineering of Addis Ababa Institute of Technology.

Fuzzy Logic is also applicable in models for seismic reitrofaction of building; performance evaluation of reinforced concrete structures, design of truss structures etc. Specific reference has not been made here as the methodologies for such study has not been investigated.

Aggarwal et al. [17] tried to predict the compressive strength of self-compacting concrete (at 28 days) using fuzzy logic and found results within $\pm 20\%$ of perfect agreement. The analysis was carried out using 60 samples obtained from different literatures. The Sugeno type fuzzy inference system was used with triangular membership functions ranging from four to nine. Perhaps one possible area of challenge is the data set used by the authors. The data is obtained from four different literatures, which may become the source of disparity in the final outputs if the nature of the constituent materials of the concrete varies. Root mean squared error was chosen as a measure of 5.626 and a mean absolute error of 4.885. Sugeno type FIS has been effective in producing an accurate compressive strength model. The model could not be further perfected as the data source used for the model was a combination of different sets with possibly different testing conditions.

Özcan et al. [22] compared the results of artificial neural network and fuzzy logic models for prediction of long-term compressive strength of silica fume concrete. Their approach was better which incorporated on meticulous description of the experimental work. Aggregate and it's grading, including chemical composition of the cement and silica fume used was addressed for the output of the 3, 7, 28, 180 and 500 day compressive strength datasets. The fuzzy rule base algorithm made use of six inputs[6] with triangular and trapezoidal membership functions ranging from 3 to 9. The FL model outputs predicted the compressive strength with $R^2$ of 0.9274.

Attempts were also made to see if these methods (including the utilization of artificial neural networks) gave a fair reflection of the effect of inclusion of silica fume on compressive strength. The simulation results showed that silica fume enhanced the short term compressive strength (up to 28 days) by 20% - 50% compared to the control concrete of Portland cement. This confirms with the reality (other things constant); that the early day compressive strength is actually enhanced by the presence of silica fume, as described by Des King [23]. Further discussion on the mechanisms is not addressed in this thesis.

Similar pursuit was undertaken by Topcu et al. [18], using fuzzy logic and artificial neural networks. The fuzzy system model incorporated a Sugeno type inference, with triangular membership functions obtained from clustering of the training data set. Results obtained were 'in harmony' with the experimental results. It was shown that the models were able to reproduce experimental results with a fairly higher accuracy, with R-squared values of 0.9769 and 0.9549 for the training and testing data sets respectively.

[6] Amount of cement, silica fume replacement, water, plasticizer, aggregate and age of samples

## 2.4 NEURAL NETWORK

### 2.4.1 Theoretical Background

Neural network is part of the revolutionary change in the mindset of human beings towards solving problems. In the continued effort towards extending machines' somewhat confined use in muscle works to intelligence works; neural network has been at the forefront, ever since the work on artificial intelligence started in the fifties.

There are several definitions of artificial neural networks. They resemble to the biological neural networks in processing and producing data. The axon, dendrites, and synapses are analogous to outputs, and weights respectively. Sometimes the common element, the neuron, is labeled as a 'processing element' in artificial neural network. Yeh I [21] succinctly described artificial neural networks as a family of massively parallel architectures that solve difficult problems via the cooperation of highly interconnected but simple computing elements (or artificial neurons).

Neural networks can range from a perceptron; which is a direct mapping of inputs to outputs, to multi-layered networks with different types of activation functions. A better understanding of artificial neural networks is achieved through classification of its types. Several methods of classification exist as shown below, depending on the behavior of the network, how the network behaves in circumstances, etc. [8]

i. **Topology of the network architecture**: According to this type of classification, the network architecture can be described as multilayered or non-multilayered. Multilayered network is characterized as one having distinct layers such as input, hidden and output layers. Furthermore, the neurons are connected with the adjacent neurons and no connection between neurons of the same layer exists. The opposite is true for a non-multilayered network architecture.

**ii**. **Direction of output:** Depending on whether the values of the output are submitted back into the network, one can have a 'recurrent (feedforward and feedbackward)' or a 'non-recurrent (feedbackward)' architecture. In a non-recurrent system, the input values propagate into the hidden layers and outputs of the hidden neurons become input values to the output layer. Here backpropagation may be applied to correct the weights. This differs greatly with a 'recurrent' system because in recurrent system; it is the outputs that can propagate backwards not the weights.

**iii.** **Form of learning**: A network might carry out the modelling process, carrying out predictions and verifying the predicted outcomes with actual outcomes already stored. Such is known as supervised learning and a good example is the backpropagation (to be discussed later). Where there is no answer already known for verification purposes; the model can also be of unsupervised learning, which depends on a given criteria to adjust itself internally.

**iv**. **Forms of activation functions:** Linear, step, sigmoid etc.

A sigmoid function gives a better result within the modelling process in neural networks, especially because softening the threshold, a gradual transformation from -1 to +1. Such smooth function is in the form of equation (2-6).

$$S(t) = \frac{1}{1+e^{-t}} \tag{2-6}$$

In the following section, selection of the type of ANN systems for a typical compressive strength predicting model will be discussed. A perceptron lacks potential where there is non-linear relationship (as is the case with the pursued predictive model) so attention has been diverted to treating multi-layered (other than the input and output layers) networks.

Moreover, in multi-layered networks, there is an input layer where the data is presented to the neural network, and an output layer that holds the response of the network to the input [21]. The inputs are transferred through weighted connections into the intermediate (hidden) layers for processing. The weights are subject to change (iteratively) according to the error observed at the final output. This process is usually backpropagation. When the error is low enough, the final outputs mark the completion of the iteration.

Backpropagation is a training procedure introduced by Rumelhart et al. [24] which repeatedly adjusts the weights of the connections in the network so as to minimize a measure of the difference between the actual output vector of the net and the desired input vector. In feed-forward neural networks, such procedure consists in an iterative optimization of a so called error function representing a measure of the performance of the network shown in equation (2-7). This error function is the mean square sum of differences between model output values and target values [25].

$$E = \frac{1}{2}\sum_{p=1}^{P}\sum_{j=1}^{N_l}\left(t_j - a_j\right)^2 \qquad (2\text{-}7)$$

A typical multilayered feed-forward neural network system (with one hidden layer) is shown in Figure 5. The network has four input nodes (1, 2, 3 and 4), four hidden layer nodes (6, 7, 8 and 9) a bias (5) and one output node (10).

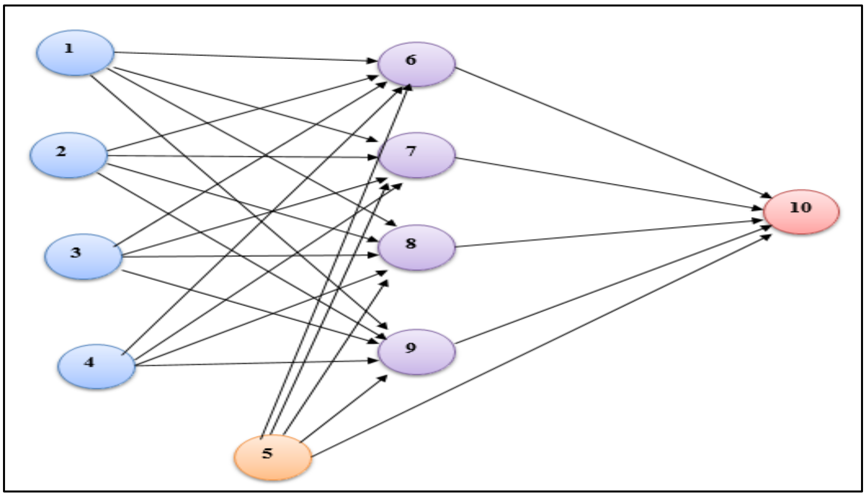


Figure 5- A typical multilayered feed-forward neural network system

The choice of the number of hidden neurons is arbitrary. Usually a smaller number of neurons is selected and then increased according to the error observed. However, some researches propose methods to help improve selection process. For 'n' number of input neurons with 'm' output neurons; Tang and Fishwick (1993) propose as many as 'n' number of hidden neurons. There are also other proposals made by different papers: Gallant [26] uses twice the number of input neurons; Nagendra [11] uses the summation of input and output neurons while Dias [27] was content with only the number of input neurons etc. Anyone can adapt their own methodology in choosing the number of hidden neurons, but such choice must be justified by an appropriate error measurement and the model's capacity to generally work on incidents outside of the training set.

The simplified procedure for using neural networks is shown in Figure 6 [15].

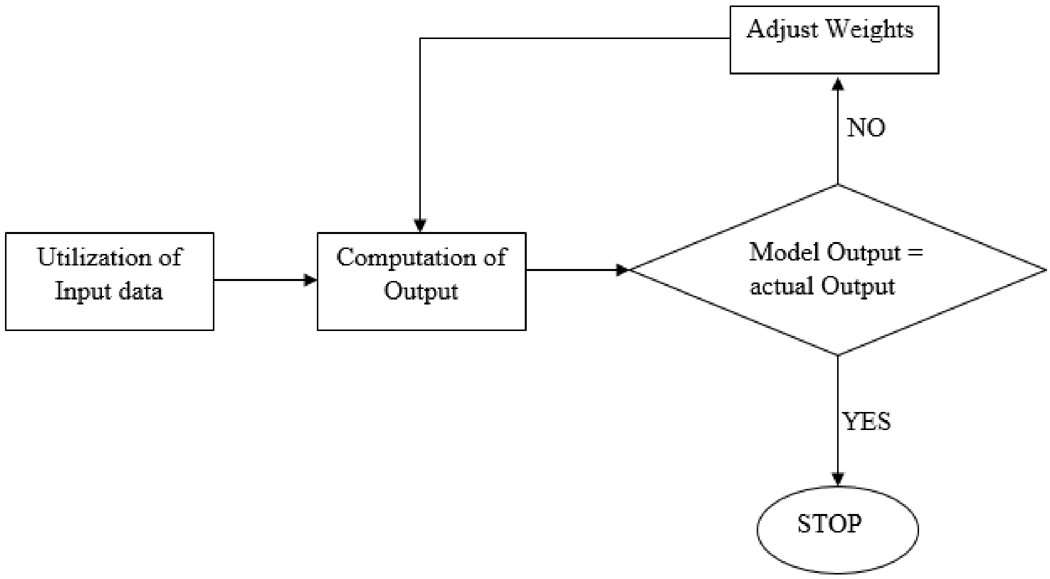


Figure 6- Simplified flowchart for modelling using Neural Network [15]

### 2.4.2 Application of Artificial Neural Networks in Civil Engineering

ANNs have been applied to the detection of structural damage, structural system identification, modeling of material behavior, structural optimization, structural control, ground water monitoring, prediction of settlement of shallow foundation, and concrete mix proportions [18].

When looking at their application in prediction models; Aggarwal et al [17] tried to also predict the compressive strength of self-compacting concrete using artificial neural networks to complement their work in fuzzy logic. The ANN model carried out 500 iteration with 6 hidden neurons in the hidden layer. Their results showed a similar success, with similar error-measurements.

The resulting model predicted the strength with $R^2 = 0.9767$, showing a better result than the one obtained using fuzzy logic. The chosen ANN architecture had a single hidden layer with 11 hidden neurons. Topcu et al. [18] found accuracy of their model increase when adding another hidden layer. The absolute percentage error found was minimum (=0.000515) at ANN architecture of 2-hidden layers with nine and eight neurons at the first and second hidden layer, respectively.

The use of multiple layers was also applied in Subasi's ANN model [12]. His model also gave due attention to the material aspect in which chemical analysis results of fly ash, gradient and chemical compositions of sand were employed. The prediction model showed a good result with $R^2 = 0.9557$ for compressive strength and 0.9119 for flexural tensile strength.

In addition to assessing the effect of silica fume, Özcan et al.'s compressive strength predicting model [28] also addressed the effect of water to binder ratio on compressive strength. They found that increasing water-binder ratio resulted in a decrease in compressive strength. Their model was able to reproduce experimental results with $R^2 = 0.9944$ and predicted the testing samples with $R^2=0.9767$.

Özturan et al. [22] tried to compare concrete strength prediction techniques with artificial neural network approach and shown that ANN approach gave a good prediction for concretes of low to medium strength concretes. Apart from some good performance observed in multiple linear regression model, ANN approach showed better results. Another approach, using Abrams' law showed the same performance (measured by the coefficient of determination, $R^2$) in all the five system models.

Compression strength predicting models can be improved if there is a better description of the system, hence, more input variables. This has been elaborated in Özturan's paper [22]. Their ANN model showed a much better performance when early strength data ($7^{th}$ day compressive strength) was added to the input layer. This signifies the utilization of more clarifiers (those that contribute in the make-up of the concrete) for a better predicting model.

This was highlighted even more by Yeh I. [19], [20], [21] in pursuit to develop a model for analyzing the compressive strength of concrete modelling the appropriate mix for high-performance concrete using neural networks. Mix design is not the focus of this thesis but one can see the significant importance of the Yeh's approach [20] towards a thorough analysis and classification of the concrete ingredients, according to certain parameters. This was to somehow mitigate the difficulty faced in the effort to correctly depict the vastly varying nature of concrete performance. This variety occurs due to the presence of different ranges of properties within the same ingredient. For example, a cement can be powdered into a various degrees of fineness and composed of several different chemical compositions [20].

This disparity in the nature of ingredients can be kept to a minimum by using a limited range for each element in the modelling process. While modelling the compressive strength of high performance concrete [21] Yeh I. deleted some concrete samples that were of larger size aggregates (larger than 20mm), special curing conditions etc. This was done in an attempt to have a more general model which can relate to concrete mixes carried out on a daily basis. However, his effort was marred because of the incredibly varying range of superplasticizers. Some of the data not only lacked required fields, but also significantly varying chemical compositions were adopted by different manufacturers. Still, his results gave a better prediction than what would have been if the filtering process were not applied.

## 2.5 THERMODYNAMIC METHOD

Thermodynamic approach based models try to predict the compressive strength of concrete using principles of thermodynamics. As strength gaining in concrete is directly related with the hydration process occurring in concrete, such approaches entail consideration of chemical reactions taking place in cement particles during hydration.

Cement owes its properties mainly to the composition of its oxide constituents. Which are described in Table 2 below [5].

Table 2- Typical Cement Constituents [5]

| **Oxide form** | **Notation** |
|---|---|
| $CaO$ | C |
| $SiO_2$ | S |
| $Al_2O_3$ | A |
| $Fe_2O_3$ | F |
| $SO_3$ | $\overline{S}$ |
| $H_2O$ | H |

The notations are so that one can avoid a lengthy description of the compounds even though this may create confusion for a first time user. Furthermore, this simplifying method is also applied when one comes across the main cement phases [5]. This simplification is described in Table 3 [5].

Table 3- Notation and nomenclature of major cement compounds [5]

| **Chemical Name** | **Chemical Formula** | **Oxide Formula** | **Cement Notation** | **Mineral Name** |
|---|---|---|---|---|
| Tricalcium Silicate | $Ca_3SiO_5$ | $3CaO.SiO_2$ | $C_3S$ | Alite |
| Dicalcium Silicate | $Ca_2SiO_4$ | $2CaO.SiO_2$ | $C_2S$ | Belite |
| Tricalcium Aluminate | $Ca_3Al_2O_6$ | $3CaO.Al_2O_3$ | $C_3A$ | Aluminate |
| Tetracalcium Aluminoferrite | $Ca_2AlFeO_5$ | $4CaO.Al_2O_3.Fe_2O_3$ | $C_4AF$ | Ferrite |
| Calcium hydroxide | $Ca(OH)_2$ | $CaO.H_2O$ | CH | Portlandite |
| Calcium sulfate dihydrate | $CaSO_4.2H_2O$ | $CaO.SO_3.2H_2O$ | $C\bar{S}H_2$ | Gypsum |
| Calcium oxide | CaO | CaO | C | Lime |

About 90 – 95% consists of the four major materials (Alite, Belite, Aluminate and Ferrite). The calcium silicates comprise around 85% of the cement clinker and are responsible for the strength development by creating the most important hydration product, the C-S-H gel. Despite not contributing to strength, aluminate hydrates very rapidly release a significant amount of heat. Hence, the dependence of the proportioning for the mineral composition depends on the intended use of the Portland cement.

In so far as concrete is concerned, the cementitious material always contains Portland cement of the traditional variety, which is 'pure' Portland cement. Therefore, when other materials are also included, it is possible to refer the ensemble of the cementitious materials used as Portland composite cements. This is a logical term, and so is the term blended Portland cements [5].

Accordingly, a cement type can be rapid hardening cement, quick setting cement, low heat cement, white cement, colored cement etc,. Factors such as the intended purpose, practicability (availability and economy); among others, determine the type of cement to be used. The variation of mineral compositions of cement as well as addition of materials like pozzolans and admixtures can help one fulfill these required behaviors in cement.

*Rapid Hardening Cement* has relatively higher lime content. It attains the majority of its strength in early days. Such type of cement is used in areas where formwork needs to be removed quickly. This type of cement is also used in fast-track construction sites. The content of alite is reduced in *Low Heat Cement*. This would allow the concrete to have a lower heat of hydration allowing it to greatly avoid thermal cracking and related degradations of concrete in massive castings, like gravity dams. *White Cement* is mostly used for its architectural dimension. The entity that gives cement its gray color is avoided by removing Iron Oxide. Thus, the raw materials are prepared free from Iron oxide. Such cement is more expensive and is used where architectural purpose outweighs economy. An example is the Jublee Church of Rome [29]. Colored cement is produced by mixing ordinary cement with mineral pigments. It is famous for its use in decorating floors.

Naming the types of cements according to their inherent features may not fit the standardization criteria. The most common nomenclature is the ASTM description which is shown in Table 4 [5].

Table 4- Main Types of Portland cement [5]

| **Traditional British Description** | **ASTM description** |
|---|---|
| Ordinary Portland | Type I |
| Rapid-hardening Portland | Type III |
| Low-heat Portland | Type IV |
| Modified cement | Type II |
| Sulfate-resisting Portland | Type V |
| White Portland | -- |
| Portland-pozzolana | Type IP |
| | Type I (PM) |
| Slag Cement | Type S |

The hydration of cement was first summarized by Le Chatelier, as a continuous process of dissolution and precipitation. The dissolution stage initiates first, allowing cement to release ions into the mix water. This continuous release of ions supersaturates the solution, making it possible for some of the dissolved ions to mix into new solid phases, which marks the beginning of precipitation. This (formation of new hydration products) somehow relieves the impediment created by the super-saturation and further promotes the dissolution process. The dissolution-precipitation process will therefore continue for most part of the hydration.

Considering the overall dissolution-precipitation as a process, one can have cement and water as reactants and the hydration outputs as the products. This 'process' strives to achieve thermodynamic equilibrium. Of the dissolution and precipitation processes continuously going on within the mix, the ones that have precipitated into solid forms are the ones that are more stable, with lower free energy (amount of chemical and thermal energy).

The above hydration process initiates microstructure formation. This process plays out differently in cement of mortar and in cement of concrete. As the cement hydration progresses, the developing microstructure which has much say in the compressive strength attained, will depend on many other factors. These factors (which will be discussed later) are to be considered while using thermodynamic approaches. The success of each model, therefore, relies heavily upon a successful representation of the microstructure formation and development in the concrete.

Clinker is the major constituent of cement. Hence, the property exhibited by a certain type of cement owes greatly to its clinker mineral composition. Therefore, in describing the hydration process, this clinker composition and its effect on the overall hydration process should be given due attention.

Apart from Le Chatelier's simplified description, the hydration process of the cement in concrete is quite complicated. This is because hydration of different components in the cement are interdependent. Furthermore, the reactions taking place during hydration are simultaneous and reaction itself is dependent on the temperature of the system, which is in turn affected by the heat given off.

Ippei et al. elaborated this intricacy as one caused by the physical and chemical aspect of cement [15]. The physical aspect being the cement matrix formed by cement particles of random particle size distribution and water that affect hydration through diffusion of ions; and the chemical aspect: the nature of a cement particle as a composition of multi-minerals that have dependency on temperature for hydration. This fact was also highlighted by Maruyama et al. [30].

With the addition of pozollans and/or admixtures, the hydration phenomenon gets further complicated as these minerals introduce their own properties. For example, powder admixtures such as blast furnace slag, fly ash and silica fume introduce a delaying effect, which brings another compound (calcium hydroxide) into play. This delaying effect cannot occur and continue without calcium hydroxide as an activator which is itself produced from hydration of the alite and belite components.

Therefore, evaluation of this interdependence among mineral components is of paramount importance for an accurate representation of the hydration process, which in turn affects the compressive strength predicting models produced.

There are several models attempting to depict the hydration model of cement. These models have attempted to correctly represent the microstructure in concrete. The challenge with this pursuit is correctly choosing the method of approach. For pixel based analysis, there is a resolution issue: a unit representative volume that is considered in a computer simulation should be small enough to correctly depict this scenario. Such task would consume longer amount of computing time and computer memory as well. Hence, proper mitigation should be carried out without compromising the microstructure model so that it can be applied on a larger scale.

Tomosawa [31] tries to model the hydration of cement as a combination of four rate determining parameters, namely, formation and destruction of initial impermeable layer, the activatied chemical reaction process and the diffusion control stage. Effects of these four parameters are incorporated as coefficients in his proposed hydration equation. This is a fair inclusion of the majority of the processes involved. However, Tomosawa employs assumptions to minimize computing time while simulating the hydration process.

These assumptions include a homogenous particle size distribution of cement, including the condition that the cement particle is always surrounded by water. This assumption eludes from the fact that any microstructure model should account for the effect of reduced free water and its effect on the overall hydration process within the cement matrix of different cement particle size.

HYMOSTRUC model describes the hydration of cement as a function of particle size distribution, the reaction temperature, chemical composition and the water to cement ratio. This is by far the best elaborate approach and also includes compelling features for a prospective user. However, hydration rate of clinker components is assumed the same throughout the hydration process. This may be regarded as an oversimplification to the actual scenario in hydration of cement. The hydration process basically goes through a multitude of variations especially within the clinker components.

This pixel-based model gives a plethora of outputs but the most intriguing feature is its 3D representation of the hydration process. While running the program, one can pause the process at any time-step and see how the hydration process is taking place. An example is shown below (Figure 7, Figure 8 and Figure 9), using already given inputs to utilize the model using a program called Hymostruc_Lite (Courtesy of TU Delft University).

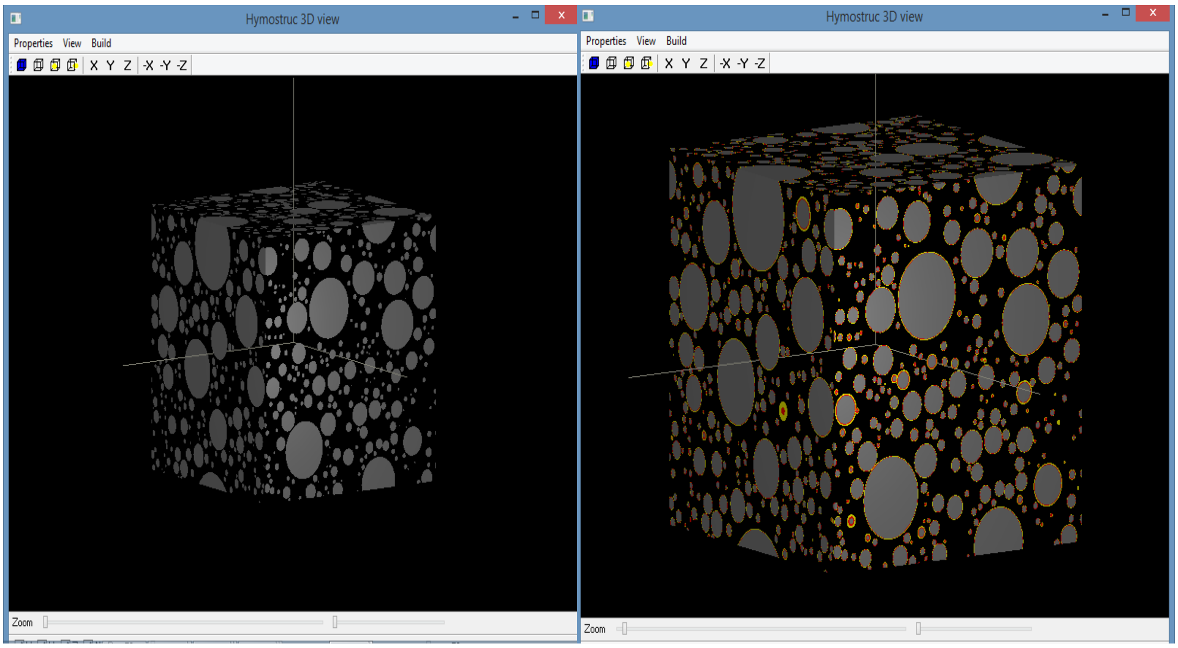


Figure 7- Hymostruc model of a cement in pixels with a Cube envelope at time = 0 Hrs (Left) and 2Hrs (Right)

The first picture shows a sample cube, with cement particles of different sizes cast randomly in space at time = 0. The pore structure within the cube is the black portion. The next picture (right) shows the changes in the cube after a continuous hydration of 2hours. One can see the hydration products formed, designated by different colors (red and yellow). Figure 8 and Figure 9 also show this hydration process at different times.

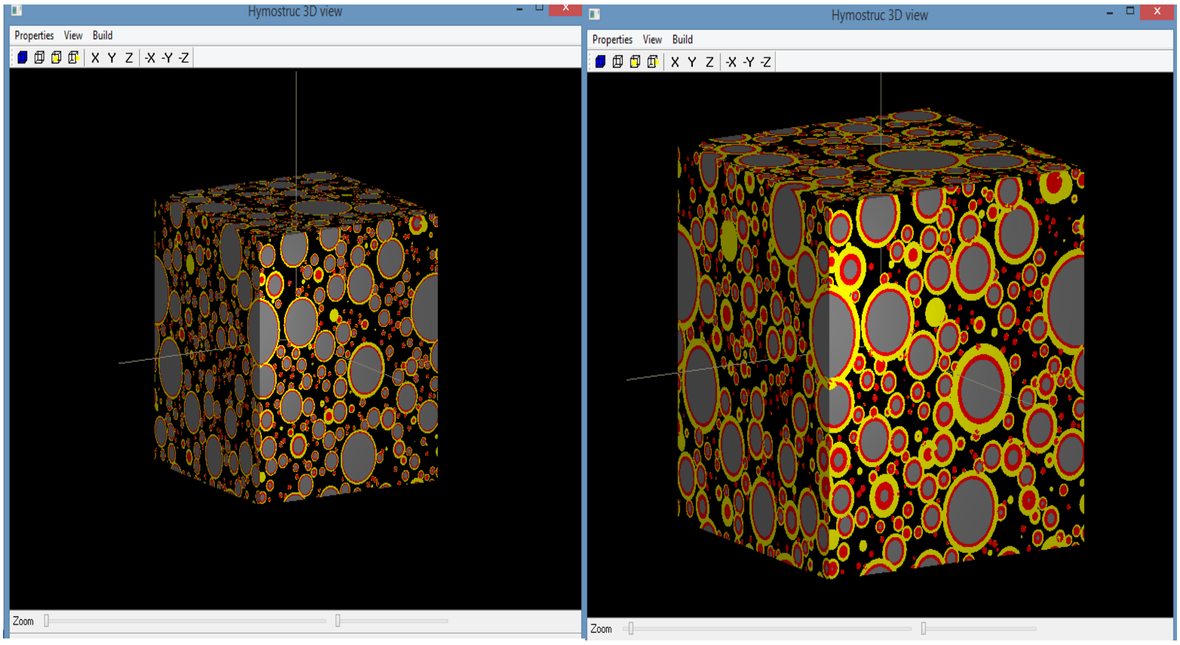


Figure 8- Hymostruc model of a cement in pixels with a Cube envelope at time = 12 Hrs (Left) and 24Hrs (Right)

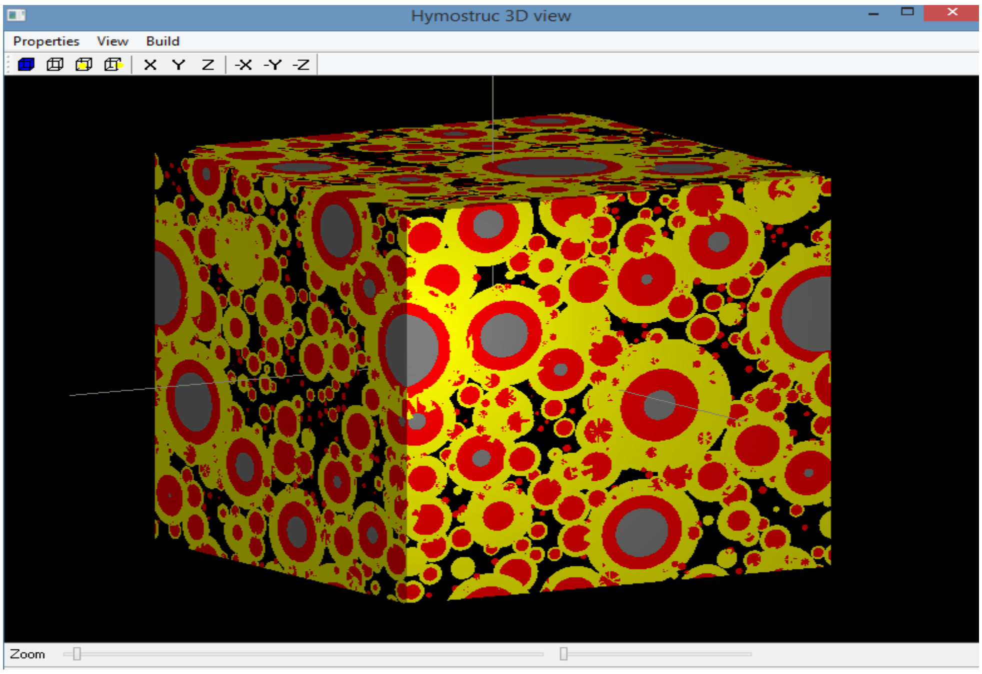


Figure 9- Hymostruc model of a cement in pixels with a Cube envelope at Day 28

According to the depiction of the 3D model, one can easily see the pattern of hydration of the cement particles. The color coding is labeled as 'un-hydrated core' for grey, 'inner layer' for red and 'outer layer' for yellow. The increase in the size of cement particles, as well as the change in the pore structures are amongst those simulated by the model. Adiabatic temperature rise curve, elastic modulus of the concrete, degree of hydration etc. are only some of the many outputs produced by the model.

Wang *et al.* [32] presented a model of Portland cement hydration that tries to include the effect of cement particle size distribution, cement particle mineral composition, water to cement ratio and curing temperature. The effect of reduced water on hydration is also incorporated in the final hydration equation. However, the model falls short of representing the interaction among different hydration products. Hydration, as a multi-component process, fairly depends on mineral interaction but this model assumes hydration of individual clinker minerals as independent and therefore, no mechanism of interaction exists among reaction components.

NIST model, referred to as CEMHYD3D, is also a computer simulation model by Bentz and Grboczi. It is a comprehensive model for the three-dimensional microstructural development of cement paste during hydration [33]. It divides the hydration process of each 'pixel' into three steps; dissolution, diffusion and reaction. One pixel has a volume of $1um^3$ and this by itself has implications on the applicability of this model on large-scale hydration computations. A possible shortcoming of this model thus lies in its demand of computers with specific attributes like random access memory. Consequently, endeavors like these would take enormous amount of CPU-computing time which necessitates the use of computers with very high speed and memory storage capacity.

Other approaches for hydration of cement in mortar and in concrete also include the works done by Uchida et al, Suzuki et al and Kishi et al. Their works make use of Arrhenius' principle of chemical reaction to quantify the hydration process. This gives precedence to the discussion of Arrhenius' principle for a better understanding of such hydration models.

For a chemical reaction, Rate law portrays the rate of the chemical reaction as a function of a rate constant, concentration of the reactant and the order of the reaction. A typical relation is of the form:

$$Rate = k\,[C]^{n} \tag{2-8}$$

Where k is the rate constant, C is the concentration and n, the order of the reaction. There are several methods to predict the rate constant. Keith J. Laidler [34] presented the history and applicability of several temperature dependence equations and found Arrhenius' equation to be the most applied and forward approach.

Arrhehius's Equation is given by the following equation (2-9).

$$k = Ae^{E_a/RT} \tag{2-9}$$

where:

k = rate constant

A = frequency factor

Ea = activation energy (usually in kJ/mol)

R = gas constant (8.314 J/mol•K)

T = Kelvin temperature

A simple look at the mathematical relationship connotes that as activation energy increases, the rate decreases and as temperature increases, the rate increases. Such influence of temperature and activation energy on the rate of almost any chemical reaction can be properly described by the above Arrhenius's equation.

Equation (2-9) can be changed into the form y = mx + b after taking the natural logarithm of both sides and rearranging. This form, finally transformed into Equation (2-10) is used while developing hydration models of cement in concrete.

$$\ln k = \frac{-E_a}{R}\left(\frac{1}{T}\right) + \ln A \tag{2-10}$$

Where y = *ln*k

m = $\frac{-E_a}{R}$

$$x = \left(\frac{1}{T}\right)$$

$$b = \ln A$$

This would mean that the slope is a function of the activation energy, which, among other methods, can be obtained graphically by running experiments at various temperatures and measuring the respective rates. Such experiments are the likes of adiabatic temperature rise tests for varying initial temperatures. This concept is extensively utilized in development of Suzuki's component model for heat of hydration of concrete and Uchida's model for prediction of temperature rise in concrete [35], [36]. The models make use of the thermal properties of cement in concrete.

The feature of these models is that the exothermic hydration properties of cement in concrete are specified by two material functions, i.e. the thermal activity and the intrinsic heat rate [37]. Temperature dependence of the reaction is described by the thermal activity which in turn is a reflection of the activation energy [37]. Activation energy is the energy barrier to a chemical reaction. Hence, energy within the system (supplied by the molecular kinetic energy) must be over this barrier in order for the reaction to start. The higher the temperature, the higher the tendency of molecules to go over this barrier and be involved in the chemical reaction process. Both thermal activity and intrinsic heat rate (heat rate at a specified constant temperature) characterize the process of heat generation of cement in the concrete. The accumulated heat is a main parameter for the rate of heat generation as well as the temperature and represents the past hydration process [38].

In order to quantify the hydration phenomenon, one needs to successfully predict the temperature rise in the concrete. Such temperature rise can be obtained by adiabatic tests of the concrete. However, there are many cases where concrete outside of the laboratory experiences non-adiabatic conditions. Hence, Uchida et al. [36] proposed an alternative, which is expressing the heat of hydration of cement.

In an attempt to simplify the complicated hydration process, their study [36] focused on the heat liberated (cement + water = hydrate + Q) where Q is the heat of hydration. This can be obtained through direct measurements with the use of microcalorimeter. Under constant conditions (mainly temperature), the author et al. were able to successfully plot the rate of heat liberation of the cement versus time; which can be interpreted to the overall temperature rise in the concrete.

However, such relationship introduces weakness because even under constant conditions, temperature varies with time due to ongoing hydration process. This in turn, affects the rate of heat liberation. Uchida et al [36] showed that as cement samples with different temperatures attained different hydration states at time $t_1$, the hydration states were found to be equal for a given cumulative heat liberation. Hence cumulative heat liberation was introduced as a parameter as it uniquely expresses the hydrated state of cement at any given time. This hydrated state coupled with the corresponding rate of heat liberation, in accordance with Arrhenius' equation, can be used to predict the temperature rise of concrete.

$$\frac{h_T}{h_o} = exp\left(\frac{-E}{R}\right)\left(\frac{1}{T} - \frac{1}{T_0}\right) \tag{2-11}$$

$$ln\left(\frac{h_T}{h_o}\right) = g(H_T) \tag{2-12}$$

$$g(H_T) = aH_T + bH_T + cH_T + dH_T \tag{2-13}$$

Where

$H_T$ = cumulative temperature at absolute temperature T and time t

$h_T$ = rate of heat liberation at time t

$h_o$ = rate of heat liberation at reference temperature $T_0$

a, b, c and d are constants

E= activation energy

R= rate constant

Hydration is a reaction process and as discussed previously; in order for any reaction to occur, it must pass a reaction barrier, called the activation energy. This activation energy varies according to cumulative heat liberation which owes to the difference in clinker components of cement. Even though the influence of each mineral in altering the activation energy of the reaction was not specifically described, Uchida et al., in their work tried to present the relation between representative cumulative heat liberation (at a reference temperature) and inclination (activation energy per rate constant); shown in Figure 10 [36].

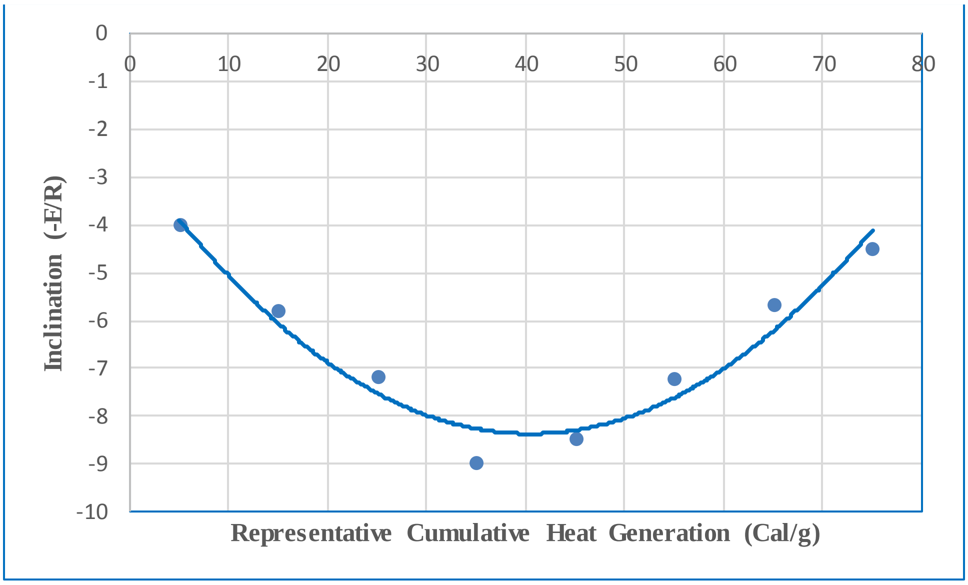


Figure 10- Representative Cumulative Heat Generation vs Inclination [36]

The overall process of Uchida et al.'s approach is summarized in a flowchart of cumulative heat liberation. The aim is to find the amount of cumulative heat at a given time (which is the summation of cumulative heat liberation of previous time steps). Corresponding to the adiabatic temperature rise test made by Suzuki, this method also establishes $g(H_T)$, which is the cumulative heat liberation's effect in influencing the activation energy. In addition, specific heats of the cements and aggregates measured are also used for analysis. At a given temperature $T_1$ and time $t_1$, the cumulative heat liberation $H_{T1}$ can be computed from already known temperatures. The rate of heat liberation at the initial temperature will be used to compute the rate of heat liberation at $T_1$ from Equation (2-15).

This equation can also be replaced with a cubical regression that fits the cumulative heat liberation versus rate of heat liberation graph (Equation **Error! Reference source not found.**). This process will be repeated all over again until the total elapsed time is reached. The model diagram is shown in Figure 11 [36].

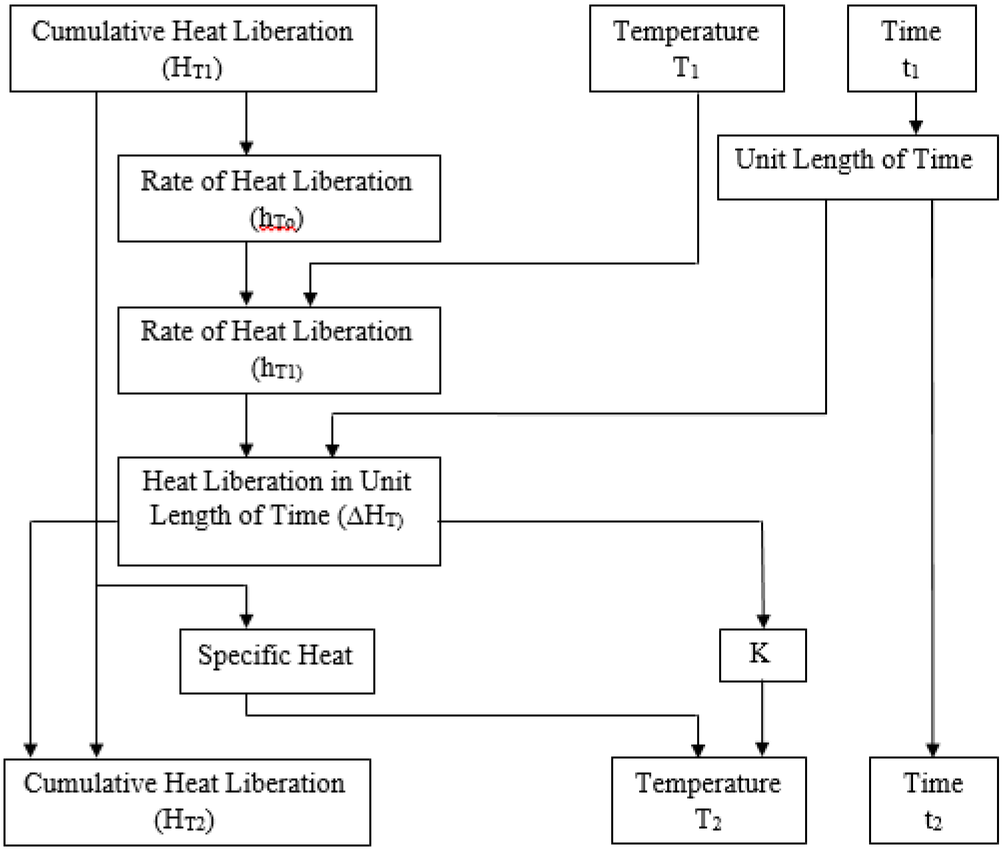


Figure 11- Flowchart for computing a time-step Cumulative Heat Liberation [36]

Despite corresponding with the actual values at some mixes, the calculations showed a great deal of disparity in mixes with larger/or smaller water to cement ratios (w/c ratio of 0.38, 0.61 and 0.785 were greatly visible). The calculation value is considerably lower than the actual value with a larger water to cement ratio and vice versa [35]. This is a testament in that the material functions described by Uchida et al. also depend on the mix proportions. This is only logical as the mix proportions (disparity in the presence of aggregates) affect the dispersion of the cement particles, varying the hydration rate. This problem is addressed in the work of Suzuki et al. [35].

Suzuki et al. refined the adiabatic temperature rise results from Uchida et al.'s approach and produced a model that can confirm with any temperature hysteresis, even without the need for a conduction type microcalori-meter. Unlike the erroneous the conventional system which relates hydration heat generation rate only with time (due to the assumption of zero activation energy), they considered its relationship with integrated calorific value (Q) and absolute temperature (T) [39]. Such consideration invokes the assumption of a constant activation energy in the reaction.

Adiabatic temperature rise can be affected by the initial atmospheric conditions as well as the behavior of the reactant. In this case: the heart of the concrete which is on a continuous heat generation process, is the cement. Consequently, the effect of a correct representation of the adiabatic rise curve in determining the total hydration of the cement will be given due attention here. This gives significance to the consideration of factors that play a key role in the adiabatic temperature rise such as the type of cement (the proportion of its ingredients), initial temperature at casting and the unit cement content in the mix [39].

Several relationships exist that can be used to predict this adiabatic temperature rise [35]. Each relationship tries to quantify the adiabatic temperature rise Q(t); *t* days after casting with respect to the ultimate temperature rise $Q_\infty$ and other experimental constants. The relationships are shown in Equation (2-14) below [37].

$$
\begin{aligned}
Q(t) &= Q_\infty(1-\exp(-rt)) \\
Q(t) &= Q_\infty(1-\exp(-rt^s)) \\
Q(t) &= Q_\infty(1-\exp(-r(t-t_{0)}))) \\
Q(t) &= Q_\infty(1-\exp(-r(t-t_{0)})^s))
\end{aligned}
\qquad (2\text{-}14)
$$

Any one of these four expressions can be chosen as a means to quantify the adiabatic temperature rise. However, Suzuki et al. [39], after studying the reliability of these approximations, found that each equation's performance differed according to the type of cement used. For example, Equation (2-14) (b) and. Equation (2-14) (d) performed well and were similar in output but Equation (2-14) (b) was found to be slightly better in blended cements. This fact also forms the basis in the authors' preference to use Equation (2-14) (b) and produce coefficients for calculations. Therefore, Equation (2-14) (b) will be used to represent a particular heat generation under adiabatic conditions with a specific concrete mix and casting temperature.

Suzuki *et al.* inversely identified the cement properties from concrete based measurements. The accumulated heat generation is specified as a main parameter for the rate of heat generation as well as the temperature in order to represent the past hydration process. The governing equation is given in Equation (2-15)

$$
H = H(T,Q) = H(T_s\,,\,Q)\exp\left[-\frac{E(Q)}{R}\left(\frac{1}{T}-\frac{1}{T_s}\right)\right] \qquad (2\text{-}15)
$$

$$
H(T_s\,,\,Q) = H_\infty(Q)\exp\left[\frac{E(Q)}{RT_s}\right] \qquad (2\text{-}16)
$$

where

H = heat generation rate per unit weight of cement

$H(T_s\,,\,Q)$ = a function of the accumulated heat Q, is the reference heat generation rate of cement at a constant temperature $Ts$

$H_\infty(Q)$ = is the ultimate reference heat generation rate of cement at infinite temperature

$E(Q)$ = activation energy of cement

R = gas constant

T = absolute temperature of concrete

Given two initial temperatures (usually three, for better accuracy), one can write material functions in terms of the accumulated heat per unit weight of cement. Such pursuit starts from producing adiabatic temperature rise curves for the initial pouring temperatures mentioned above. Once the adiabatic temperature rise curve of concrete is established, it will be multiplied by the average heat capacity of concrete and divided by the cement content per unit volume of concrete to obtain the quantity of the corresponding accumulated heat (Q) (named as the 'integrated calorific value' in Suzuki et al.'s work [35]). The graph of the accumulated heat vs. Time may be used to compute the hydration heat rate ($= \partial Q / \partial t$) which is also the gradient of the respective curve.

This plot of the hydration heat rate H (at different temperature) vs. the accumulated heat can be converted to Arrhenius' plot by taking the logarithmic scale. This Arrhenius plot is a logarithm of the hydration heat rate vs. the inverse of time graph, and may be interpreted to arrive to the derivation of material properties of cement hydration [37]. The important material properties, namely reference heat rate and thermal activity are thus obtained. Summary of the entire process is addressed in Figure 12 below [35].

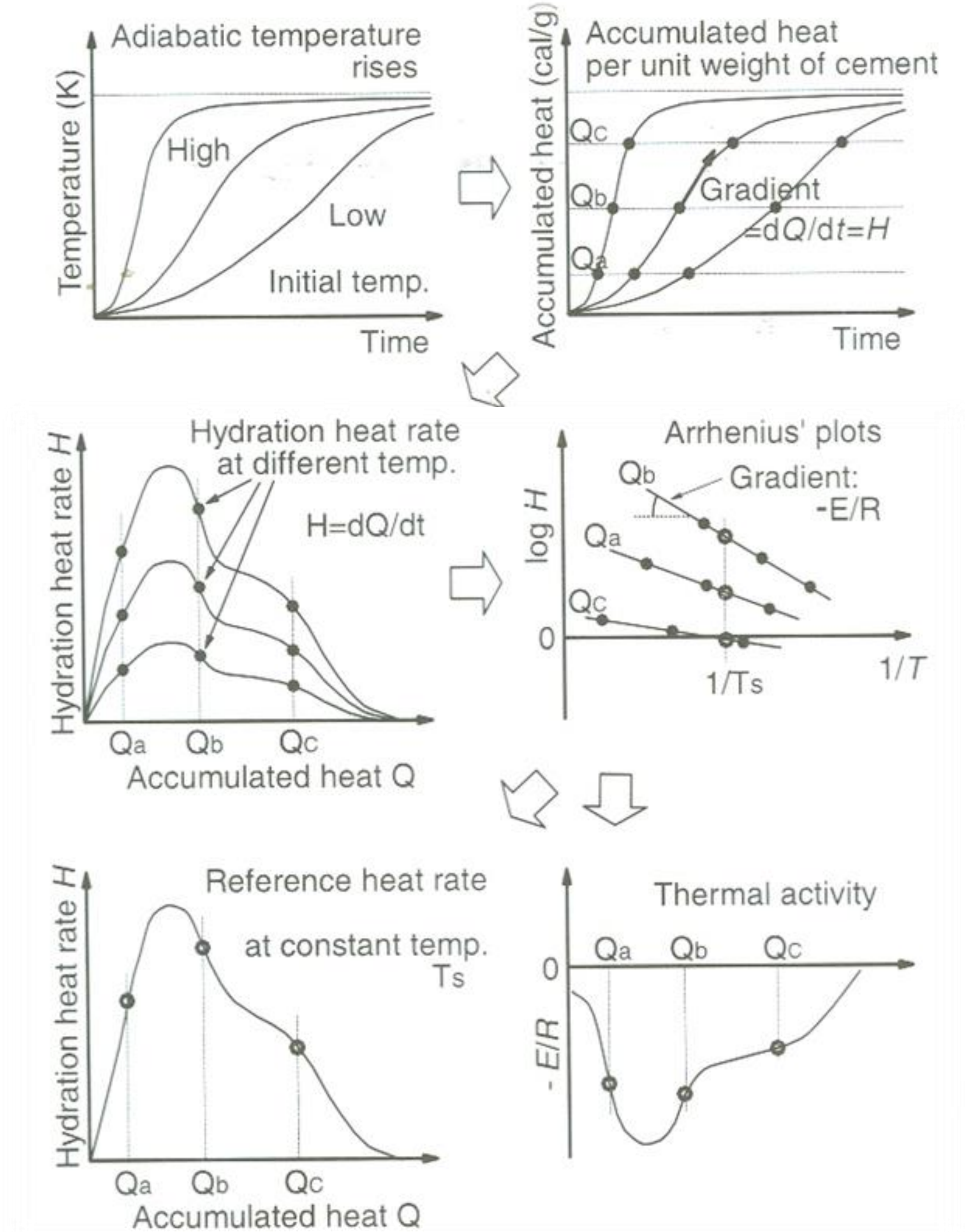


Figure 12- Procedures to derive thermal properties of cement hydration from adiabatic temperature rise tests [35]

In quantitatively evaluating the temperature-dependent hydration-heat generation rate described by Suzuki et al., the logH vs. 1/T graph shown above is used. The value where the graph intersects the ordinate represents the logarithm of the limit hydration-heat generation rate ($\log H_{\infty}$), at ultimate hydration. The thermal activity of cement (-E/R) is also determined as the gradient of the Arrhenius' plot.

Studies made by Uchida et al. and Suzuki et al.; utilizing Arrhenius' Law to quantify the related heat properties of cement during hydration, were further broadened by Kishi et al. to produce a model of hydration of cement by independently addressing the mineral reactions. The heat liberation process, as the combined effect of individual clinker mineral components was addressed by Kishi et al. in their multi-component model for hydration heating of Portland cement [40].

The Multi-component model tries to address actual conditions at construction sites. The versatility offered by concrete would mean making the model applicable to changes not only in the cement composition, but also in cases where pozzolans and/or admixtures are to be introduced.

The difference in clinker mineral compositions is the main reason behind the variety in cement properties. These clinker minerals undergo individual reactions throughout the hydration process. Some minerals become active as soon as the cement comes into contact with water and some minerals become involved at the later stages. Hence, the multi-mineral component concept separately addresses the simultaneous reactions, giving attention to the interaction among minerals [38].

The minerals treated in the multi-component model are those major clinker compounds making up cement (alite, belite, ferrite and aluminate) and gypsum. The hydration process of each mineral is computed as a function of material properties introduced by Suzuki et al., namely, the reference heat rate and the thermal activity. The heat rate for the cement as a whole, Hc, including blending powders, is shown in Equation (2-17) below [40].

$$
\begin{aligned}
Hc &= \Sigma p_i H_i \\
&= p_{C_3A}(H_{C_3AET} + H_{C_3A}) + p_{C4AF}(H_{C4AFET} + H_{C4AF}) + p_{C_3S}H_{C_3S} + p_{C_3S}H_{C_3S} \\
&+ p_{SG}H_{SG} + p_{FA}H_{FA}
\end{aligned}
\tag{2-17}
$$

Where

$H_i$ = heat generation rate of mineral $i$ per unit weight

$p_i$ = the weight composition ratio

$H_{C_3AET}$ *and* $H_{C_4AFET}$ = heat generation rates of $C_3A$ and $C_4AF$ (respectively) during the formation of ettringite

$H_{C_3A}$ *and* $H_{C_4AF}$ = hydration heat generated by $C_3A$ and $C_4AF$ respectively

The interdependence of reactions stated previously is quantified by coefficients which take into account the effects of the shared environmental temperature, the amounts of mixing water, and changes in the heat generation rates for minerals that are affected by certain conditions and the delaying effect of admixtures.

$$
\begin{aligned}
H_i &= \gamma_i \, \beta_i \, \lambda_i \, \mu_i \, H_{i,T_0}(Q_i) \exp\left\{\frac{-E_i}{R}\left(\frac{1}{T} - \frac{1}{T_0}\right)\right\} \\
Q_i &= \int H_i dt
\end{aligned}
\tag{2-18}
$$

Where

$E_i$ is the activation energy of component i

R= gas constant

$H_{i,T_0}$ = the reference heat-generation rate of component i at constant temperature $T_0$ (also a function of the accumulated heat $Q_i$)

$\gamma_i$ = delaying effect of the chemical admixture and fly ash in the initial exothermic hydration process

$\beta_i$ = reduction in the heat generation due to the reduced availability of free water (precipitation space)

$\lambda$ = the change in the heat generation rate of powder admixtures (blast furnace slag, fly ash and silica fume), due to lack of calcium hydroxide in the liquid phase

$\mu_i$ = change in the heat-generation rate in terms of the interdependence between alite and belite in Portland cement (shown in Equation (2-20) below)

$$\mu = 1.4 \cdot \left\{ 1 - exp\left[ -0.48 \cdot \left( \frac{\rho C_3S}{\rho C_2S} \right)^{1.4} \right] \right\} + 0.1 \qquad (2\text{-}19)$$

The multi-component approach will be the main focus of this paper mainly due to its vast nature of applicability. Its benefits range from assessment of thermal cracking to the analysis durability and strength gain in concrete for material design. Accordingly, a thorough discussion of the major aspects in the make-up of the model is paramount. These are: modelling of the temperature dependence and the reference heat generation rate, modelling of the Ettringite formation, consideration of interdependence of mineral reactions and modelling of the delaying effect of organic admixtures [40]. Further discussion will therefore be presented in the consequent section.

In an attempt to see the physical hydration process of cement, the conventional method of relating hydration with time may be of use here. Accordingly, cement hydration can be considered a multi-stage process. General stages in the exothermic hydration process in OPC was shown by Uchikawa's time-domain division of cement hydration, shown in Figure 13 [37].

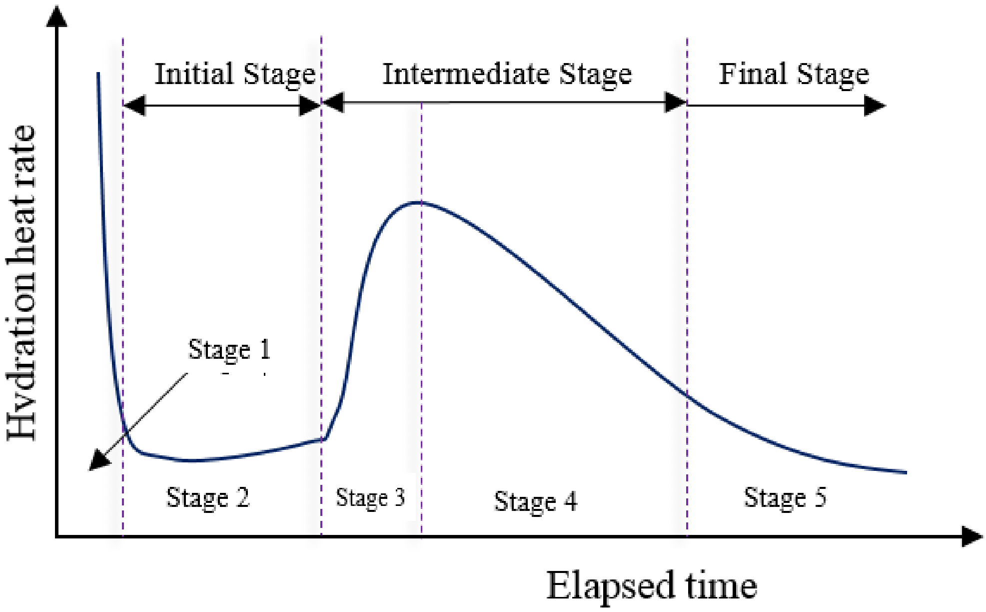


Figure 13- General stages in the exothermic hydration process in OPC [37]

Stage I is the first peak in the exothermic process of hydration. Right from the onset of mixing, this is where rapid heat liberation occurs due to formation of ettringite. The reaction process will then slow dow n shortly after this peak in heat liberation. This is due to ettringite formation. Collision of cement particles with water will be less as a protective layer of C-S-H and a hard coating of ettringite are produced on the surface of cement particles. This coating prevents hydration, significantly reducing the exothermic reaction of the cement. This stage is usually called the 'dormant period'.

Wang *et al.* [32] explained this stage as one in which the reaction resistance increases with the increase of degree of hydration in each particle (film formation) followed by a period in which the reaction resistance decreases with increasing thickness of inner products. The expression for the rate coefficient is shown in the relation below:

$$k_d = \frac{B}{(\alpha_i^j)^{1.5}} + C(r_0^j - r_t^j)^4 \qquad (2\text{-}20)$$

Where:

B and C are rate determining coefficients

$r_i^j$ is radius of anhydrous cement core

$\alpha_i^j$ denotes hydration degree of mineral component in a given cement particle where *i* denotes clinker mineral component and *j* denotes cement particle number.

This representation of the dormant model by Wang *et al.* assumes the same coefficient for each mineral component.

Stage II is mainly dominated by the active hydration of alite and conversion of ettringite to monosulphate hydrate. As the ettringite that was continuously being formed on the surface of cement particles in Stage I crumbles, the surface of the cement exposed and alite gets the chance for hydration [37].

Stage III is diffusion-controlled hydration process. The probability of contact between water and un-hydrated cement is extremely low as the surface area of the un-hydrated particles becomes small. Nagashima [41] separates this diffusion control phase into two parts according to the rate of heat generation. The first part is where the rate of heat generation becomes gradually slower. Where the rate of hydration is remarkably reduced by the thicker later of hydrates around particles forms part two of the diffusion control phase.

The heat generation rate ($H_{i,To}$ ) at a reference temperature of 293 K (20 $^0$C) is shown in Figure 14 for the different clinker components taking part in the hydration process [37]. The values of the heat generation rate at different values of the accumulated heat (and at the reference temperature) will be used as material functions for each mineral

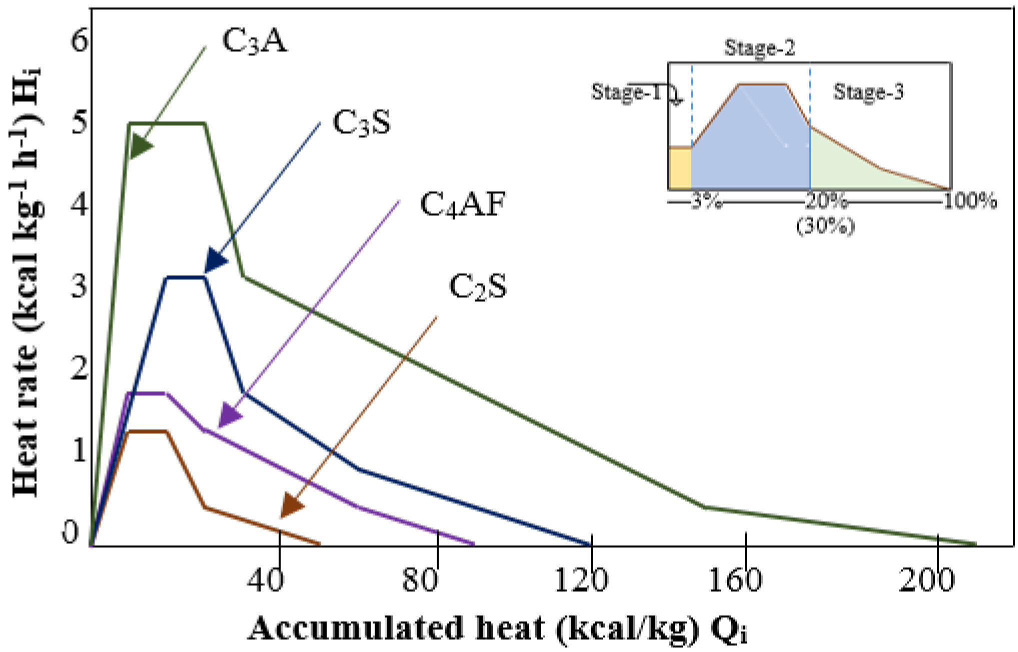


Figure 14- Accumulated heat vs. heat rate at reference temperature [37]

The final heat output achieved by 100% hydration ($Q_{i,\infty}$) is the accumulated heat at which the reference heat rate of a particular mineral is certainly zero [38]. The heat generated during hydration may vary depending on the level of reaction reached by the individual clinker minerals but each clinker mineral generates a certain amount of heat at complete (pure) hydration. $C_3S$ generates 504J/g (129kcal/kg), $C_2S$ generates 260J/g (62kcal/kg), $C_3A$ generates 870J/g (270kcal/kg) and $C_4AF$ generates 420J/g (100kcal/kg). [38]

Another material property that also needs to be written in terms of accumulated heat is the thermal activity. Thermal activity gives a picture of temperature dependence of mineral reactions within the hydration process. The individual mineral relationships should reflect the non-linear variation of thermal activity with increasing accumulated heat for the whole cement which was studied by Suzuki et al.

Such endeavor was achieved by considering the reactivity of each mineral from the onset of hydration. Suzuki's values for the thermal activity of cement were used as reference and were interpreted at each stage of hydration. Maekawa *et al.* [37] explained the reference generation rate by dividing the reaction process into three stages.

The values for each stage were set through analysis (Figure 14). Stage 1 is the period until 1% of the total heat output is reached. This corresponds to the temperature increment during the initial dormant period of the cement hydration process. Stage 2 (thought to be a reaction control process; analogous to temperature increment of the second exothermic peak) is up to 25% for $C_3S$ and up to $C_2S$. In the case where large amount of superplasticizer is added, these values are affected. This was not addressed in the authors' work. Stage 3 is the diffusion control process, defined as percentages above these values. This is also the stage where heat generation rate drastically decreases. The reference heat generation curve developed for the entire cement [35] was used to quantify the decrease in reference heat rate due to diffusion resistance.

Kichi et al. [40] set the thermal activity of $C_3A$ and $C_4AF$ as constant throughout the hydration process as they believed simultaneous elution of ions from unhydrated surfaces and precipitation of hydrated products took place which evens out the energy demand. These minerals give precedence to reacting with gypsum and produce ettringite ($C_3A.3CS.H_{32}$) if there exists gypsum in the system. Thus, ettringite forms rapidly and then slows down as the minerals get covered with the reaction products. The ettringite formation model consequently takes this into account in setting the reference heat rate.

The ettringite formation model bases on the assumption that ettringite still continues to form as long as there is un-reacted gypsum present. This notion is capitalized on by considering the amount of $SO_4^{2-}$ left. As the gypsum gets consumed, such halt in the reaction process undermines the stability of the ettringite and so it crumbles. This ettringite reacts with unreacted belite and ferrite to produce monosulfate (until there is no more ettringite). It is then that the hydrates from the unreacted $C_3A$ and $C_4AF$ start to precipitate.

This calls for a representation of the ettringite formation process and its conversion to monosulphate. Even though the ettringite forms rapidly compared with the overall hydration process, it has influence in the hydration of unreacted $C_3A$ and $C_4AF$.

The formation of ettringite and its inevitable transformation to monosulphate and hydration is represented by the chemical reaction shown in **Error! Reference source not found.**. .

$$
\begin{aligned}
&C_3A + C_3A \cdot 3C\bar{S}H_2 + 26H \rightarrow C_3A \cdot 3C\bar{S} \cdot H_{32} \\
&C_4AF + 3C\bar{S}H_2 + 27H \rightarrow C_3(AF) \cdot 3C\bar{S} \cdot H_{32} + CH
\end{aligned}
\tag{2-21}
$$

$$
\begin{aligned}
&where,\ C \equiv CaO,\ A \equiv Al_2O_3,\ F \equiv Fe_2O_3,\ H \equiv H_2O,\ CH \equiv Ca(OH)_2, \\
&\bar{S} \equiv SO_3
\end{aligned}
$$

The formation of ettringite will continue until all the gypsum is consumed. Therefore, the authors' model will compute the heat generation corresponding to the first peak and will continue to do so until the amount of gypsum remaining is zero. From the reaction in **Error! Reference source not found.**, one can calculate the amount of gypsum consumption. When the consumption reaches the original amount of gypsum present, the process stops.

After the collapse of ettringite layers due to the absence of $SO_4^{-2}$ in the liquid, elution from unreacted $C_3A$ and $C_4AF$ takes place simultaneously, which in turn convert whatever ettringite is left to monosulphate. This stage stops when there is no unconverted gypsum remaining. The overall reaction is summarized in Equation **Error! Reference source not found.** below. For every amount of unreacted aluminates and ferrites, the heat generation is computed.

$$
\begin{aligned}
&2C_3A + C_3A \cdot 3C\bar{S} \cdot H_{32} + 4H \rightarrow 3\left[C_3A \cdot C\bar{S} \cdot H_{12}\right] \\
&2C_4AF + C_3(AF) \cdot 3C\bar{S} \cdot H_{32} + 6H \rightarrow 3\left[C_3(AF) \cdot C\bar{S} \cdot H_{12}\right] + 2CH
\end{aligned}
\tag{2-22}
$$

As the individual mineral components have been treated, it will be necessary to address the mineral interactions. One possible ground for interaction is the amount of water minerals share during reactions. As stated previously, Tomosawa's model incorporates this by focusing on the residual amount of water content which, in his model, leads to the decline in the reaction rate.

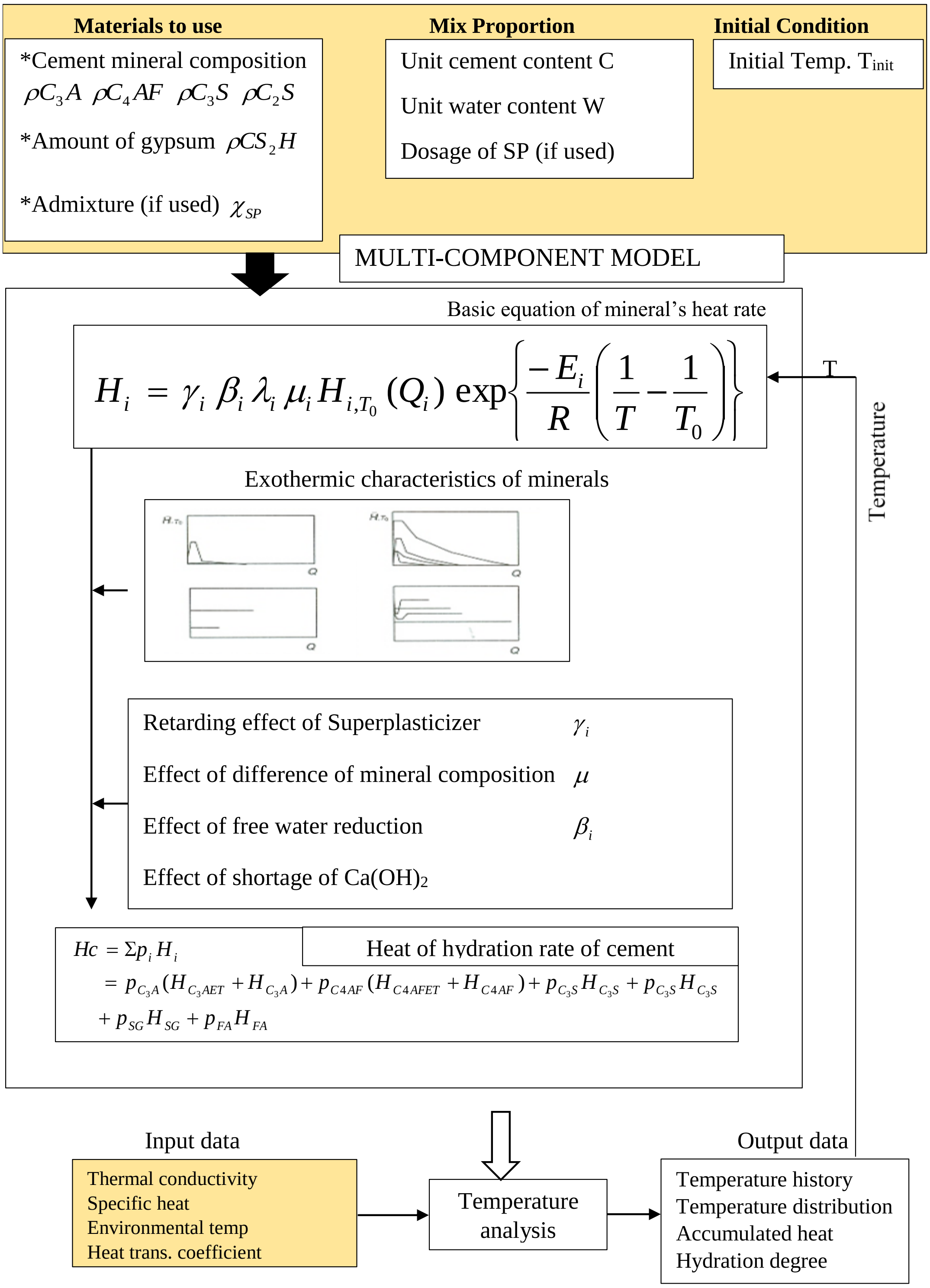


Figure 15- Structure of the Multicomponent heat of hydration computation [37]

### 2.5.1 Multi-Compressive Strength Model

The multi-component compressive strength model accounts four minerals (C3S, C2S, slag and fly ash) to be responsible for the evolution of compressive strength [37]. The relation is given in the equation **Error! Reference source not found.**.

$$fc' = \int df_c' , \quad df_c' = 25dQ_{3S} + 40dQ_{2S} + 27dQ_{SG} + 40dQ_{FA}$$
$$dQ_i = \frac{p_i}{W_{total}} d\phi_i , \quad \phi_i = \frac{Q_i}{Q_\infty} \qquad (2\text{-}23)$$

Where

$fc'$ = Compressive strength (MPa)

$p_i$ = weight ratio of the *i*-th clinker material

$\phi_i$ = the degree of hydration of the *i*-th clinker material, indicated by the accumulated heat normalized by the final heat generated.

In this thesis, strength development prediction models (using thermodynamic model) were carried out for OPC cement type. Hence, the accumulated heat of slag and fly ash will not be used as an input. After a stepwise computation of the accumulated heat of alite and belite, the compressive strength can thus be predicted at any age.

# 3. PREDICTION OF COMPRESSIVE STRENGTH USING REGRESSION, FUZZY LOGIC, NEURAL NETWORK AND THERMODYNAMIC METHODS

## 3.1 DATASETS

In this section, the datasets used for producing the prediction models will be analyzed and discussed. The first dataset used for this project (Dataset-1) is obtained online from UCI machine learning repository. The original owner and donor of the data is Prof. I-Cheng Yeh, Chung-Hua University, Taiwan. The data set has 1,030 instances and the number of attributes is 9 with 8 input quantitative variable and 1 quantitative output variable. The compressive strength is the output variable and has a unit of MPa. The input variables in accordance with their units are listed in Table 5. The values listed below are individual values obtained by comparing the values of the entire dataset.

Table 5- Descriptive Statistics of Dataset I

| Attributes | Lower Bound | Upper Bound | Mean | Standard Deviation |
|---|---|---|---|---|
| Cement ($kg/m^3$) | 102 | 540 | 281.17 | 104.51 |
| Fly ash ($kg/m^3$) | 0 | 200.1 | 54.19 | 64 |
| Blast furnace slag ($kg/m^3$) | 0 | 359.40 | 73.90 | 86.28 |
| Water ($kg/m^3$) | 121.75 | 247.00 | 181.57 | 21.36 |
| Superplasticizer ($kg/m^3$) | 0 | 32.20 | 6.20 | 5.97 |
| Coarse aggregate ($kg/m^3$) | 801 | 1145 | 972.92 | 77.75 |
| Fine aggregate ($kg/m^3$) | 594 | 992.60 | 773.58 | 80.18 |
| Age (Days) | 1 | 365 | 45.7 | 63.17 |
| Compressive Strength (MPa) | 2.3 | 82.6 | 35.8 | 16.71 |

With an aim to compare the model produced using the dataset above, another (local) dataset will also be used (Dataset 2). This dataset is obtained from the Materials Laboratory of Addis Ababa Institute of Technology, Addis Ababa University. The dataset has 328 instances and the number of attributes is 6 with 5 input quantitative variable and 1 quantitative output variable.

The compressive strength is the output variable and has a unit of MPa. For testing days of 3, 7 and 28; the input variables in accordance with their units are listed in Table 6 below.

Table 6-Descriptive Statistics of Dataset II

| **Attributes** | **OPC** | | | | **PPC** | | | |
|---|---|---|---|---|---|---|---|---|
| | Lower Bound | Upper Bound | Mean | Standard deviation | Lower Bound | Upper Bound | Mean | Standard deviation |
| Cement (kg/m3) | 230 | 536 | 356.41 | 44.55 | 240 | 400 | 344.66 | 32.76 |
| Water (kg/m3) | 150 | 215 | 184.76 | 11.62 | 160 | 196.1 | 181.40 | 19.52 |
| Fine Aggregate (kg/m3) | 893.63 | 1262.2 | 1098.03 | 70.87 | 1021.6 | 1253.99 | 1120.08 | 59.93 |
| Coarse Aggregate (kg/m3) | 581.24 | 998.961 | 732.87 | 60.64 | 631.546 | 946.987 | 729.33 | 57.73 |

The clinker composition for OPC cement was a courtesy of Mr. Getu (Data used in his study of Autogenous Shrinkage of Cement) , shown in Table 7. The data was collected from the five cement producing companies in the country; namely Dangote, Derba, Mesebo, Muger and National Cements. Of the data obtained, only the clinker compositions of Derba, Mesebo and Muger were used. This was primarily due to test sample availability. There was no other specific criteria for selection. Table 7-shows the composition of each mineral's mass in percent. The presence of gypsum was taken to be 4.5 (mass in percent) for all of the samples.

Table 7-Mineral composition of cement used by cement manufacturers

| **No.** | **Factory** | **$C_3S$** | **$C_2S$** | **$C_3A$** | **$C_4AF$** |
|---|---|---|---|---|---|
| **1.** | Dangote | 57.29 | 22.22 | 5.45 | 10.25 |
| **2.** | Derba | 57.0 | 22.0 | 8.5 | 11.0 |
| **3.** | Mesebo | 59.66 | 14.89 | 6.64 | 11.73 |
| **4.** | Muger | 37.0 | 35.53 | 7.31 | 12.59 |
| **5.** | National Cement | 24.68 | 46.63 | 10.94 | 9.49 |

In producing the model for determination of compressive strength, simplifications have been implemented as higher number of input variables may complicate the modeling process. In this regard, 'age of testing' is considered a constant. A separate model is produced that is categorized according to the required compressive strength at a given age (in days).

Furthermore, the applicability of Dataset-2 does not match with Dataset-1 as there are additional input parameters in the latter. The presence of Blast Furnace Slag, Admixtures and Superplastisizers could divert the nature of the concrete to one, differing from normal strength concrete. This necessitated for additional simplification in Dataset-1. Therefore, samples which did not contain these three ingredients were selected, as shown in Table 8. The final, formatted data set will have cement, aggregates and water as inputs with compressive strength as an output at a specific 'age' of testing.

Table 8- Descriptive statistics of modified Dataset-1

| **Attributes** | **OPC** | | | |
|---|---|---|---|---|
| | **Lower Bound** | **Upper Bound** | **Mean** | **Standard deviation** |
| Cement (kg/m$^3$) | 200.0 | 525.0 | 336.0 | 73.31 |
| Water (kg/m$^3$) | 175.0 | 228.0 | 190.2 | 9.03 |
| Fine Aggregate (kg/m$^3$) | 594.0 | 945.0 | 776.7 | 61.02 |
| Coarse Aggregate (kg/m$^3$) | 838.4 | 1125.0 | 1033.7 | 71.37 |

As it was seen in the literature review, the compressive strength of concrete does depend on the water to cement ratio. This correlation will be checked using Dataset II for both OPC and PPC cement types. Each dataset will be then used separately to produce models that can predict the compressive strength according to methods which have been discussed in the previous section.

## 3.2 PREDICTION OF COMPRESSION STRENGTH USING REGRESSION ANALYSIS

### 3.2.1 Model Parameters (Dataset II)

Regression analysis is carried out only for the ordinary Portland cement (OPC) type. The dataset containing samples of test results is divided into 3rd, 7th and 28th day samples. A total of six experiments is carried out as shown in Table 9, which included an added clarifier (w/c ratio) to see its effect on the prediction model.

Table 9-Description of experiment sets for modelling

| No. | Experiment | Description (Both for training and testing set) |
|---|---|---|
| 1 | E-1 | 3rd day sample, all data utilized |
| 2 | E-2 | 3rd day sample, w/c ratio = 0.49 - 0.53 |
| 3 | E-3 | 7th day sample, all data utilized |
| 4 | E-4 | 7th day sample, w/c ratio = 0.49 - 0.53 |
| 5 | E-5 | 28th day sample, all data utilized |
| 6 | E-6 | 28th day sample, w/c ratio = 0.5 - 0.53 |

The results of the regression analysis is shown in Table 10 . R-squared as well as regression coefficients have been computed for each experiment set. The regression equation is in the form of:

$$Y = a*C + b*W + c*FA + d*CA \qquad (3\text{-}1)$$

Where,

a, b, c and d are regression coefficients for C (Cement), W (Water), FA (Fine Aggregate) and CA (Coarse Aggregate) respectively. Y- is the resulting compressive strength in MPa.

### 3.2.2 Results and Discussion

The following section shows the results of the regression analysis.

Table 10-Results of Regression Analysis

| Experiment | $R^2$ | | Regression Coefficients | | | |
|---|---|---|---|---|---|---|
| | Training | Testing | a | b | C | d |
| E-1 | 0.939 | 0.27 | 0.077 | -0.061 | -0.061 | 0.005 |
| E-2 | 0.937 | 0.153 | -0.209 | 0.542 | -0.030 | 0.030 |
| E-3 | 0.921 | 0.34 | 0.034 | 0.074 | -0.022 | 0.0278 |
| E-4 | 0.911 | 0.45 | -0.019 | 0.194 | -0.026 | 0.028 |
| E-5 | 0.992 | 0.68 | 0.155 | -0.093 | -0.006 | 4.9E-05 |
| E-6 | 0.995 | 0.77 | 0.118 | -0.05 | 0.01 | -0.0198 |

Table 10 shows the results of the regression analysis. In an attempt to portray a picture of the strength predicting models, experiments E-5 and E-6 are shown in Figure 16 and Figure 17 respectively.

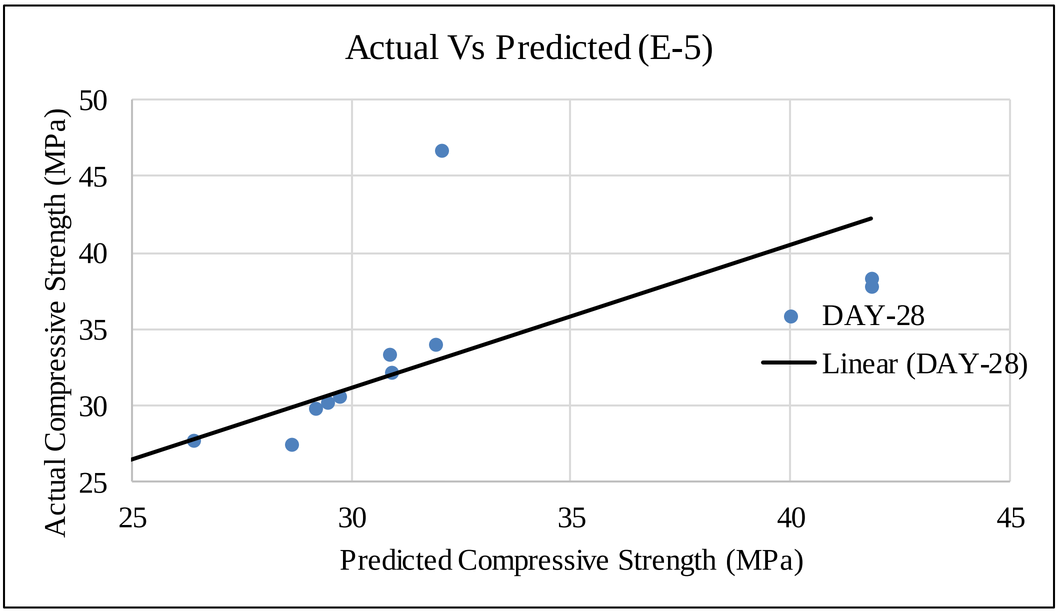


Figure 16- Predicted and Actual compressive strength of the training set using regression

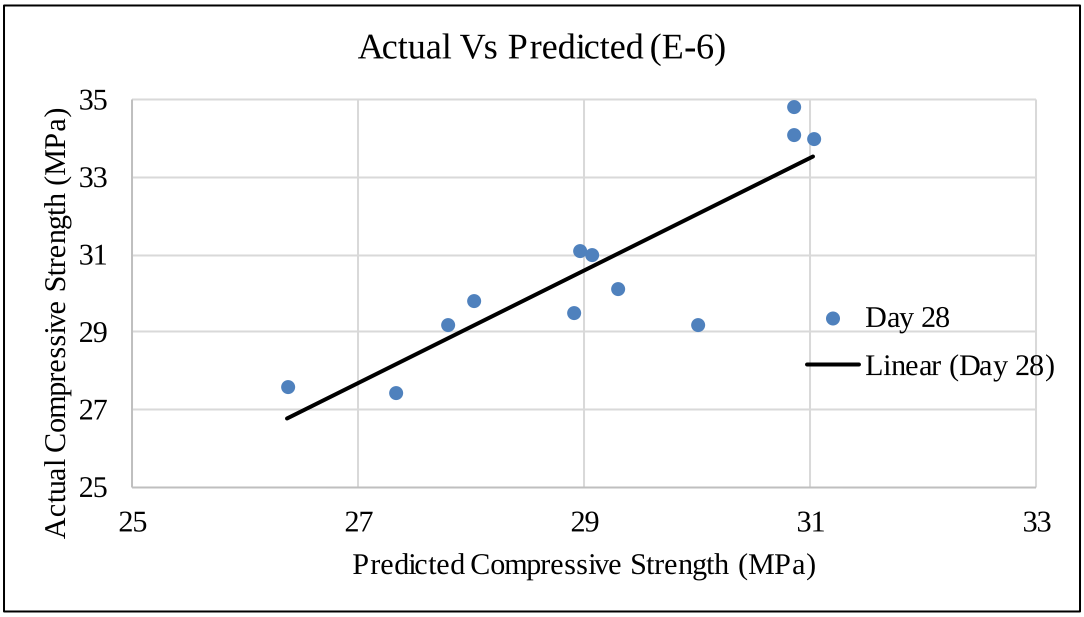


Figure 17- Predicted and Actual compressive strength of the training set using regression

The results from the regression analysis seem to be giving a fair picture of the compressive strength. Increasing R-squared values imply that refining the dataset in terms of water to cement ratio somehow gave strength to the prediction models. However, another experimental study was carried out which introduced one random sample[7] into the evaluation set. The inclusion of this sample greatly compromised the model, dropping the R-squared value of E-6 from 0.77 to 0.02.

[7] Cement=360kg/m$^3$, Water=187.2 kg/m$^3$, C.A=1041.18 kg/m$^3$, F.A=799.97 kg/m$^3$

## 3.3 PREDICTION OF COMPRESSION STRENGTH USING FUZZY LOGIC

### 3.3.1 The Fuzzy Inference Process and Model Parameters

This process entails defining the model parameters according to the five major steps as discussed in the literature review. From the list of available options, the ones selected in coming up with the prediction models are shown.

Both Mamdani and Sugeno types have been chosen in the modelling process. Matlab's fuzzy inference system generator, 'genfis 3' is used in this thesis as it allows for both subtractive clustering and fcm (fuzzy c-means clustering).

The fuzzy inference process has been carried out according to the previous discussions and the appropriate options are selected in the interface shown in Figure 18 .

Dataset I and Dataset II have been used to produce a model according to Mamdani and Sugeno types for different membership functions with the aim to explore the relationship between cluster types, fuzzy types and the strength of each predictive model. This task is easily supported on the features of the personalized GUI.

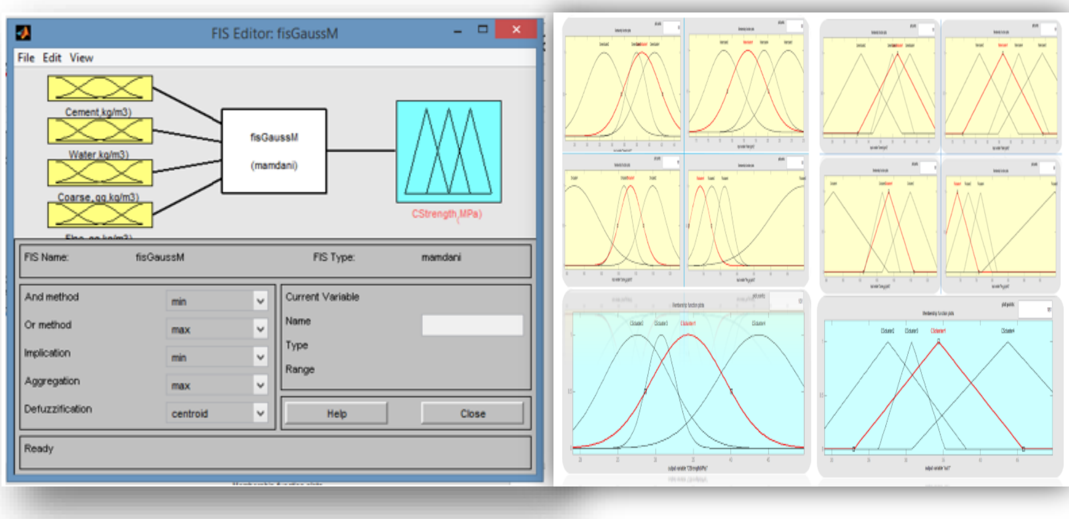


Figure 18- Setting up of the FIS _ FIS Editor (left) and Membership function editor (right)

Subtractive clustering is chosen for a sample calculation which will be carried out using the 28$^{th}$ day OPC test sample from data set II. Fcm clustering has been applied while producing the personalized graphical user interface.

The input and output parameters are crisp sets, obtained from the data described previously. A simple combination of ‘and’ for the implication process was achieved by the ‘minimum’ operator. Each rule is believed to contribute equally to the output set so a rule weight of 1 has been applied to each rule. For a single consequent (*y1*), outputs from all rules have been aggregated using ‘max’ for its relative simplicity in application when computer aided algorithms are not available. While using the Mamdani type, defuzzification has been carried out using the centroid method as the alternatives gave a less accurate result. ‘Wtaver’ method, which is also the default method is chosen for Sugeno-type FIS. Table 11 is a summary of the fuzzy inference process with the model parameters listed according to each FIS type.

Table 11- Summary of Inference Methods and Model Structure

| **Inference methods** | **Mamdani** | **Sugeno** |
|---|---|---|
| Fuzzy operator (AND) | Min | Product |
| Implication | Min | Min |
| Aggregation | Max | Sum |
| Defuzzification | Centroid | Weighted average |
| Number of membership functions | Variable | Variable |
| Type of input membership function | Variable | Variable |

### 3.3.2 Results and Discussion

The model carried out employing a subtractive clustering gave 3-cluster centers for both Mamdani and Sugeno inference types. MAPE and RMS-errors were computed (Table 12 and Table 13) and the errors show the produced model's efficiency tested against the training set and the validation set.

Table 12- Errors for the Training set

| **ERROR** | **MAMDANI** | | **SUGENO** | | |
|---|---|---|---|---|---|
| | Triangular MF | Gaussian MF | Triangular MF | Trapezoidal MF | Gaussian MF |
| **RMS** | 3.6 | 3.74 | 4.02 | 4.48 | 3.31 |
| **MAPE** | 12.77% | 11.9% | 11.0% | 11.0% | 6.8% |

Table 13 - Errors for the Testing set

| **ERROR** | **MAMDANI** | | **SUGENO** | | |
|---|---|---|---|---|---|
| | Triangular MF | Gaussian MF | Triangular MF | Trapezoidal MF | Gaussian MF |
| **RMS** | 3.6 | 3.74 | 4.01 | 4.48 | 3.31 |
| **MAPE** | 10.16% | 10.69% | 10.15% | 11.13% | 7.78% |

Figure 19 and Figure 20 comparatively show the model outputs for the Mamdani and Sugeno fuzzy inference types.

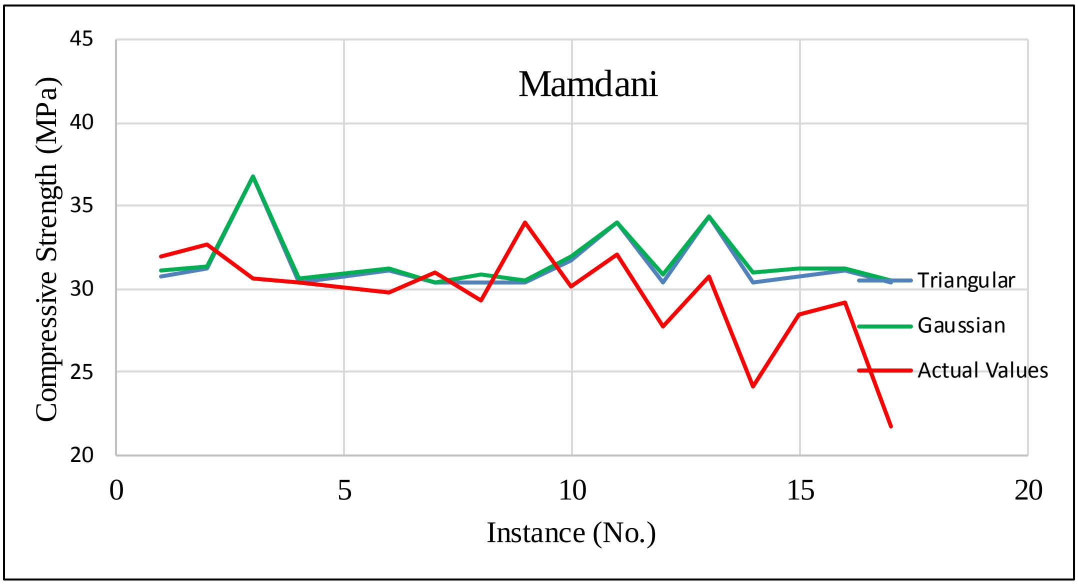


Figure 19- Model Output for Mamdani Type (different membership functions)

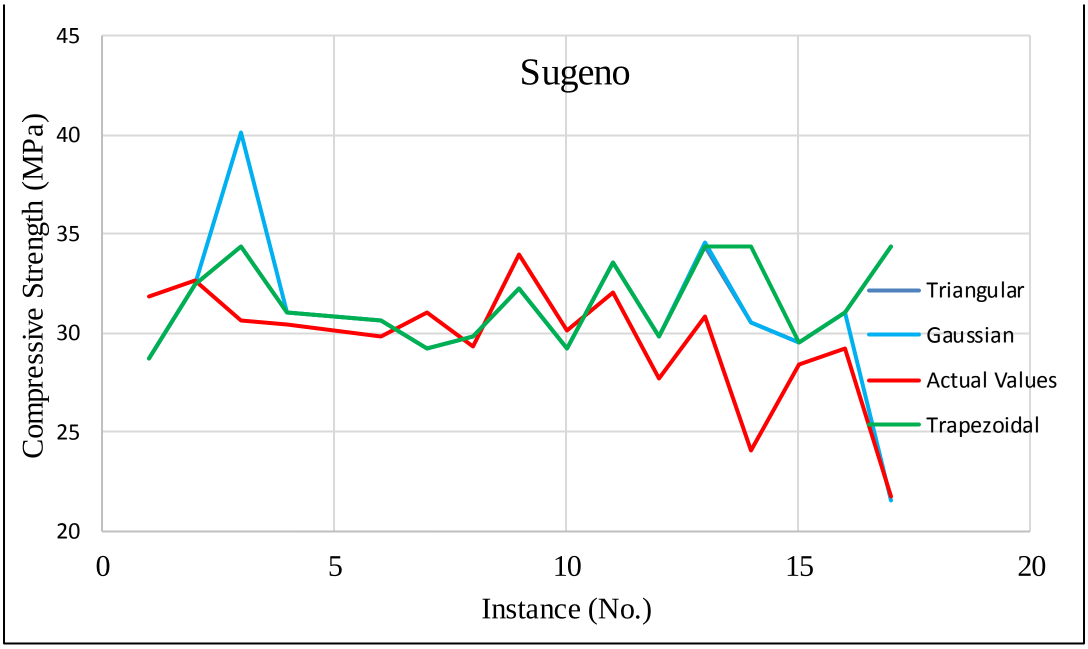


Figure 20- Model output for Sugeno Type (different membership functions)

The results show that Gaussian membership function with Sugeno type fuzzy inference system gives the best prediction both in the training and testing sets. Hence, this model parameter has been selected to further carry out interpretations on common knowledge (effect of W/C on concrete). This is shown in Figure 21, as the effect of water and cement at compressive strength surface for Gaussian membership functions

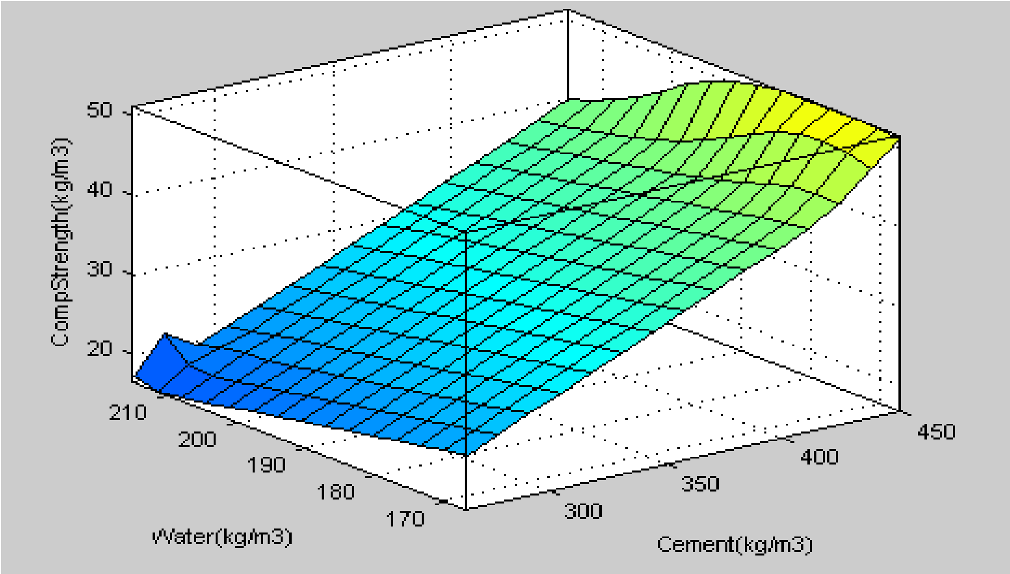


Figure 21- Water and Cement inputs with Comp. Strength surface

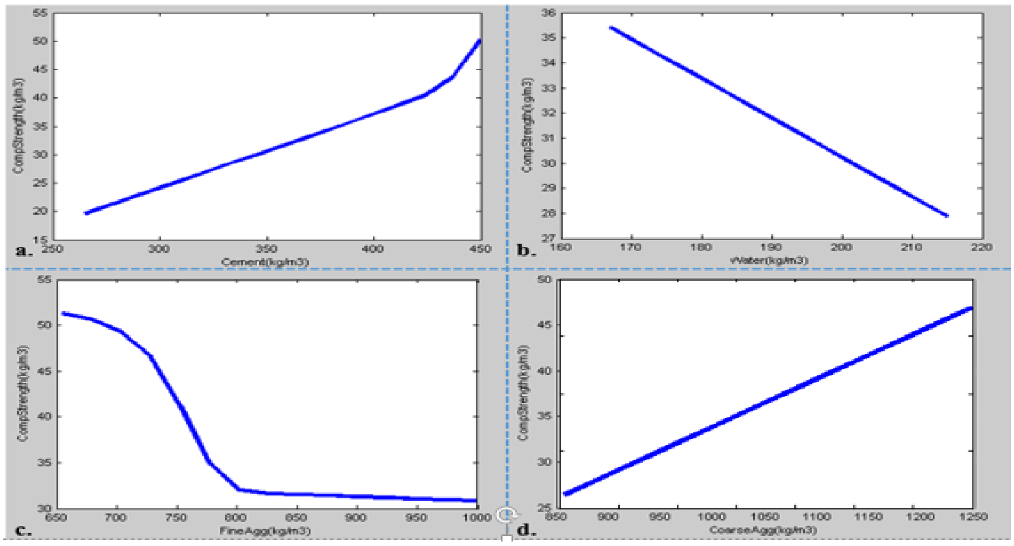


Figure 22-(a) Effect of cement on CS; (b) Effect of water on CS; (c) Effect of Fine Aggregate on CS; (d) Effect of Coarse Aggregate on CS

Figure 21 and Figure 22 try to capture the effect of ingredient proportions on compressive strength of concrete. The surface diagram shown in Figure 21 seems plausible as strength decreases with increasing water content and increases with increasing cement. Effect of aggregates on compressive strength was somehow depicted in the succeeding figure despite the fact that concrete strength is dictated by strength of the paste for normal strength concrete. Furthermore, as aggregates are inert materials, their properties are defined by other parameters like moisture content, porosity etc., and these properties are not included in the model.

Matlab "Personalized Graphical User Interface" has been adopted in the next section as a user-friendly and simpler method of computation.

### 3.3.3 Personalized Graphical User Interface

The interface has a format as shown below. After the data to be used to form the model is compiled, it is saved in .xls or .csv format. This Matlab program strongly encourages the use of .xls format so that multiple sheets can be handled. The user is required to input the path of the file name which is already prepared in a certain format. The format is prepared in such a way that the dataset to be used is categorized within training and testing divisions. The testing data (with respective inputs and outputs) should also precede the evaluation data in the excel file. The sheets in Ms. Excel will then take the form: "XTest, YTest, XEval, YEval". The user is required to prepare these inputs before going to the Matlab interface.

The file path/s will be copied in "File Name". This will give freedom to the user, as different datasets can be prepared at different files which the program will then concatenate before utilizing it in producing the model. The user may then choose the fuzzy logic type and the number of clusters to be used from the drop down option given. The "Evaluate Files" button will trigger generation of the Fismat needed to produce the model.

The user is faced with two options hereafter. Information about the input data set can be obtained from the "Show Graph" and "Show Table" option. The "Show Table" option has an extra feature that shows the variation of cluster numbers, fuzzy types and their accuracy. The other option is utilized if the result of a mix design is needed.

The inputs are attributes: cement, water and aggregates in kg/m$^3$. The "Evaluate Inputs" button will use the generated Fismat model to predict the compressive strength attained by the given mix proportion. The predicted compressive strength (MPa) will be displayed with the respective errors of the training dataset. These different types of errors are displayed so that the user will be the one to decide whether to use the predicted output in comparison with the computed error of the produced model.

The interface of the Matlab program is shown in Figure 23 with its features already explained.

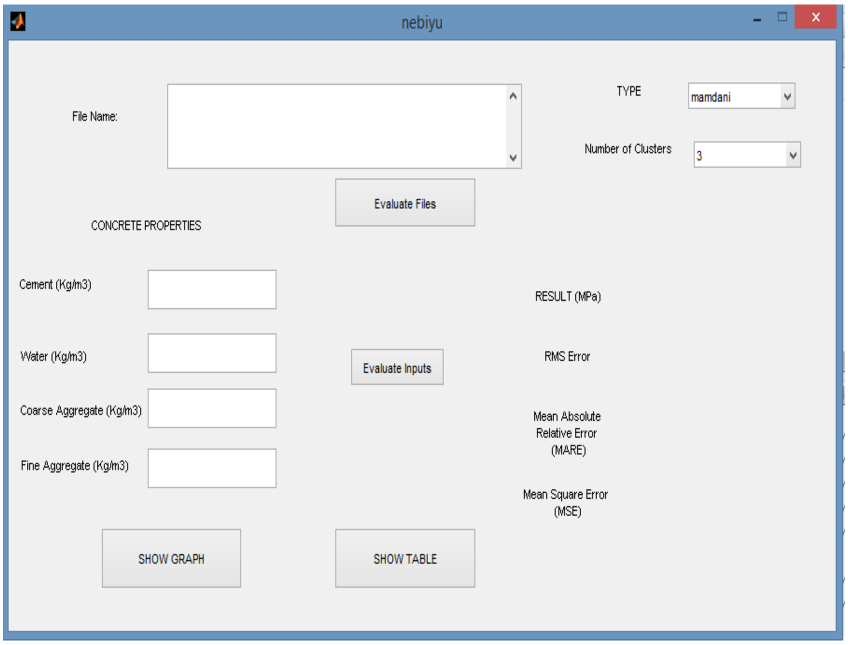


Figure 23- Matlab personalized graphical user interface

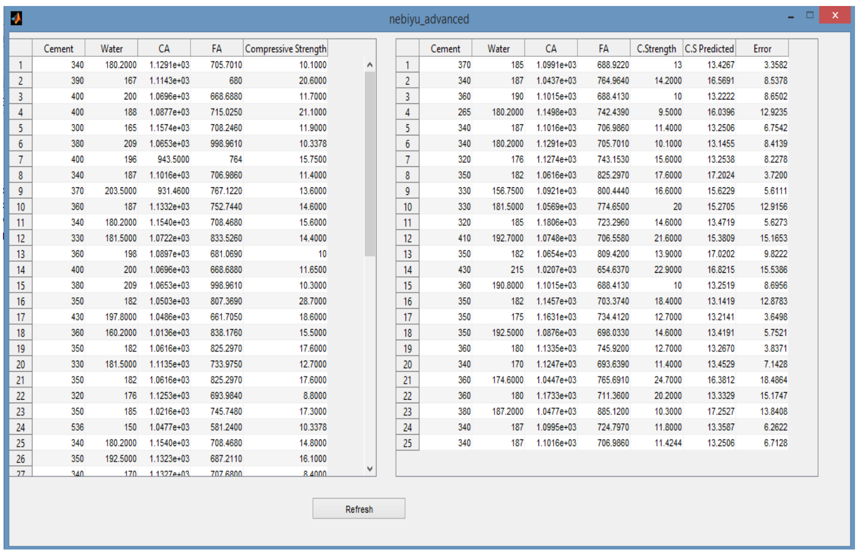


Figure 24- Output format for training and testing samples

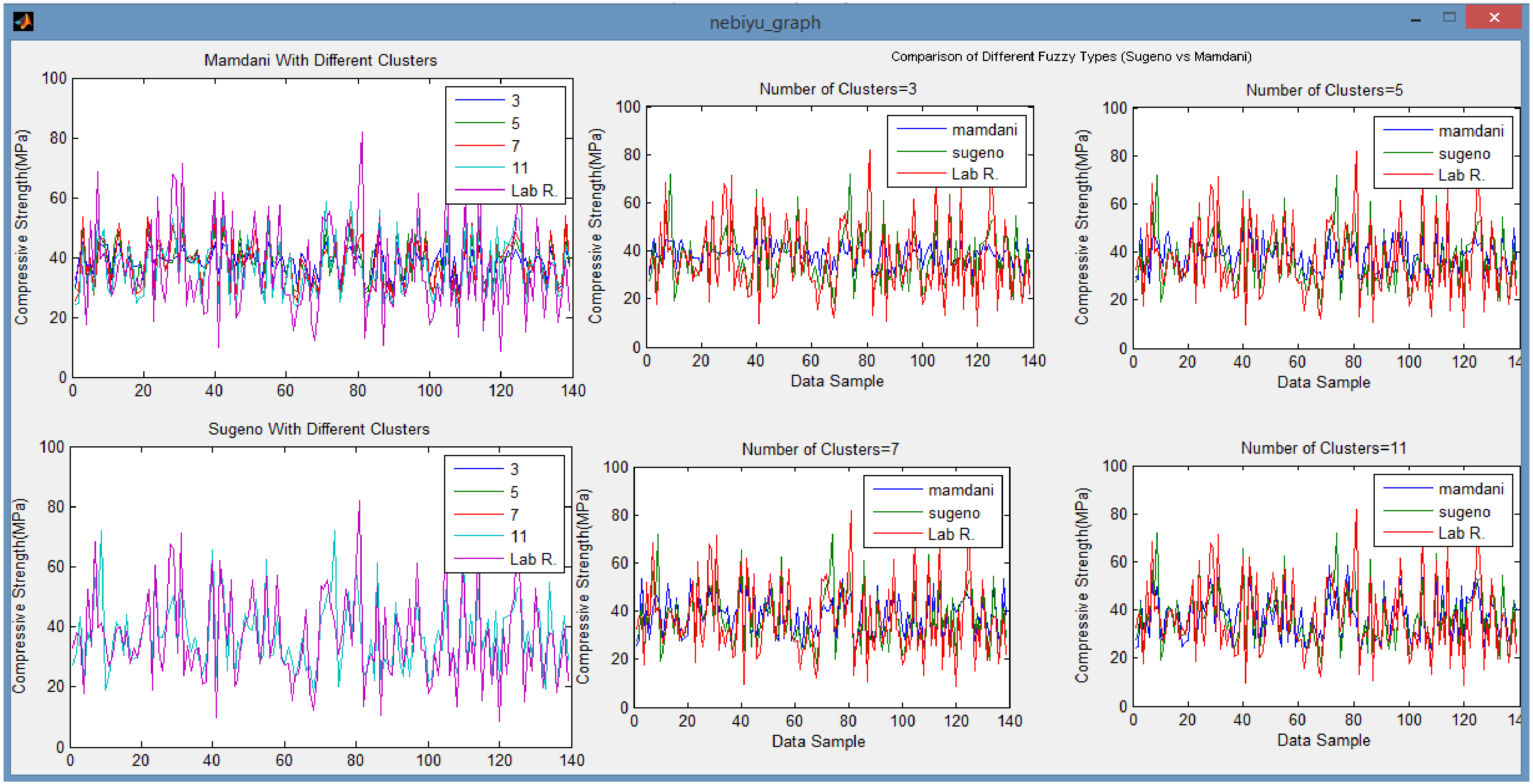


Figure 25- Comparison of Mamdani and Sugeno Fuzzy types for Dataset I (unmodified).

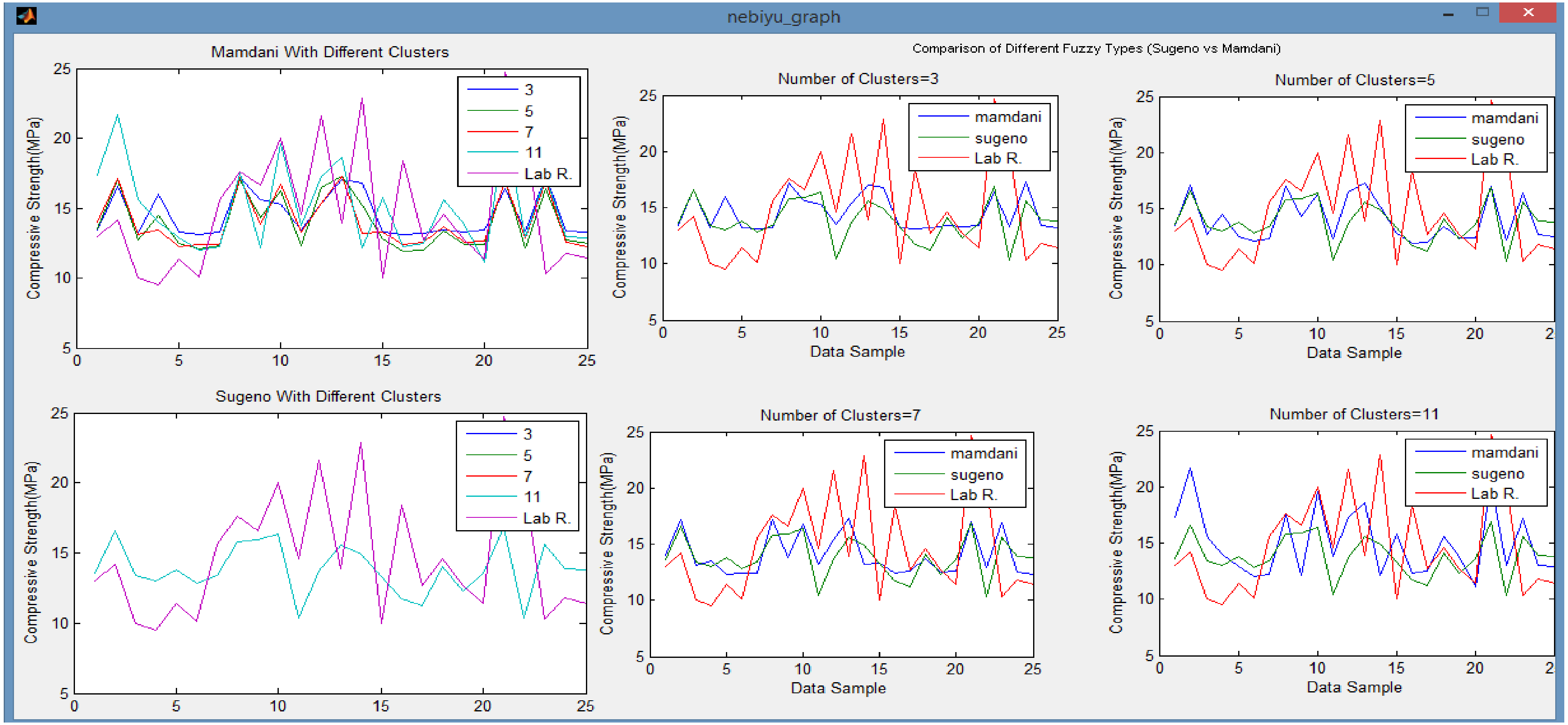


Figure 26- Comparison of Mamdani and Sugeno fuzzy types for Dataset II

The above analysis was done to compute the efficiency of the fuzzy logic model produced for dataset I. As the dataset was later modified to account for similarities with dataset II, analysis was done again with cement, water, coarse aggregate and fine aggregate as the new inputs for $28^{th}$ day compressive strength of dataset I. Mandani and Sugeno types with Gaussian membership functions and subtractive clustering method (all other modelling parameters similar) were considered. The results are shown in Figure 27.

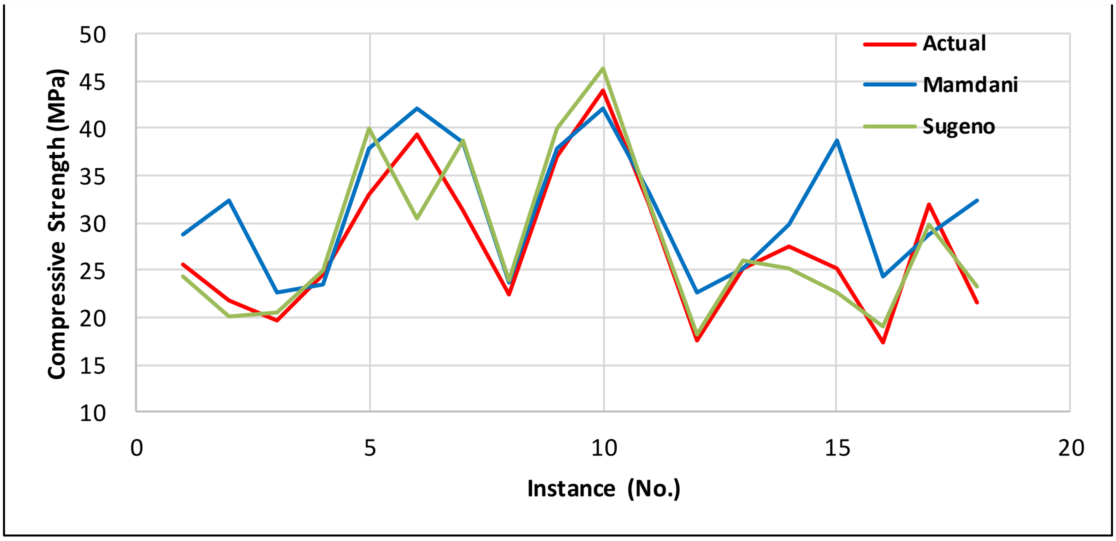


Figure 27- Comparison of Mamdani and Sugeno Types for Dataset I (modified)

Sugeno FIS with Gaussian membership function was already established to give a better prediction. This was shown at greater depth in Figure 27with the model outputs of dataset I (modified). The fact that much better predictions were achieved can be attributed to the quality of the dataset.

## 3.4 PREDICTION OF COMPRESSION STRENGTH USING ARTIFICIAL NEURAL NETWORK

### 3.4.1 ANN Procedure and Model Parameters

The following steps were followed for the modelling using artificial neural network method in the Matlab Neural Network toolbox.

**Step-1:** Start Matlab (Matlab version R2009b was used in this thesis)

**Step-2:** Import input and target data set (Dataset II): input and target values were imported from MS Excel which was already prepared in a matrix form for use in Matlab.

**Step-3:** Create Network: during creation of the network, feed-forward back propagation type of network was selected among the available network types. This is due to the efficiency and relative ease of this type of network compared to the other available options.

**Step-4:** Choose training function (for batch training): A network training function that adaptively updates weight and bias values according to gradient descent was selected. This selection was made keeping the network type in mind. Other alternatives also showed less learning capacity.

**Step-5:** Choose performance function: An MSE performance function was selected. It measures network performance according to the mean of squared errors.

**Step-6:** Choose number of hidden layers and number of neurons: One hidden layer was chosen as it has proven to be sufficient in many cases, and 4 hidden neurons were selected according to Tang et al.'s proposition. The number of neurons was increased until there was a significant improvement in the accuracy was observed.

**Step-7:** Choose transfer function: logistic Sigmoid (LOGSIG) and Tan Sigmoid (TANSIG) functions were used.

The neural network tool enables a user to create networks by first calling the network/data manager interface shown in Figure 26. Several data can be imported as input or output.

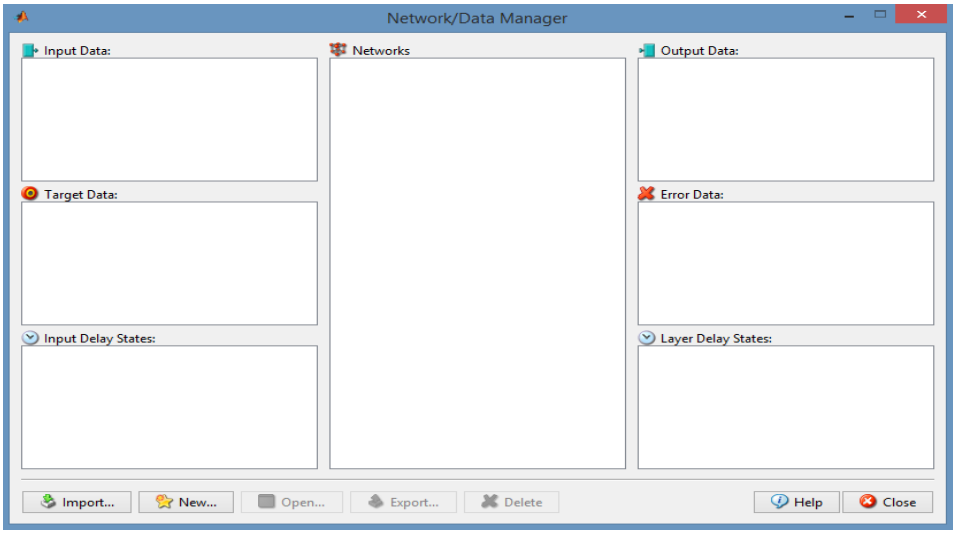


Figure 28- Data manager interface of the NN tool

Different network structures were experimented by varying the number of neurons in the hidden layer (4 up to 8), transfer function (LOGSIG and TANSIG) and learning rate (0.1, 0.6 and 1). After the network is created, the training process can begin.

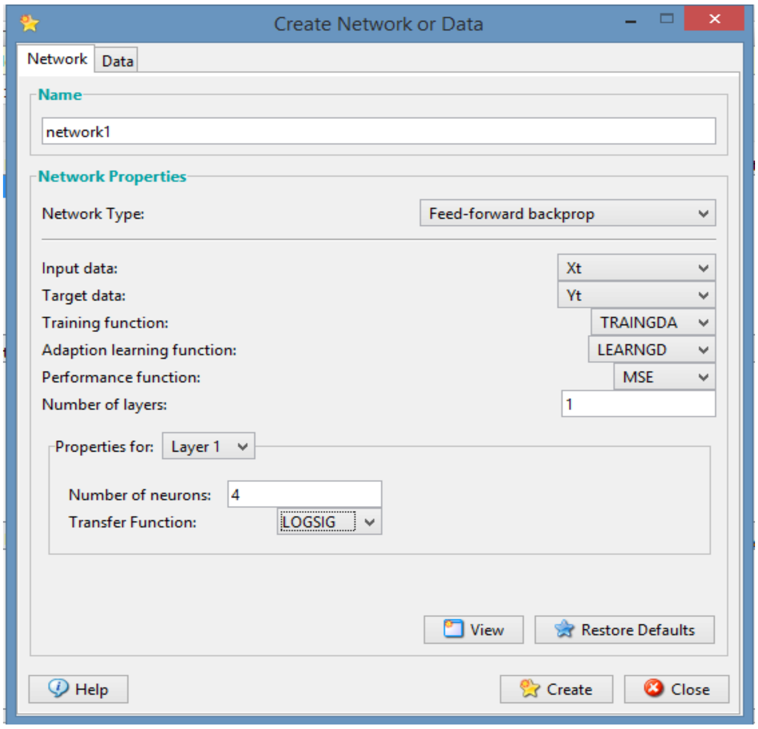


Figure 29- Network Creation in the NN toolbox

**Step-8:** Training the neural network: training information and parameters are set as shown in Figure 29. Ten networks were developed (Table 14) and trained by varying the transfer function and learning rate This shall make up for a total of 30 experiments, carried out for 3rd, 7th and 28th day compressive strength samples from data set 2. Figure 30 shows the incorporation of the network into Matlab for processing. For the purpose of simplicity, network number and learning rate (a=0.1, b=0.6, c=1) are used for nomenclature of the experiments carried out. This shall hold for all the subsequent steps.

Table 14- NN Model Parameters

| No. | NETWORK | No. of Neurons | Transfer Function | Learning Rate |
|---|---|---|---|---|
| **1** | 1 | 4 | LOGSIG | 0.1 |
| **2** | | | | 0.6 |
| **3** | | | | 1 |
| **4** | 2 | 4 | TANSIG | 0.1 |
| **5** | | | | 0.6 |
| **6** | | | | 1 |
| **7** | 3 | 5 | LOGSIG | 0.1 |
| **8** | | | | 0.6 |
| **9** | | | | 1 |
| **10** | 4 | 5 | TANSIG | 0.1 |
| **11** | | | | 0.6 |
| **12** | | | | 1 |
| **13** | 5 | 6 | LOGSIG | 0.1 |
| **14** | | | | 0.6 |
| **15** | | | | 1 |
| **16** | 6 | 6 | TANSIG | 0.1 |
| **17** | | | | 0.6 |
| **18** | | | | 1 |
| **19** | 7 | 7 | LOGSIG | 0.1 |
| **20** | | | | 0.6 |
| **21** | | | | 1 |
| **22** | 8 | 7 | TANSIG | 0.1 |
| **23** | | | | 0.6 |
| **24** | | | | 1 |
| **25** | 9 | 8 | LOGSIG | 0.1 |
| **26** | | | | 0.6 |
| **27** | | | | 1 |
| **28** | 10 | 8 | TANSIG | 0.1 |
| **29** | | | | 0.6 |
| **30** | | | | 1 |

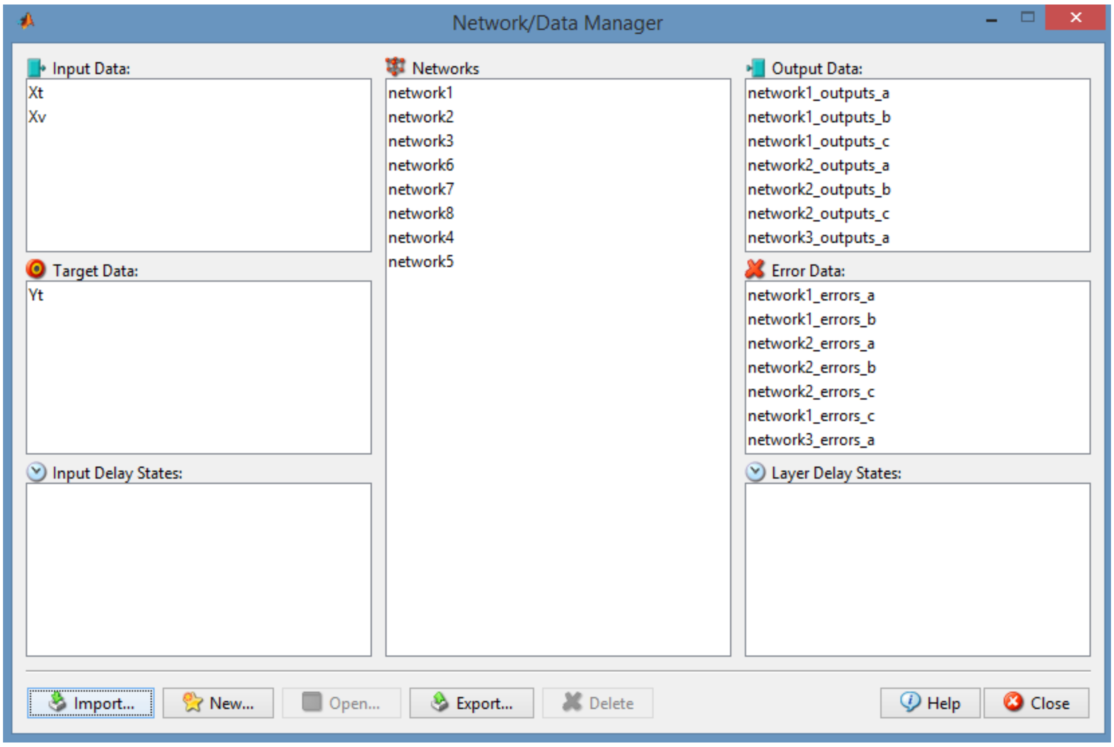


Figure 30- List of different networks created

**Step-9**: View the network performance: the network performance was viewed by using the various plots available in the network as shown in Figure 31.

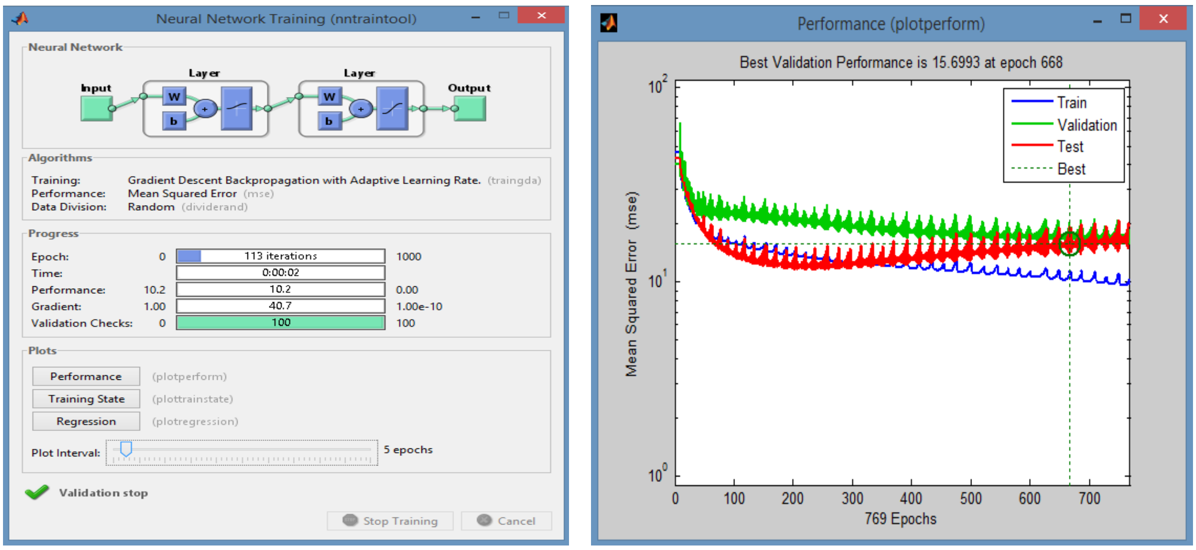


Figure 31-Network Performance and training

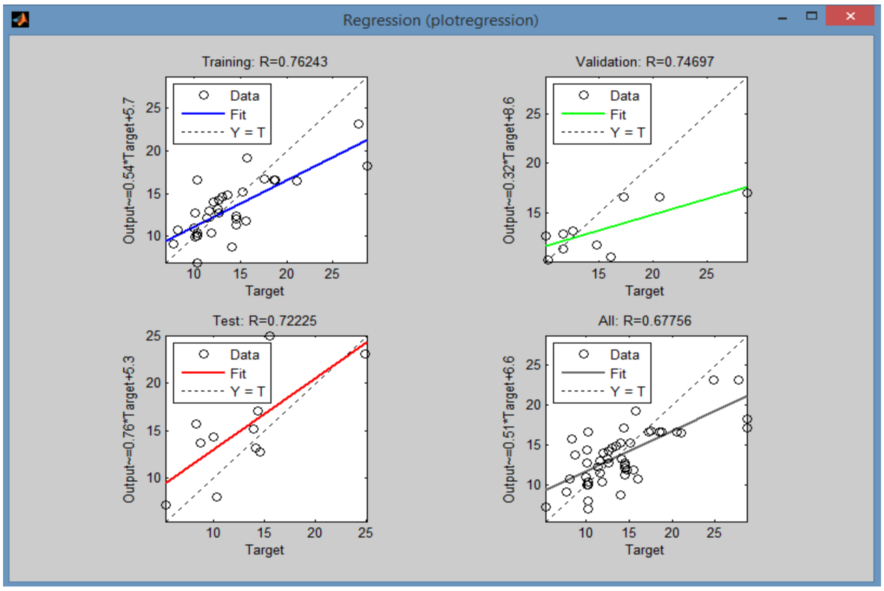


Figure 32- Example of regression plot

**Step-10**: Simulate the trained network: the trained network is simulated to obtain its response to the inputs in the training set. The outputs of the simulations are compiled in the results below.

Table 15 shows the network parameters for the ANN prediction models discussed above.

Table 15- Summary of Network Parameters

| | |
|---|---|
| Network Type: Multilayer feed forward back propagation<br>Learning function: Gradient descent method with momentum weight and bias<br>Performance function: Mean square error<br>Initial weight: Randomized<br>Stopping Criteria: Minimum gradient magnitude and validation checks | **LM training parameters**<br>▪ Minimum gradient : $1x10^{-10}$<br>▪ Validation Checks (Maximum fail): 100<br>▪ Maximum training epochs: 1000<br>▪ Performance goal: 0<br>▪ Learning rate: 0.1<br>▪ Lr_inc = 1.05<br>▪ Lr_dec= 0.7 |

### 3.4.2 Results and Discussion

After experimenting with a variety of network parameters, the observed performance and correlation coefficients are summarized in Table 16 and Table 17.

Table 16- Results of different network parameters (Day 3)

| NETWORK TYPE-CASE | R- Values | | | | Best Performance _ at Epoch-E |
|---|---|---|---|---|---|
| | Training | Testing | Validation | All -R | |
| 1-a | 0.717 | 0.756 | 0.666 | 0.71 | 17.395_E5 |
| 1-b | 0.66 | 0.706 | 0.784 | 0.699 | 6.96_E16 |
| 1-c | 0.697 | 0.895 | 0.584 | 0.7 | 11.305_E17 |
| 2-a | 0.84 | 0.848 | 0.555 | 0.782 | 10.024_E20 |
| 2-b | 0.824 | 0.565 | 0.843 | 0.79 | 5.233_E19 |
| 2-c | 0.813 | 0.646 | 0.466 | 0.793 | 4.678_E17 |
| 3-a | 0.15 | 0.19 | 0.43 | 0.238 | minimum grade reached |
| 3-b | -0.29 | -0.1 | -0.258 | -0.238 | |
| 3-c | -0.15 | -0.49 | -0.529 | -0.238 | |
| 4-a | 0.766 | 0.554 | 0.667 | 0.6397 | 6.717_E23 |
| 4-b | 0.87 | 0.03 | 0.12 | 0.62 | 16.01_E101 |
| 4-c | 0.719 | 0.904 | 0.593 | 0.747 | 7.73_E56 |
| 5-a | 0.81 | 0.867 | 0.666 | 0.757 | 2.0791_48 |
| 5-b | 0.807 | 0.786 | 0.961 | 0.827 | 23.768_E987 |
| 5-c | 0.863 | 0.889 | 0.448 | 0.827 | 3.363_E20 |
| 6-a | 0.801 | 0.607 | 0.273 | 0.637 | 10.97_E12 |
| 6-b | 0.733 | 0.807 | 0.487 | 0.674 | 15.18_E32 |
| 6-c | 0.724 | 0.742 | 0.643 | 0.689 | 17.25_E20 |
| 7-a | 0.311 | 0.286 | 0.598 | 0.304 | 21.58_E61 |
| 7-b | 0.42 | 0.77 | 0.307 | 0.343 | 35.839_E15 |
| 7-c | 0.273 | 0.047 | 0.823 | 0.336 | 11.9_E17 |
| 8-a | 0.748 | 0.51 | 0.455 | 0.666 | 20.947_E16 |
| 8-b | 0.783 | 0.5 | 0.169 | 0.638 | 20.277_E21 |
| 8-c | 0.778 | 0.199 | 0.494 | 0.692 | 8.83_E124 |
| 9-a | 0.63 | 0.645 | 0.181 | 0.521 | 17.77_E111 |
| 9-b | 0.891 | 0.516 | 0.508 | 0.796 | 19.95_561 |
| 9-c | 0.789 | 0.944 | 0.588 | 0.802 | 6.191_E15 |
| 10-a | 0.837 | 0.582 | 0.47 | 0.702 | 21.48_E15 |
| 10-b | 0.848 | 0.172 | 0.802 | 0.736 | 7.639_E126 |
| 10-c | 0.718 | 0.77 | 0.819 | 0.726 | 8.86_E40 |

Table 17- Results of different network parameters (Day 7)

| NETWORK TYPE-CASE | R- Values | | | | Best Performance _ at Epoch-E |
|---|---|---|---|---|---|
| | Training | Testing | Validation | All -R | |
| 1-a | 0.79 | 0.64 | 0.62 | 0.73 | 23.34_E249 |
| 1-b | 0.80 | 0.78 | 0.12 | 0.64 | 37.6_E0 |
| 1-c | 0.80 | 0.71 | 0.47 | 0.71 | 36.35_E0 |
| 2-a | 0.80 | 0.55 | 0.89 | 0.75 | 13.25_E0 |
| 2-b | 0.88 | 0.77 | 0.59 | 0.80 | 26.81_E21 |
| 2-c | 0.90 | 0.77 | 0.74 | 0.85 | 16.76_E18 |
| 3-a | 0.80 | 0.26 | 0.05 | 0.59 | 29.8_E32 |
| 3-b | 0.66 | 0.67 | 0.21 | 0.57 | 49.9_E0 |
| 3-c | 0.83 | 0.39 | 0.44 | 0.68 | 45.43_E120 |
| 4-a | 0.91 | 0.57 | 0.54 | 0.82 | 32.86_E525 |
| 4-b | 0.92 | 0.33 | 0.56 | 0.83 | 16.65_E950 |
| 4-c | 0.87 | 0.81 | 0.87 | 0.84 | 15.67_E0 |
| 5-a | 0.87 | 0.92 | 0.47 | 0.72 | 47.9_E0 |
| 5-b | 0.92 | 0.11 | 0.37 | 0.77 | 26_E0 |
| 5-c | 0.86 | 0.68 | 0.09 | 0.72 | 16.5_E0 |
| 6-a | 0.78 | 0.74 | 0.64 | 0.73 | 50.5_E1000 |
| 6-b | 0.90 | 0.73 | 0.29 | 0.78 | 22.52_E83 |
| 6-c | 0.89 | 0.69 | 0.78 | 0.79 | 9.6_E395 |
| 7-a | 0.65 | 0.54 | 0.84 | 0.55 | 19.31_E412 |
| 7-b | 0.78 | 0.73 | 0.59 | 0.72 | 31.26_E121 |
| 7-c | 0.72 | 0.82 | 0.77 | 0.71 | 26.26_E999 |
| 8-a | 0.88 | 0.78 | 0.62 | 0.79 | 20.69_E26 |
| 8-b | 0.80 | 0.90 | 0.29 | 0.78 | 24.8_E940 |
| 8-c | 0.88 | 0.81 | 0.86 | 0.83 | 12.35_E23 |
| 9-a | 0.80 | 0.77 | 0.43 | 0.75 | 17.12_E962 |
| 9-b | 0.85 | 0.87 | 0.69 | 0.81 | 17.28_E181 |
| 9-c | 0.80 | 0.74 | 0.70 | 0.77 | 21.81_E31 |
| 10-a | 0.87 | 0.43 | 0.47 | 0.68 | 43_E53 |
| 10-b | 0.84 | 0.70 | 0.18 | 0.59 | 55_E0 |
| 10-c | 0.90 | 0.45 | 0.15 | 0.65 | 49.15_E0 |

After experimenting with several network parameters, the tangent sigmoid activation function with 4 neurons in the hidden layer was found to be more efficient in both cases. Learning rate of 0.1 showed a higher performance, measured by the amount of mean squared error. Hence, for the specific set of experiments carried out given the previously defined modelling parameters, the tangent sigmoid activation function with 4 hidden neurons was able to train better at a learning rate of 0.1 and map the testing values with a higher performance.

This model parameter was used for modelling the 28$^{th}$ day compressive strength of concrete. The result of the model is shown in Table 18. Furthermore, 30% of the dataset's sample was reserved for simulation, with the results shown in Figure 33-Simulation of the ANN model.

Table 18-Result of the 28$^{th}$ day strength predicting model

| NETWORK TYPE-CASE | R- Values | | | | Best Performance _ at Epoch-E |
|---|---|---|---|---|---|
| | Training | Testing | Validation | All -R | |
| 1-a | 0.92 | 0.92 | 0.8 | 0.9 | 3.21_E19 |

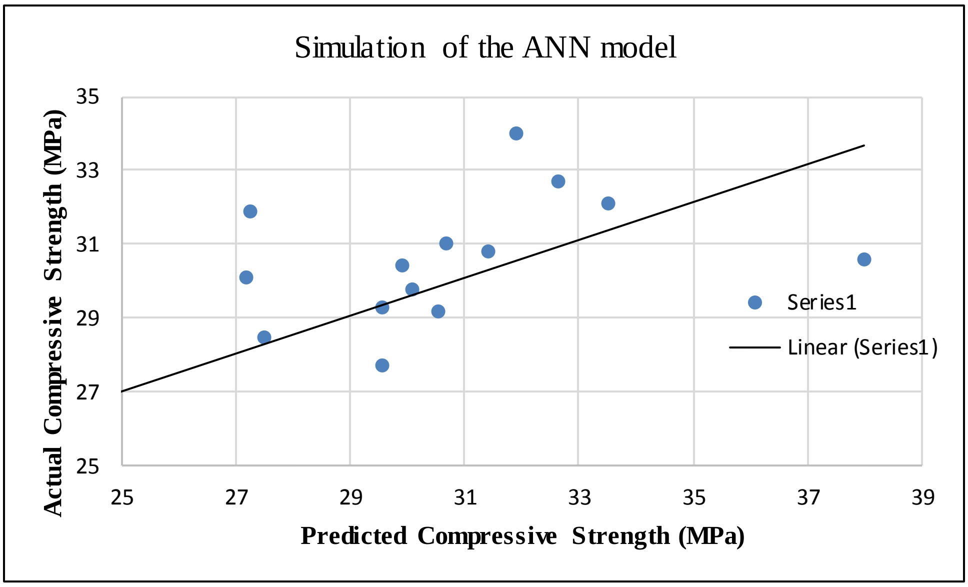


Figure 33- Simulation of the ANN model

## 3.5 PREDICTION OF COMPRESSION STRENGTH USING THERMODYNAMIC METHOD

As discussed in the literature review, hydration of cement plays a key role in the strength gain of concrete. In order to get a clear picture of this strength gain process, one needs to quantify the cement hydration occurring in the concrete mix. This method tries to predict the compressive strength of concrete basing such hydration.

### 3.5.1 Compressive Strength vs. Water to Cement Ratio

For a 'fully' compacted concrete (about 1% of air voids [5]), the strength is inversely proportional to the water to cement ratio. This has been quantified by Duff Abrams in 1919, with an empirical formula shown in Equation (3-2) [5].

$$fc = \frac{K_1}{K_2^{w/c}} \qquad (3\text{-}2)$$

Where

fc = compressive strength

$K_1$ and $K_2$ = empirical constants

w/c = water to cement ratio

The relationship between strength and water to cement ratio has been discussed in the literature review. As one of the fundamental tools used in the mix design of concrete, the effect w/c ratio has on the overall strength of a prepared concrete was analyzed using the laboratory results. Hence, the datasets were interpreted according to this concept. And dataset-2 was even more specifically defined in terms of the type of cement involved. The results of this analysis are displayed below and interpreted later.

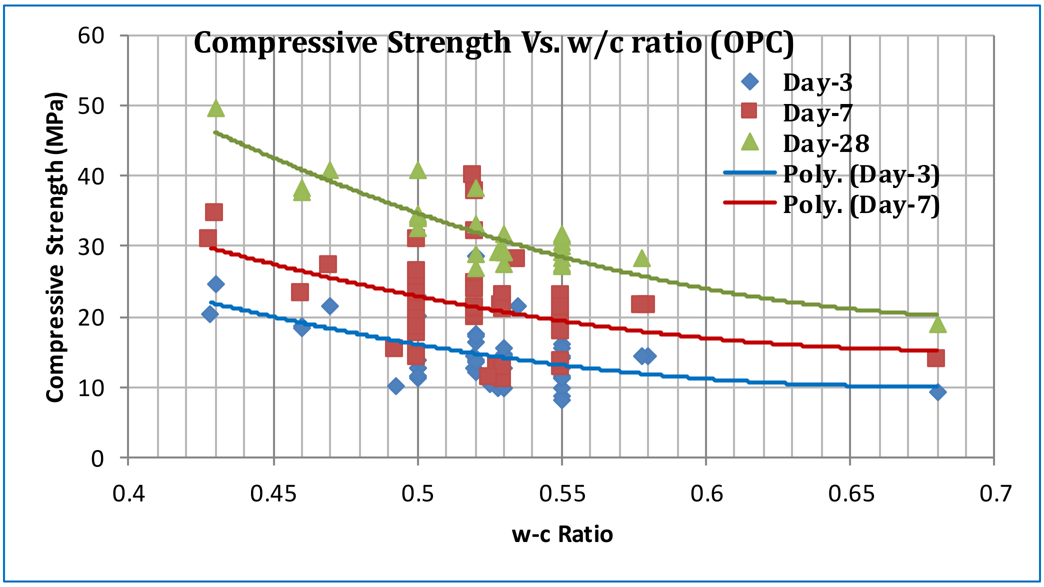


Figure 34- Compressive Strength vs. w-c ratio for concrete with OPC- type cement

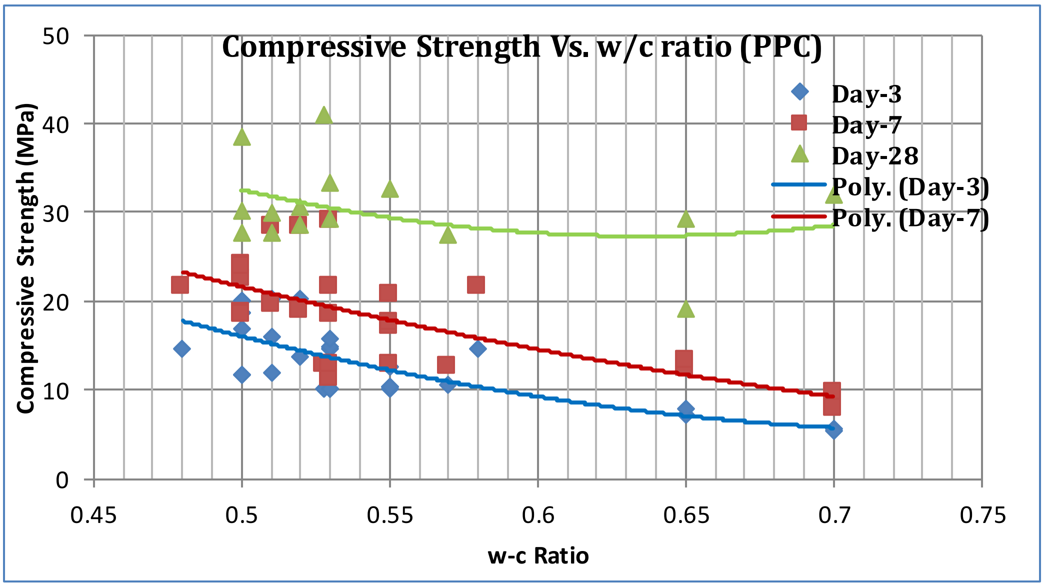


Figure 35- Compressive Strength vs. w-c ratio for concrete with PPC- type cement

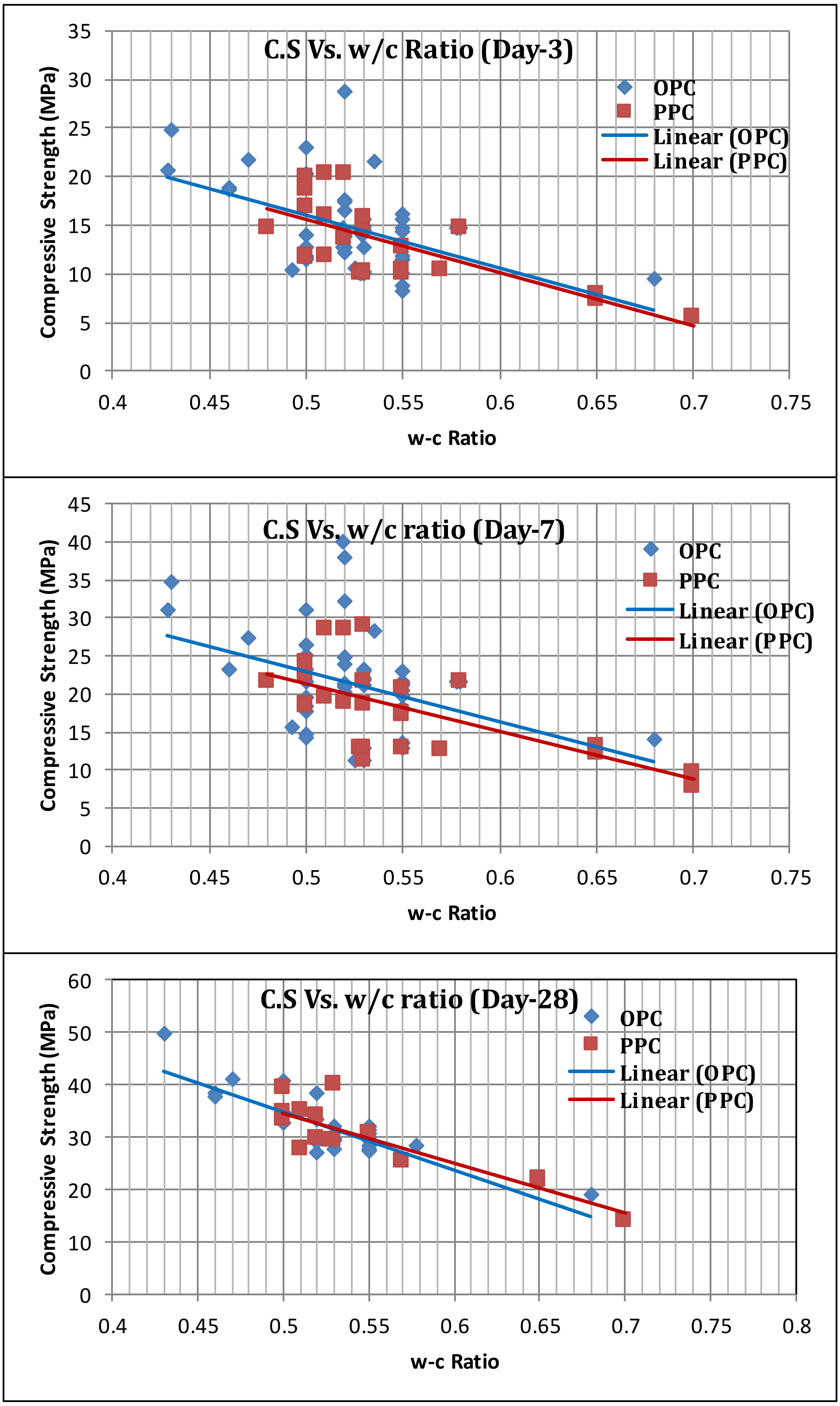


Figure 36- Compressive Strength vs. w/c ratio for OPC and PPC cement types at different days of testing

Two things can be inferred from the results obtained.

- The relationship between water to cement ratio and compressive strength was fairly reflective of the relationship proposed by Duff Abrams [5].
- The 28th day compressive test results of concrete with PPC type cement (Figure 34) were found to be higher when compared with that of OPC test results (Figure 35) at higher water to cement ratios. This is probably due to the secondary hydration of pozollans (in PPC type cement) which activates at later age.

The compressive strength development of OPC and PPC cement types is shown in Figure 36. For a given concrete with a fixed water to cement ratio, it can be seen that the compressive strength at early ages is higher in OPC type cement. The delaying effect encountered with the inclusion of pozollans became apparent at the third and seventh day of testing. Consequently, a delayed strength gain was visible in concretes with PPC cement type at 28$^{th}$ day of testing. A much better distinction could be done if the mineral composition of the pozollanic cement were known.

### 3.5.2 Model Parameters and Calculation

Analysis was carried out for the three types of cement locally available: Derba, Muger and National Cement. The concrete sample Table 7 can be inferred for mineral composition of these cement types. Three different casting temperatures; 10 $^0$C, 20 $^0$C and 32 $^0$C, with varying mix proportions were examined. The experiment parameters are listed in Table 19 and Table 22.

The analysis process has two phases:

- Verification of the model's outputs with laboratory results for testing days of 3, 7 and 28 for different mixes and cement types. Samples with the same cement content were chosen tacitly to also see the effect of water to cement ratio on the development of strength (which also paves the way to the second phase).
- After verification, further analysis of the model's outputs will be carried out. The relationship between adiabatic temperature rises, degree of hydration and development of compressive strength is studied for different initial

temperatures and cement types (which vary according to cement mineral compositions).

Three OPC cement types with varying clinker compositions are chosen to represent this analysis process (Derba, Muger and National Cement)[8] due to the difference of their mineral composition, especially alite to belite ratio (National Cement vs. the rest). In this regard, the effect of alite to belite ratio in affecting the hydration rate is also captured.

Furthermore, ettringite formation and monosulphate conversion processes, as well as the progression of hydration rate vs. accumulated heat in each mineral component is studied for varying initial temperatures.

Table 19- Experiment Parameters for Thermodynamic Analysis

| | **W/C (%)** | **Cement ($kg/m^3$)** | **Coarse Aggregate ($kg/m^3$)** | **Fine Aggregate ($kg/m^3$)** | **Specific Gravity** | | | **Cement Type** |
|---|---|---|---|---|---|---|---|---|
| | | | | | **Cement** | **C.A** | **F.A** | |
| **C-1** | 0.55 | 350 | 1132.28 | 687.21 | 3.15 | 2.79 | 2.54 | Derban |
| **C-2** | 0.52 | 350 | 1050.25 | 807.37 | 3.15 | 2.78 | 2.61 | Derban |
| **C-3** | 0.55 | 350 | 1087.30 | 698.03 | 3.15 | 2.68 | 2.58 | Derban |
| **C-4** | 0.52 | 350 | 1145.73 | 703.37 | 3.15 | 2.78 | 2.56 | Muger |
| **C-5** | 0.58 | 320 | 1180.55 | 723.30 | 3.15 | 2.84 | 2.61 | Mesobo |

[8] Mineral composition can be found at Table 7.

### 3.5.3 Results and Discussion

These samples were used to carry out phase one. The 3rd, 7th and 28th day compressive strength tests were consequently compared with the DuCOM analysis results. These comparisons are shown in Table 20.

Table 20- Experimental vs. DuCOM analysis results

| | Day-3 | | Day-7 | | Day-28 | |
|---|---|---|---|---|---|---|
| | **Actual** | **Predicted** | **Actual** | **Predicted** | **Actual** | **Predicted** |
| **C-1** | 16.1 | 17.31 | 23 | 25.74 | 30.1 | 30.1 |
| **C-2** | 28.7 | 15.45 | 32.1 | 26.18 | 38.4 | 38.33 |
| **C-3** | 14.2 | 13.09 | 22 | 23.1 | 29.3 | 34.2 |
| **C-4** | 16.5 | 7.59 | 20.1 | 21.05 | 29.1 | 38.7 |
| **C-5** | 14.6 | 3.76 | 21.6 | 10.10 | 28.3 | 28.4 |

### 3.5.4 Further Applications of the Thermodynamic Analysis

The advantage with the thermodynamic analysis is we can determine a progressive development of compressive strength, temperature, degree of hydration, water content, porosity, relative humidity etc. This has very important applications in modifying properties like durability of the concrete. Hence, the following section tries to capture the relationship between the different cement types (Derba, Muger and National Cement) versus the possible compressive strength, temperature and degree of hydration attained with different water to cement ratios and casting temperatures.

#### *3.5.4.1 Model Parameters*

The previous endeavor was pursued by considering various scenarios, performing several simulations that are based on thermodynamic principles. A total of 28 experiments were carried out with parameters shown in Table 22. Accordingly, experiments F-1 up to F-27 were completed with the same mix design (C-1). There was no specific reason for choosing this specific mix, only the need to compare the behaviors on the same platform.

In order to achieve good results at phase two, analysis using DuCOM was carried out in a total of 96 steps. In an attempt to capture the early hydration process, more steps were added at the early days of hydration. The choice of the time step is shown in Table 21.

Table 21- Time step for DuCOM analysis

| STEP | Time Step (Day) | Total Time Step (Day) | Total Time Average (Day) |
|---|---|---|---|
| 1 – 10 | 0.01 | 0.1 | 0.1 |
| 10 – 20 | 0.02 | 0.2 | 0.3 |
| 20 – 34 | 0.05 | 0.7 | 1 |
| 34 – 54 | 0.1 | 2 | 3 |
| 54 – 74 | 0.2 | 4 | 7 |
| 74 – 96 | 1 | 22 | 29 |

Table 22-Simulations for comparative study

| Experiment | Cement Type | T( $^0$C) | w/c (% weight) |
|---|---|---|---|
| F-1 | Derba | 20 | 0.55 |
| F-2 | Muger | 20 | 0.55 |
| F-3 | N.Cement | 20 | 0.55 |
| F-4 | Derba | 10 | 0.55 |
| F-5 | Muger | 10 | 0.55 |
| F-6 | N.Cement | 10 | 0.55 |
| F-7 | Derba | 32 | 0.55 |
| F-8 | Muger | 32 | 0.55 |
| F-9 | N.Cement | 32 | 0.55 |
| F-10 | Derba | 20 | 0.2 |
| F-11 | Muger | 20 | 0.2 |
| F-12 | N.Cement | 20 | 0.2 |
| F-13 | Derba | 10 | 0.2 |
| F-14 | Muger | 10 | 0.2 |
| F-15 | N.Cement | 10 | 0.2 |
| F-16 | Derba | 32 | 0.2 |
| F-17 | Muger | 32 | 0.2 |
| F-18 | N.Cement | 32 | 0.2 |
| F-19 | Derba | 20 | 0.65 |
| F-20 | Muger | 20 | 0.65 |
| F-21 | N.Cement | 20 | 0.65 |
| F-22 | Derba | 10 | 0.65 |
| F-23 | Muger | 10 | 0.65 |
| F-24 | N.Cement | 10 | 0.65 |
| F-25 | Derba | 32 | 0.65 |
| F-26 | Muger | 32 | 0.65 |
| F-27 | N.Cement | 32 | 0.65 |

### *3.5.4.2 Results and Discussion*

The following section shows result of DuCOM analysis. The outputs try to show the effect of cement type and water to cement ratio on the progression of properties such as compressive strength, degree of hydration and temperature rise in concrete.

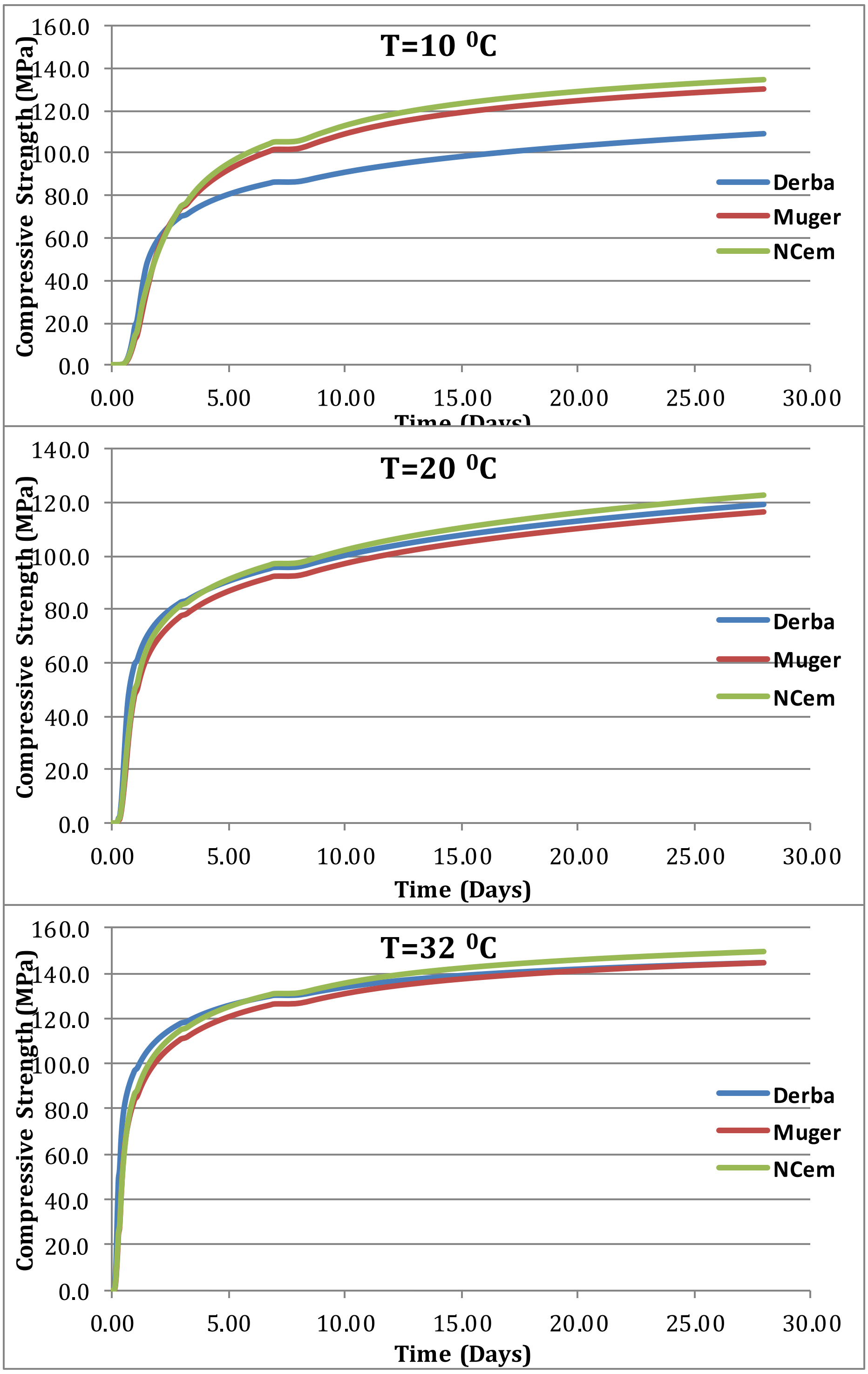


Figure 37- Compressive Strength vs. time for different cement types at varying initial temperatures for (W/C=0.2)

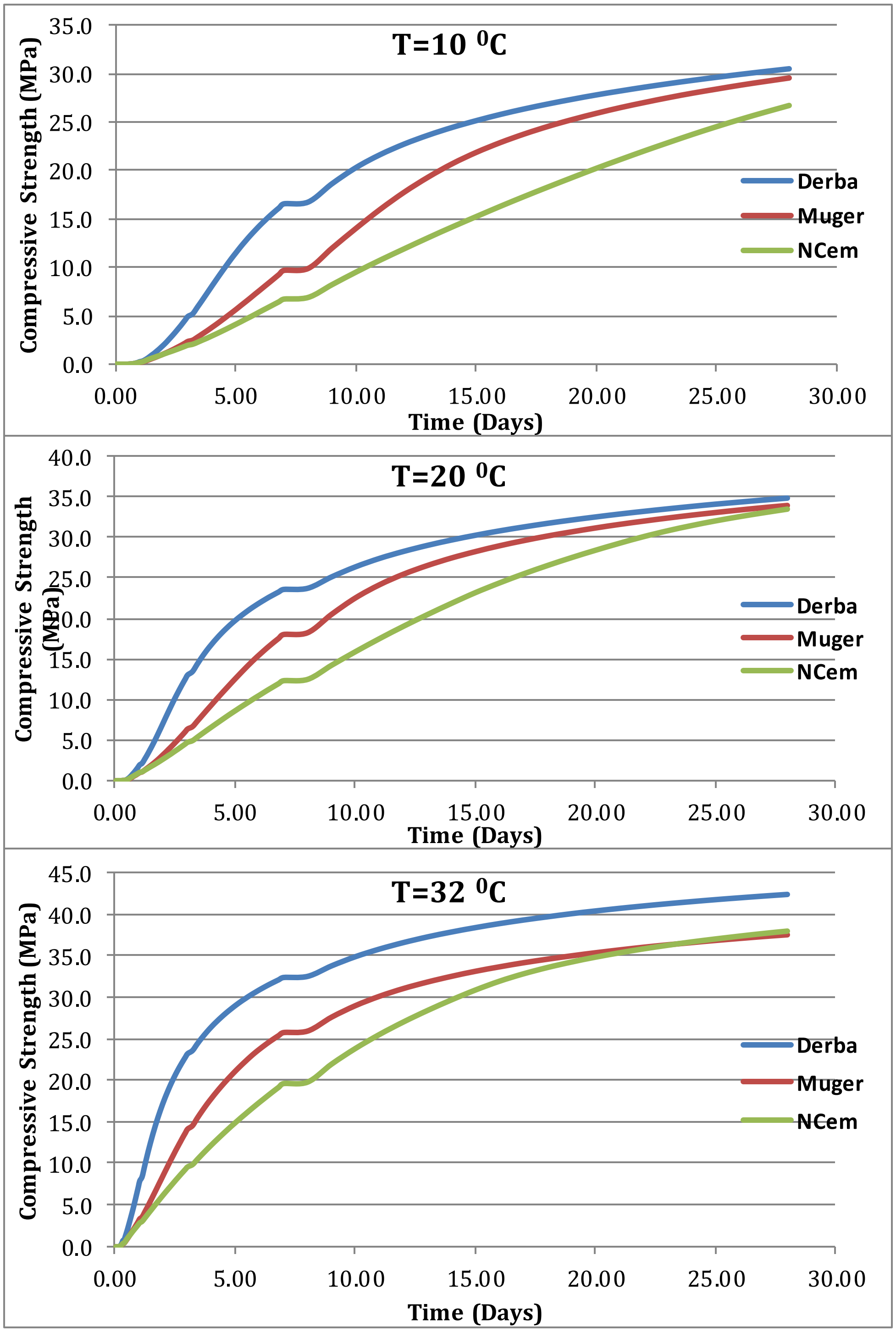


Figure 38- Compressive Strength vs. time for different cement types at varying initial temperatures for (W/C=0.55)

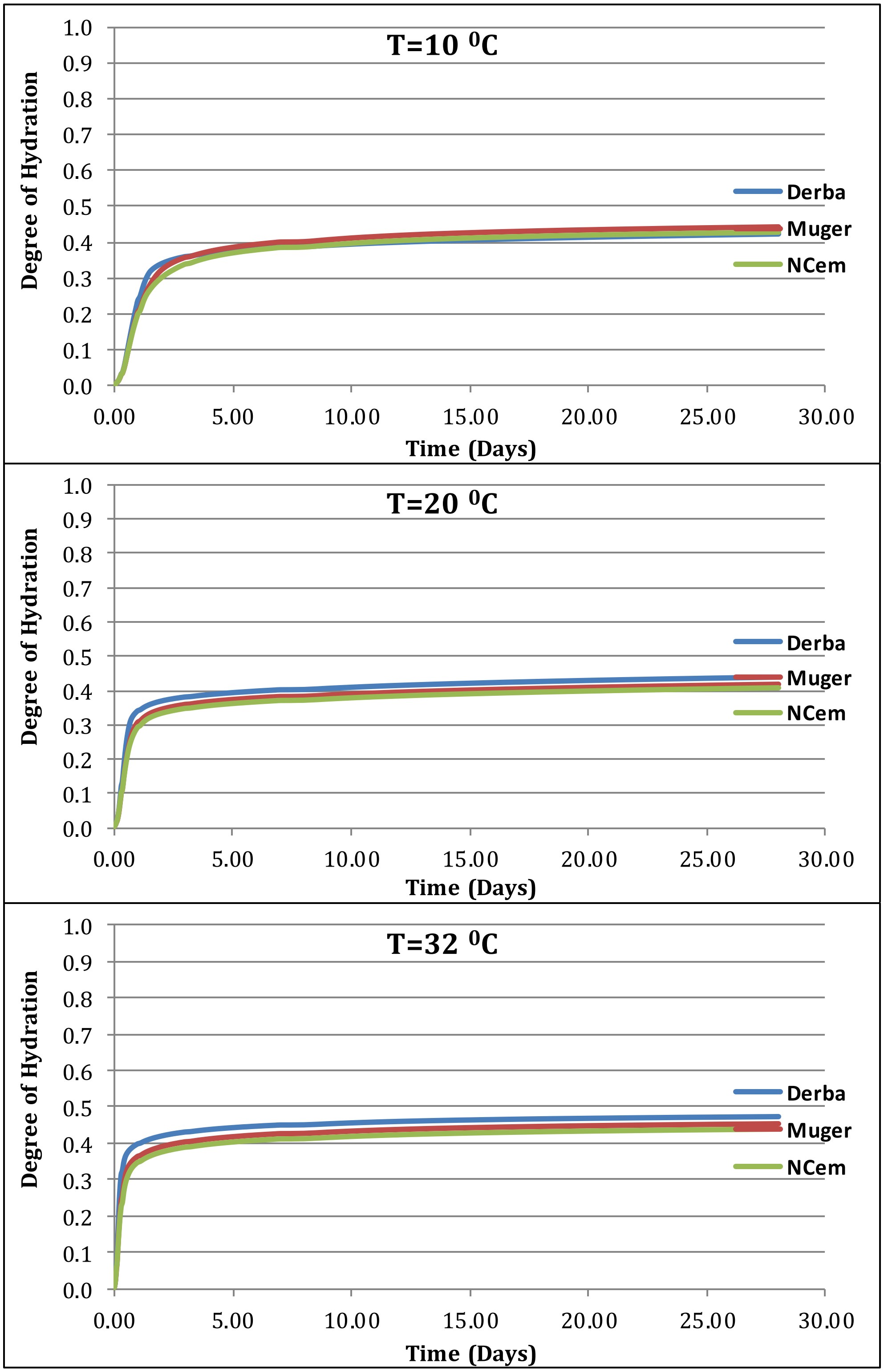


Figure 39- Degree of Hydration vs. time for different cement types at varying initial temperatures for (W/C=0.2)

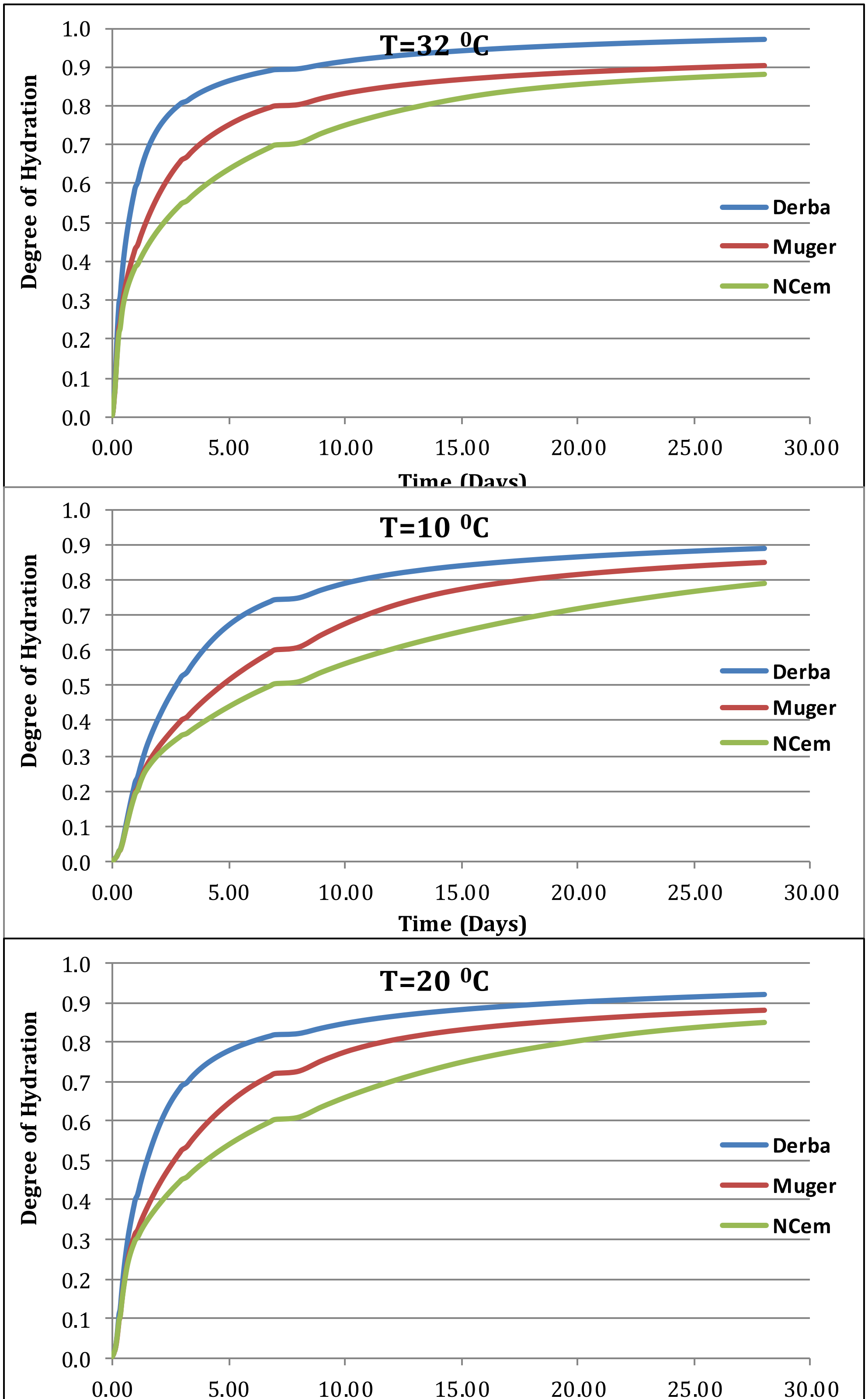


Figure 40- Degree of Hydration vs. time for different cement types at varying initial temperatures for (W/C=0.55)

Figure 37 and Figure 38 show the progression of compressive strength within the extent of the 28-day time step set by the model. A lot of information can be extracted from the figures. Perhaps the most important one is the progression of early age strength at different temperatures. One can easily see the curves at early age get more benign as the water to cement ratio increases and vice versa. Compressive strength gain gets faster at higher temperatures which may be related with the facilitation of hydration.

However, hydration occurrence does not necessitate increase in compressive strength. This is shown in Figure 39 and Figure 40. Keeping water to cement ratio constant, one can easily relate the degree of hydration with the achieved compressive strength from previous figures and see that compressive strength is actually lower in cases where the degree of hydration is higher.

This phenomenon can be explained by porosity. At higher water to cement ratios, the porous space occupied by water is filled with hydration products. Therefore, the creation of hydration products is actually necessary for strength gain. However, at lower water to cement ratios, hydration is governed by the availability of space. More un-hydrated cement particles exist; which is actually very good as cement is stronger, un-hydrated. If there is enough water to enable creation of paste for binding purposes, higher strength concrete can be achieved.

Figure 41 shows the temperature rise. Relationship between such temperature rise and its contribution to hydration is one of the many information that can be extracted. The temperature spikes are higher at higher temperatures; and even much higher at lower water to cement ratios. This is important while considering massive concrete structures at very warm environments.

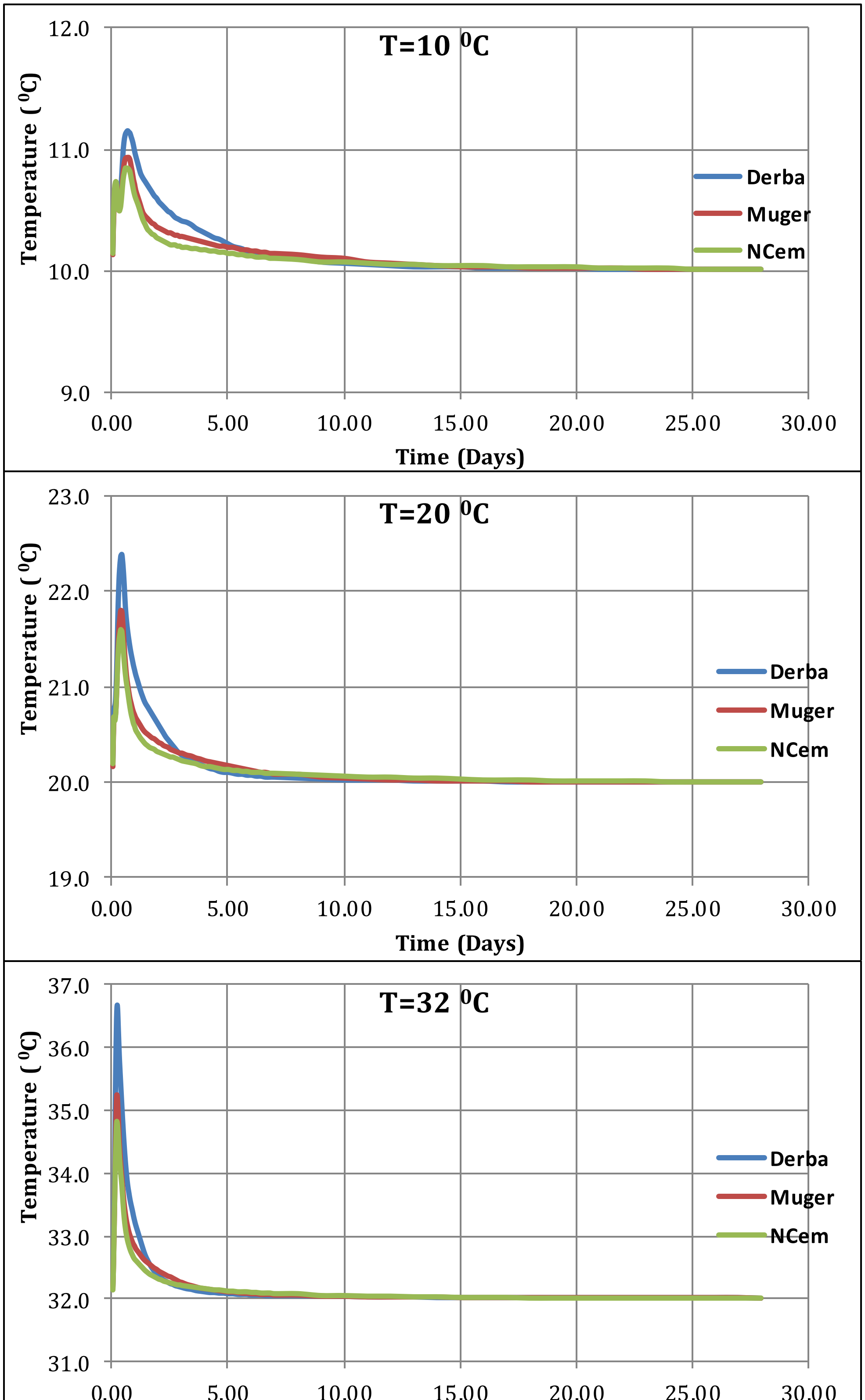


Figure 41-Temperature rise vs. time for different cement types at varying initial temperatures for (W/C=0.55)

# 4. CONCLUSION AND RECOMMENDATION

## 4.1 CONCLUSION

- Regression models performed better when the data was refined against water to cement ratio. Refining seemed to minimize the samples which behaved differently owing to varying water content in the mix. However, the prediction capacity was observed to become significantly compromised with introduction of new data. As the interaction of concrete ingredients is non-linear, the linear regression model adopted cannot be used for prediction.

- Sugeno type fuzzy inference system performed much better under all the experimental conditions. Unlike Mandani type FIS, it appeared to give similar results for varying the number of clusters within the personalized graphical user interface. The predictions made by the Sugeno type FIS with Gaussian membership functions and 3-clusters can be used as a strength prediction model with a safety margin of ($\pm 5$ MPa). This can be greatly improved if the data used for the modelling (dataset II) is refined. This observation is bolstered by the fact that the modified data (dataset I) gave superior predictions.

- Analysis based on Artificial Neural Network also gave good results. As the initial weights are set randomly, it cannot be possible to repeat an experiment and get the same results. However, after recurring experiments, it was found that the tangent sigmoid function with 4 nodes in the hidden layer was enough to accurately model the compressive strength.

- The predictions made using dataset I were far superior to dataset II; which begs the question of reliability. As the alternative approach of utilizing data to instantly predict the compressive strength (among other properties) has been shown to be possible; experiments carried out should be properly handled and recorded for future use. A data-banking system is a good way forward that facilitates contributions of data from different laboratories to one common entity.

- The thermodynamic model gave good predictions as well. The DuCOM analysis was better in prediction for Muger Cement type. Because this approach gives a stepwise strength development of concrete it may be more opted for. Concrete properties needed for durability considerations can be extracted with the use of this approach. Such approach is not dependent on the amount and quality of data on a macro level.

- This brings the notion of 'applicability' of each models. Thermodynamic approach is appealing for research purposes and in cases where concrete properties like thermal gradient, porosity etc. are needed as design parameters. On the other hand, Artificial Intelligence and statistical approaches are attractive for commercial uses, especially in fast track construction endeavors, as trial mixes and waiting for accelerated laboratory testing are avoided in mix design.

## 4.2 RECOMMENDATION

- Engineers in the research community have to consider the prospect of AI- as a tool for modelling.
- There needs to be a data-banking system for compressive strength tests performed locally, as they can serve as a major input to AI- predictive models. They can also be used to study specific material properties.
- AI- models produced may include the effect of inert constituents as a parameter to get a better prediction; provided there is replete data.
- The hydration model produced using thermodynamic approach must be incorporated with porosity to depict a clear image of the microstructure of concrete.
- The thermodynamic approach needs to be further investigated for non-adiabatic conditions where there's a coupled material and temperature ingress for a wider applicability.

# 5. BIBLIOGRAPHY


[1] Bennet D., Innovations in Concrete, Thomas Telford, 2002.

[2] Darwin D., Nilson A. and Charles W., Design of Concrete Structures- 14th Edition, New York: McGraw-Hill Companies, Inc., 2010.

[3] Department of Materials Science and Engineering;, *The History of Concrete,* Urbana-Champaign: University of Illinois, 2013.

[4] Wight J.; MacGregor G., Reinforced Concrete Mechanics and Design, Canada, 2012.

[5] Neville A., Properties of Concrete-Fourth Edition, Malaysia: John Wiley & Sons, Inc., 2000.

[6] Ministry of Works, and Urban Development, "Ethiopian Building Code Standard, Structural Use of Concrete, (EBCS 2-1995)", Addis Ababa, 1995.

[7] Ahmed M., "Statistical Modelling and Prediction of Compressive Strength of Concrete," *Concrete Research Letters,* vol. V.3, 2012.

[8] Munakata T., Fundamentals of the New Artificial Intelligence, USA: Springer-Verlag London Ltd, 2008.

[9] Silarbi S., Abderrahmane B. and Benyettou A., "Adaptive Network Based Fuzzy Inference System for Speech Recognition Through Subtractive Clustering," *International Journal of Artificial Intelligence & Applications (IJAIA),* vol. 5, no. 6, 2014.

[10] M. Zain , "Multiple Regression Model for Compressive Strength Prediction of High Performance Concrete," *Asian Network for Scientific Information,* vol. 9, no. 1, pp. 155-160, 2009.

[11] Nagendra S., Practical Aspects of Using Neural Networks: Necessary Preliminary Specifications, Technical Paper, GE Research and Development Center, 1998.

[12] Subasi S., "Prediction of Mechanical Properties of Cement Containing Class C Fly Ash by Using Aritificial Neural Network and Regression Technique," 2009.

[13] Witold Pedrycz and Fernando Gomide, Fuzzy Systems Engineering: Towards Human-Centric Computing, New Jersey: A John Wiley & Sons, Inc., 2007.

[14] Michael Negenevitsky, Artificial Intelligence, A Guide to Intelligent Systems, 2nd Edition, England: Pearson Education Ltd., 2005.

[15] Robinson A., *Artificial Intelligence and Automation in Construction-Fuzzy Logic,* Canada: Hole School of Engineerring, 2012.

[16] The MathWorks Inc., "Documentation of Matlab Software," 1994-2015.

[17] Aggarwal P. and Aggarwal Y., "Prediction of Compressive Strength of Self-Compacting Concrete with Fuzzy Logic," vol. V.5, no. World Academy of Science, Engineering and Technology, 2011.

[18] Tpocu I. and Saridemir M., "Prediction of Mechanical Properties of Recycled Aggregate Concrete Containing Silica Fume Using Artificial Neural Networks and Fuzzy Lofic," 2007.

[19] Yeh I., "Analysis of Strength of Concrete Using Design Experiments and Neural Networks," *ASCE*, 2006.

[20] Yeh I., "Design of High-Performance Concrete Mixture Using Neural Networks and Nonlinear Programming," *ASCE*, 1999.

[21] Yeh I., "Modelling of Strength of High-Performance Concrete Using Artificial Neural Networks," Elsevier Science Ltd, USA, 1998.

[22] Özturan M., Kutlu B. and Özturan T., "Comparison of Concrete Strength Prediction Techniques with Artificial Neural Network Approach," *Building Research Journal,* vol. 56, 2008.

[23] Des King., "The Effect of Silica Fume on the Properties of Concrete as Defiened in Concrete Society Report 74," *37th Conference on Our World in Concrete & Structures,* 2012.

[24] Rumelhart D., Hinton G. and Williams R., "Learning Representations by Back-Propagating Errors," *Nature*, vol. 323, 1986.

[25] Moreira M. and Fiesler E., "Neural Networks With Adaptive Learning Rate and Momentum Terms," 1995.

[26] Gallant S., Neural Network Learning and Expert Systems, Cambridge: MIT Press, 1993.

[27] Dias W. and Pooliyadda S., "Neural Networks for Predicting Properties of Concretes with Admixtures," *Construction and Building Materials*, vol. V.15, pp. 371-379, 2001.

[28] Atis C., Karahan O., Uncuoglu E. and Tanyildizi H., "Comparison of Artificial Neural Network and Fuzzy Logic Models for Prediction of Long-term Compressive Strength of Silica Fume Concrete," 2009.

[29] Luigi C., Carmine P., Giampietro T. and Giampietro L., "White Cement for Architectural Concrete, Possessing Photocatalytic Properties," *11th Int. Congr. on the Chemistry of Cement*, 2003.

[30] Maruyama I., Matsushita T. and Noguchi T., "Numerical Modeling of Portland Cement Hydration Based on Particle Kinetic MOdel and Multi-Component Concept," 2007.

[31] Tomosawa F., "A Hydration Model of Cement," *Proc. of Annual Meeting on Cement Technology*, vol. 28, pp. 53-57, 1974.

[32] Wang X., Lee H., Lee S., Lim S. and Jewoon K., "A Multi-Component Hydration Model of Portland Cement".

[33] Bentz D., "Modelling Cement Microstructure: Pixels, Particles and Property Prediction," *Materials and Structures*, vol. 32, pp. 187-195, 1999.

[34] Keith J. Laidler, "The Development of the Arrhenius Equation," Canada, 1984.

[35] Suzuki Y., Tsuji Y., Maekawa K. and Okamura H., "Quantification of Hydration-Heat Generation Process of Cement in Concrete," *JCSE*, no. 414, 1990.

[36] S. H. Uchida K., "Formulation of the Heat Liberation Rate of Cement and Prediction Method of Temperature Rise Based on Cumulative Heat Liberation," *JSCE*, no. No.9, 1987.

[37] Maekawa K., Chaube R. and Kishi T., "Modelling of Concrete Performance: Hydration, Microstructure Formation and Mass Transport," *JSCE*, vol. 16, pp. 111-124, 1999.

[38] Okamura H., , Pimanmas A. and Maekawa K., Non Linear Mechanics of Concrete, Spon Press, 2003.

[39] Suzuki Y., Harada S., Maekawa K. and Yukikazu T., "Evaluation of Adiabatic Temperature Rise of Concrete Measured With the New Testing Apparatus," *JCSE*, no. 396, 1988.

[40] Kishi T. and Maekawa K., "Multi-Component Model for Hydration Heating of Portland Cement," *JCSE*, vol. 29, no. 526, 1995.

[41] Nagashima M., "Hydration Setting and Hardening, Cement and Concrete," no. 544, pp. 36-44, 1992.

# APPENDIX I: MATLAB CODE FOR GUI- AIDED COMPRESSIVE STRENGTH PREDICTION USING MAMDANI AND SUGENO FUZZY INFERENCE SYSTEMS

```
function varargout = nebiyu(varargin)
% NEBIYU M-file for nebiyu.fig
% Please note that NEBIYU M-file is has plenty of room for improvements and further modifications
%      NEBIYU, by itself, creates a new NEBIYU or raises the existing
%      singleton*.
%
%      H = NEBIYU returns the handle to a new NEBIYU or the handle to
%      the existing singleton*.
%
%      NEBIYU('CALLBACK',hObject,eventData,handles,...) calls the local
%      function named CALLBACK in NEBIYU.M with the given input arguments.
%
%      NEBIYU('Property','Value',...) creates a new NEBIYU or raises the
%      existing singleton*.  Starting from the left, property value pairs are
%      applied to the GUI before nebiyu_OpeningFcn gets called.  An
%      unrecognized property name or invalid value makes property application
%      stop.  All inputs are passed to nebiyu_OpeningFcn via varargin.
%
%      *See GUI Options on GUIDE's Tools menu.  Choose "GUI allows only one
%      instance to run (singleton)".
%
% See also: GUIDE, GUIDATA, GUIHANDLES

% Edit the above text to modify the response to help nebiyu

% Last Modified by GUIDE v2.5 16-Aug-2015 18:16:55

% Begin initialization code - DO NOT EDIT
gui_Singleton = 1;
gui_State = struct('gui_Name',       mfilename, ...
                   'gui_Singleton',  gui_Singleton, ...
                   'gui_OpeningFcn', @nebiyu_OpeningFcn, ...
                   'gui_OutputFcn',  @nebiyu_OutputFcn, ...
                   'gui_LayoutFcn',  [] , ...
                   'gui_Callback',   []);
if nargin && ischar(varargin{1})
    gui_State.gui_Callback = str2func(varargin{1});
end

if nargout
    [varargout{1:nargout}] = gui_mainfcn(gui_State, varargin{:});
else
    gui_mainfcn(gui_State, varargin{:});
end
% End initialization code - DO NOT EDIT

% --- Executes just before nebiyu is made visible.
function nebiyu_OpeningFcn(hObject, eventdata, handles, varargin)
% This function has no output args, see OutputFcn.
```

```
% hObject    handle to figure
% eventdata  reserved - to be defined in a future version of MATLAB
% handles    structure with handles and user data (see GUIDATA)
% varargin   command line arguments to nebiyu (see VARARGIN)

% Choose default command line output for nebiyu
handles.output = hObject;

% Update handles structure
guidata(hObject, handles);

% UIWAIT makes nebiyu wait for user response (see UIRESUME)
% uiwait(handles.figure1);
 % --- Outputs from this function are returned to the command line.
 function varargout = nebiyu_OutputFcn(hObject, eventdata, handles)
% varargout  cell array for returning output args (see VARARGOUT);
% hObject    handle to figure
% eventdata  reserved - to be defined in a future version of MATLAB
% handles    structure with handles and user data (see GUIDATA)

% Get default command line output from handles structure
varargout{1} = handles.output;

 function filesListEditText_Callback(hObject, eventdata, handles)
% hObject    handle to filesListEditText (see GCBO)
% eventdata  reserved - to be defined in a future version of MATLAB
% handles    structure with handles and user data (see GUIDATA)

% Hints: get(hObject,'String') returns contents of filesListEditText as text
%        str2double(get(hObject,'String')) returns contents of filesListEditText as a double
 % --- Executes during object creation, after setting all properties.
function filesListEditText_CreateFcn(hObject, eventdata, handles)
% hObject    handle to filesListEditText (see GCBO)
% eventdata  reserved - to be defined in a future version of MATLAB
% handles    empty - handles not created until after all CreateFcns called

% Hint: edit controls usually have a white background on Windows.
%       See ISPC and COMPUTER.
if ispc && isequal(get(hObject,'BackgroundColor'), get(0,'defaultUicontrolBackgroundColor'))
    set(hObject,'BackgroundColor','white');
end

function cementEditText_Callback(hObject, eventdata, handles)
% hObject    handle to cementEditText (see GCBO)
% eventdata  reserved - to be defined in a future version of MATLAB
% handles    structure with handles and user data (see GUIDATA)

% Hints: get(hObject,'String') returns contents of cementEditText as text
%        str2double(get(hObject,'String')) returns contents of cementEditText as a double

% --- Executes during object creation, after setting all properties.
function cementEditText_CreateFcn(hObject, eventdata, handles)
% hObject    handle to cementEditText (see GCBO)
% eventdata  reserved - to be defined in a future version of MATLAB
% handles    empty - handles not created until after all CreateFcns called

% Hint: edit controls usually have a white background on Windows.
```

```
%       See ISPC and COMPUTER.
if ispc && isequal(get(hObject,'BackgroundColor'), get(0,'defaultUicontrolBackgroundColor'))
    set(hObject,'BackgroundColor','white');
end

function waterEditText_Callback(hObject, eventdata, handles)
% hObject    handle to waterEditText (see GCBO)
% eventdata  reserved - to be defined in a future version of MATLAB
% handles    structure with handles and user data (see GUIDATA)

% Hints: get(hObject,'String') returns contents of waterEditText as text
%        str2double(get(hObject,'String')) returns contents of waterEditText as a double

% --- Executes during object creation, after setting all properties.
function waterEditText_CreateFcn(hObject, eventdata, handles)
% hObject    handle to waterEditText (see GCBO)
% eventdata  reserved - to be defined in a future version of MATLAB
% handles    empty - handles not created until after all CreateFcns called

% Hint: edit controls usually have a white background on Windows.
%       See ISPC and COMPUTER.
if ispc && isequal(get(hObject,'BackgroundColor'), get(0,'defaultUicontrolBackgroundColor'))
    set(hObject,'BackgroundColor','white');
end

function caEditText_Callback(hObject, eventdata, handles)
% hObject    handle to caEditText (see GCBO)
% eventdata  reserved - to be defined in a future version of MATLAB
% handles    structure with handles and user data (see GUIDATA)

% Hints: get(hObject,'String') returns contents of caEditText as text
%        str2double(get(hObject,'String')) returns contents of caEditText as a double

% --- Executes during object creation, after setting all properties.
function caEditText_CreateFcn(hObject, eventdata, handles)
% hObject    handle to caEditText (see GCBO)
% eventdata  reserved - to be defined in a future version of MATLAB
% handles    empty - handles not created until after all CreateFcns called

% Hint: edit controls usually have a white background on Windows.
%       See ISPC and COMPUTER.
if ispc && isequal(get(hObject,'BackgroundColor'), get(0,'defaultUicontrolBackgroundColor'))
    set(hObject,'BackgroundColor','white');
end

 function faEditText_Callback(hObject, eventdata, handles)
% hObject    handle to faEditText (see GCBO)
% eventdata  reserved - to be defined in a future version of MATLAB
% handles    structure with handles and user data (see GUIDATA)

% Hints: get(hObject,'String') returns contents of faEditText as text
%        str2double(get(hObject,'String')) returns contents of faEditText as a double

% --- Executes during object creation, after setting all properties.
function faEditText_CreateFcn(hObject, eventdata, handles)
% hObject    handle to faEditText (see GCBO)
% eventdata  reserved - to be defined in a future version of MATLAB
```

```
% handles    empty - handles not created until after all CreateFcns called

% Hint: edit controls usually have a white background on Windows.
%       See ISPC and COMPUTER.
if ispc && isequal(get(hObject,'BackgroundColor'), get(0,'defaultUicontrolBackgroundColor'))
    set(hObject,'BackgroundColor','white');
end

function fuzzyTypePopUp_Callback(hObject, eventdata, handles)
% hObject    handle to fuzzyTypePopUp (see GCBO)
% eventdata  reserved - to be defined in a future version of MATLAB
% handles    structure with handles and user data (see GUIDATA)

% Hints: get(hObject,'String') returns contents of fuzzyTypePopUp as text
%        str2double(get(hObject,'String')) returns contents of fuzzyTypePopUp as a double

% --- Executes during object creation, after setting all properties.
function fuzzyTypePopUp_CreateFcn(hObject, eventdata, handles)
% hObject    handle to fuzzyTypePopUp (see GCBO)
% eventdata  reserved - to be defined in a future version of MATLAB
% handles    empty - handles not created until after all CreateFcns called

% Hint: edit controls usually have a white background on Windows.
%       See ISPC and COMPUTER.
if ispc && isequal(get(hObject,'BackgroundColor'), get(0,'defaultUicontrolBackgroundColor'))
    set(hObject,'BackgroundColor','white');
end

function numberOfClustersPopUp_Callback(hObject, eventdata, handles)
% hObject    handle to numberOfClustersPopUp (see GCBO)
% eventdata  reserved - to be defined in a future version of MATLAB
% handles    structure with handles and user data (see GUIDATA)

% Hints: get(hObject,'String') returns contents of numberOfClustersPopUp as text
%        str2double(get(hObject,'String')) returns contents of numberOfClustersPopUp as a double
% --- Executes during object creation, after setting all properties.
function numberOfClustersPopUp_CreateFcn(hObject, eventdata, handles)
% hObject    handle to numberOfClustersPopUp (see GCBO)
% eventdata  reserved - to be defined in a future version of MATLAB
% handles    empty - handles not created until after all CreateFcns called

% Hint: edit controls usually have a white background on Windows.
%       See ISPC and COMPUTER.
if ispc && isequal(get(hObject,'BackgroundColor'), get(0,'defaultUicontrolBackgroundColor'))
    set(hObject,'BackgroundColor','white');
end

% --- Executes on button press in showAdvancedPushButton.
function showAdvancedPushButton_Callback(hObject, eventdata, handles)
% hObject    handle to showAdvancedPushButton (see GCBO)
% eventdata  reserved - to be defined in a future version of MATLAB
% handles    structure with handles and user data (see GUIDATA)

nebiyu_advanced

% --- Executes on button press in evaluateFilesButton.
function evaluateFilesButton_Callback(hObject, eventdata, handles)
```

```
% hObject    handle to evaluateFilesButton (see GCBO)
% eventdata  reserved - to be defined in a future version of MATLAB
% handles    structure with handles and user data (see GUIDATA)

 %first read the files and save them into an array
tempNumberOfClusters=str2double(get(handles.numberOfClustersPopUp,'String'));
val=get(handles.numberOfClustersPopUp,'Value');
numberOfClusters=tempNumberOfClusters(val);

tempType=get(handles.fuzzyTypePopUp,'String');
val=get(handles.fuzzyTypePopUp,'Value');
type=tempType(val);

%the code below is used to delete the trailing and endign ' that
%the selected string has.
temp=strfind(type,'mamdani');
if(temp{1}==1)%this means that the selected type is mamdani
    type='mamdani';
else
    type='sugeno';
end

%get the file names as much as the user has given.
fileNames=get(handles.filesListEditText,'String');
[xtest,ytest,xeval,yeval]=readFiles(fileNames);

%after saving the values in the files into an array create the fismat
'Generating fuzzy logic'
global fismat;
fismat=genfis3(xtest,ytest,type,numberOfClusters);

'finished generating fuzzy logic'
%after creating the fismat calculate the evaluation data.
yresult=evalfis(xeval,fismat);
yerror=abs((yeval.^2)-(yresult.^2)).^0.5;
yrms=sum(yerror)/length(yerror);

mare=sum((abs(yeval-yresult))./yeval)*100/length(yeval);
mse=sum((yeval-yresult).^2)/length(yeval);

set(handles.rmsErrorStaticText,'string',yrms);
set(handles.mareErrorStaticText,'string',mare);
set(handles.mseErrorStaticText,'string',mse);

setappdata(0,'xtest',xtest);
setappdata(0,'ytest',ytest);
setappdata(0,'xeval',xeval);
setappdata(0,'yeval',yeval);
setappdata(0,'yresult',yresult);
setappdata(0,'yerror',yerror);
 %after the evaluation data is evaluated display the average rms.
 function [xtest,ytest,xeval,yeval] = readFiles(fileNames)
xtest=[];
ytest=[];
xeval=[];
yeval=[];
```

```
numberOfFiles=size(fileNames);
numberOfFiles=numberOfFiles(1);
counter=1;
while(counter<=numberOfFiles)
    fileName=fileNames(counter,:);
    'Reading...'
    fileName
    xtest=cat(1,xtest,xlsread(fileName,'XTest'));
    ytest=cat(1,ytest,xlsread(fileName,'YTest'));
    xeval=cat(1,xeval,xlsread(fileName,'XEval'));
    yeval=cat(1,yeval,xlsread(fileName,'YEval'));

    counter=counter+1;
end

function writeFiles(fileName,xtest,ytest,eval,yeval,yerror)
xlswrite(fileName,xtest,'XTest');
xlswrite(fileName,ytest,'YTest');
xlswrite(fileName,xeval,'XEval');
xlswrite(fileName,yeval,'YEval');
xlswrite(fileName,yerror,'YError');

% --- Executes on button press in evaluateInputsButton.
function evaluateInputsButton_Callback(hObject, eventdata, handles)
% hObject    handle to evaluateInputsButton (see GCBO)
% eventdata  reserved - to be defined in a future version of MATLAB
% handles    structure with handles and user data (see GUIDATA)
cement=str2double(get(handles.cementEditText,'string'));
water=str2double(get(handles.waterEditText,'string'));
ca=str2double(get(handles.caEditText,'string'));
fa=str2double(get(handles.faEditText,'string'));

if(isnan(cement)||isnan(water)||isnan(ca)||isnan(fa)||cement<=0||water==0||ca==0||fa==0)
    set(handles.resultStaticText,'string','Please  enter a correct Data');
    return;
end

xinput=[cement,water,ca,fa];
global fismat;
try
    lastwarn('');
    error(lastwarn);
    youtput=evalfis(xinput,fismat);
    error(lastwarn);
catch exception
    youtput=exception.message;
end

'finished evaluating inputs'
set(handles.resultStaticText,'string',youtput);
 % --- Executes on button press in showGraphButton.
function showGraphButton_Callback(hObject, eventdata, handles)
% hObject    handle to showGraphButton (see GCBO)
% eventdata  reserved - to be defined in a future version of MATLAB
% handles    structure with handles and user data (see GUIDATA)
nebiyu_graph

function initialize(handles)
```

```
xtest=getappdata(0,'xtest');
ytest=getappdata(0,'ytest');
xeval=getappdata(0,'xeval');
yeval=getappdata(0,'yeval');
yresult=getappdata(0,'yresult');
yerror=getappdata(0,'yerror');

mamdani3=evalfis(xeval,genfis3(xtest,ytest,'mamdani',3));
mamdani5=evalfis(xeval,genfis3(xtest,ytest,'mamdani',5));
mamdani7=evalfis(xeval,genfis3(xtest,ytest,'mamdani',7));
mamdani11=evalfis(xeval,genfis3(xtest,ytest,'mamdani',11));

sugeno3=evalfis(xeval,genfis3(xtest,ytest,'sugeno',3));
sugeno5=evalfis(xeval,genfis3(xtest,ytest,'sugeno',5));
sugeno7=evalfis(xeval,genfis3(xtest,ytest,'sugeno',7));
sugeno11=evalfis(xeval,genfis3(xtest,ytest,'sugeno',11));

x=1:1:length(mamdani3);
axes(handles.axes1);

plot(x,mamdani3,x,mamdani5,x,mamdani7,x,mamdani11,x,yeval);
title('Mamdani  With Different Clusters');
ylabel('Compressive Strength(MPa)');
legend('3','5','7','11','Lab  R.');

axes(handles.axes2);
plot(x,sugeno3,x,sugeno5,x,sugeno7,x,sugeno11,x,yeval);
title('Sugeno With Different Clusters');
xlabel('Data Sample');
ylabel('Compressive Strength(MPa)');
legend('3','5','7','11','Lab  R.');
axes(handles.axes3);
plot(x,mamdani3,x,sugeno3,x,yeval);
title('Number of Clusters=3');
xlabel('Data Sample');
ylabel('Compressive Strength(MPa)');
legend('mamdani','sugeno','Lab  R.');
axes(handles.axes4);
plot(x,mamdani5,x,sugeno5,x,yeval);
title('Number of Clusters=5');
xlabel('Data Sample');
ylabel('Compressive Strength(MPa)');
legend('mamdani','sugeno','Lab  R.');
axes(handles.axes5);
plot(x,mamdani7,x,sugeno7,x,yeval);
title('Number of Clusters=7');
xlabel('Data Sample');
ylabel('Compressive Strength(MPa)');
legend('mamdani','sugeno','Lab  R.');
axes(handles.axes6);
plot(x,mamdani11,x,sugeno11,x,yeval);
title('Number of Clusters=11');
xlabel('Data Sample');
ylabel('Compressive Strength(MPa)');
legend('mamdani','sugeno','Lab  R.');
```